

SPATIO-TEMPORAL MAPPING OF SUB-ARCTIC BENTHIC COMMUNITIES

by © Kaitlyn Charmley

A Thesis submitted to the

School of Graduate Studies in partial fulfillment

of the requirements for the degree of

Master of Science

Fisheries Science and Technology

Marine Institute -Memorial University of Newfoundland and Labrador

May 2023

St. John's, Newfoundland and Labrador

Abstract

Spatial studies of benthic communities rarely incorporate a temporal aspect into their construction, despite the fact that organisms can exhibit spatio-temporal patterns. Construction of benthic community maps often involve the association of spatially-continuous acoustic layers with *in situ* samples (ground-truthing); often image and/or video data. Most current habitat mapping studies are built from a single ground-truthing event, which makes the maps a simple snapshot of the distribution of organisms and does not consider temporal variability.

The goal of this thesis was to explore the importance of incorporating seasonality into investigations on benthic organisms habitat selection, at both the community and species levels. The first objective explores the spatio-temporal changes that occur in the communities and the implications in the production of benthic community maps. The second objective focuses on one economically-important species, snow crab (*Chionoecetes opilio*) and investigates the abiotic factors influencing its habitat selection and how these drivers change seasonally. The community maps produced in part one presented two to five different communities depending on the season, with map differences caused by the changes in densities and location of individual taxa. Part two revealed that fine-scale habitat preferences of snow crab was driven by temperature, slope, and in the winter, seafloor hardness. Recommendations are made to researchers regarding timing and frequency of ground-truthing data collection.

This study is one of the first to produce predictive maps based on a spatio-temporal seafloor dataset for a sub-Arctic megabenthic community in Canada. It emphasized the importance of incorporating temporal coverage into benthic research to accurately represent communities. This will increase the effectiveness of management of these marine areas , so they can remain biodiverse and economically productive.

Acknowledgements

Many people contributed to the completion of this thesis, both professionally and personally. Firstly, I'd like to thank Dr. Kathleen Robert (Canada Research Chair in Ocean Mapping) for your expertise, and your consistent academic support throughout this project. You always made time to meet with me, to edit my drafts, and to push me to be the best scientist that I could be. I thank my co-supervisor Dr. Krista Baker for your academic and moral support, and for knowing when I needed each most. Additionally, I'd like to thank my committee member Dr. Darrell Mullowney for the knowledge and guidance you have provided throughout this thesis.

A big thanks to my field team, Adam Templeton, Kirk Regular, Poppy Keogh, Shreya Nemanji, and Rylan Command, for your assistance collecting this data in Holyrood on both the sunny days, and the not so sunny days. I'd like to thank all the experts who have assisted in species identification for this thesis: Dr. Annie Mercier, Philip Sargent, Jackson Chu, Vonda Hayes, William Coffey, and Dr. Darrell Mullowney. I'd also like to thank Dr. Krista Baker, and Dave Fifield for your guidance and knowledge on GAM modelling.

Thank you to the following organizations for providing the funding for this research: Marine Environmental Observation Prediction and Response network (MEOPAR), Fisheries and Oceans Canada (DFO), and Memorial University's School of Graduate Studies.

Lastly, I would like to express my utmost gratitude and appreciation to my family and friends for your support during this thesis, especially during the period that I was completing it part-time, and especially to Poppy Keogh, Dr. Andrew Nicholson, and Dr. Evan Pugh. This period was not easy and would not have been possible without you three. Evan, you have been such an incredibly supportive, loving, and patient partner during this process, thank you for everything you do.

Table of Contents

Abstract	i
Acknowledgements	ii
Table of Contents	iii
List of Tables	v
List of Figures	vi
List of Abbreviations	x
1. Introduction.....	1
1.1. Benthic Communities.....	1
1.1.1. Spatial Patterns.....	2
1.1.2. Temporal Patterns	4
1.1.3. Benthic Commercial Species- Snow Crab	6
1.1.4. Management.....	8
1.2. Mapping Benthic Communities	8
1.2.1. Creating a Benthic Community Map	8
1.2.2. Uses of Benthic Community Maps	12
1.3.3. The Issue with Current Practices	12
1.3. Approach	13
1.4. Study Site	14
2. Materials and Methods.....	17
2.1. Acoustic Survey	17
2.2. Environmental Variables.....	17
2.3. Ground-Truthing	23
2.4. Video Annotation	24
2.5. Community Clustering	25
2.6. Community Mapping	26
2.7. Modelling Snow Crab Presence	28
3. Results.....	29
3.1. Species Accumulation Curves.....	29
3.2. Community Clusters.....	30
3.3. Description of Clusters and their Seasonal Change	33

3.4. Variables Influencing Clusters	39
3.5. Spatially-Continuous Community Maps and Variable Importance	44
3.6. Variables Driving Snow Crab Presence	48
4. Discussion	52
4.1. Overview	52
4.2. Abiotic Patterns	53
4.3. Biotic Patterns	55
4.3.1. Community-Level	55
4.3.2. Species Driving Community Change.....	57
4.3.3. Snow Crab Fine-Scale Habitat Preferences	60
4.4. Broader Implications	62
5. Conclusions and Future Directions	64
5.1. Key Findings	64
5.2. Recommendations	65
References	67
Appendix A – Rasters of Environmental Variable	98
Appendix B – Species Catalogue	123
Annelida.....	123
Arthropoda	123
Chordata.....	126
Cnidaria.....	129
Echinodermata	134
Mollusca.....	139
Porifera.....	145
Unclassified.....	148
Appendix C – SIMPER, IndVal, ANOSIM Results	149
SUMMER	149

List of Tables

Table 1. List of variables used in the analyses, the packages used for their calculation, the range of scales, and a brief description.....	Error! Bookmark not defined.
Table 2. Total density of organisms and individual species densities of taxa of interest, of the sampled sites in Holyrood Bay in all seasons.....	30
Table 3. Model performance statistics and important non-correlated variables and their associated scales for the final random forest models. Variables are listed in their order of importance determined using VarImp.	44
Table 4. Summary of the model output describing the parametric and smoothed terms of the snow crab Presence/Absence Generalized Additive Model.	49

List of Figures

Figure 1. Maps of the study site Holyrood Bay, (A) Denoting its geographical location at the head of Conception Bay in Newfoundland and Labrador, Canada. The red rectangle denotes the extent of the study site. (B-C) The primary continuous data layers used as explanatory variables, bathymetry and backscatter. Numbers on the bathymetry (and associated circles on the backscatter) denote the ground-truthing sites..... 15

Figure 2. Species accumulation curves for Holyrood Bay sampled from July 2020 to April 2021 for (A) all seasons combined and (B) each season independently..... 30

Figure 3. Photos documenting examples of each community observed throughout the seasons, based on Unweighted Pair-Group Method with Arithmetic Averages (UPGMA) hierarchical clustering of Holyrood Bay site observations from July 2020- April 2021. The communities are: (A) star and sand dollar dominated, (B) urchin dominated, (C) star and urchin dominated, (D) sea cucumber dominated, (E) brittle star dominated, (F) sea cucumber and brittle star dominated, (G) decapod dominated, and (H) flatfish dominated..... 31

Figure 4. UPGMA hierarchical clustering of all sites across the four seasons in Holyrood Bay. (Summer (n=64), Fall (n=66), Winter (n=65), and Spring (n=67)). Coloured rectangles denote the cluster grouping for each season..... 32

Figure 5. A flow chart depicting the change in important taxa for each cluster throughout the seasons. Bolded taxa are the defining taxa for each cluster. Asterix's denote that a taxa was not an indicator taxa but still significantly contributed to the difference between clusters (using

SIMPER). Numbered taxa represent morphospecies names. X's denote when a cluster was not present in a season. (Created with BioRender.com) 33

Figure 6. Bubble map of (A) Brittle stars (*Ophiuroidea* spp.), (B) Brown psolus (*Psolus phantapus*), (C) Green sea urchin (*Strongylocentrotus droebachiensis*), and (D) Common sand dollar (*Echinarachnius parma*) densities at sample sites in Holyrood Bay in all four seasons. The average density of each morphospecies for the total area observed is at the bottom of each plot. The maps use a UTM projection in zone 22N. X's denote absence of the morphospecies at a site. 36

Figure 7. Non-metric dimensional scaling plots of the morphospecies present in each season. The coloured points represent the important taxa for the corresponding cluster in that season, with points with two colours being dominant in two different clusters in a season. Labels represent species that were further discussed in this study..... 38

Figure 8. Boxplots of broad-scale GLCM Mean (21x21). (A) Comparing the GLCM Mean values of the different clusters (all seasons merged), and (B) Comparing the GLCM mean value of the primary substrata that were recorded at each site. Algae occurred across a range of seafloor hardness and were only used as a 'substrate' when it obscured all view of the substrate. (D-F) The most important scale of GLCM Mean by cluster for each of the seasons..... 40

Figure 9. Violin plots of the (A) Brown psolus (*Psolus phantapus*) and (B) Brittle stars (*Ophiuroidea* spp.) abundances by depth, binned by season. 41

Figure 10. Boxplots of Bathymetric Position Index (BPI) by the cluster for each of the seasons
(A) Summer, (B) Fall, (C) Winter, and (D) Spring. 42

Figure 11. Violin plots and associated boxplots of (A) overall sampling density, and (B) green sea urchin (*Strongylocentrotus droebachiensis*) abundance, by depth. 43

Figure 12. Maps showing the predicted spatial coverage of each community as predicted by the random forest models for all four seasons in Holyrood Bay A) summer 2020, B) fall 2020, C) winter 2021, and D) spring 2021. See Figure 5 for community descriptions. 45

Figure 13. Boxplots of temperature by the cluster for each of the seasons (A) Summer, (B) Fall, (C)Winter, and (D) Spring. The dashed lines denotes the mean temperature of the study area (2.23°C in summer, 2.62°C in fall, 0.70°C in winter, and 0.94°C in spring). 47

Figure 14. Presence/Absence map of snow crab (*Chionoecetes opilio*) at sample sites in Holyrood Bay across the four seasons. The maps use a UTM projection in zone 22N. 50

Figure 15. Partial-effects plots of the smoother relationships from the snow crab (*Chionoecetes opilio*) binomial GAM model converted to the probability scale with the model intercept, and the intercept uncertainty added to the smooth uncertainty. Significant covariates (A) global temperature, (B) global slope (25x25), and (C) GLCM Mean (3x3) by season are illustrated. Hashes on the x-axis denote the presence or absence of snow crab from in-situ data collected in Holyrood Bay from 2020-2021, which was used to inform the model. 51

Figure 16. Boxplots of the (A) depths and (B) temperatures of the study sites sampled in Holyrood Bay with snow crabs (*Chionoecetes opilio*) absent (light grey), and with snow crabs present (dark grey) across the four seasons from July 2020 to April 2021. 52

List of Abbreviations

ANOSIM	Analysis of Similarities
BPI	Bathymetric Position Index
CTD	Conductivity, Temperature, Depth
EBM	Ecosystem-Based Management
FPS	Frames Per Second
GAM	Generalized Additive Model
GLCM	Grey Level Co-Occurrence Matrices
GPS	Global Positioning System
HD	High Definition
ID	Inner Diameter
IndVal	Indicator Value Index
MBES	Multibeam Echosounders
NAO	North Atlantic Oscillation
NMDS	Non-Metric Multidimensional Scaling
OD	Outer Diameter
RDMV	Relative Difference from the Mean Value
SIMPER	Similarity Percentages
TASSE	Terrain Attribute Selection for Spatial Ecology
UPGMA	Unweighted Pair-Group Method with Arithmetic Averages
UTM	Universal Transverse Mercator
VARS	Video Annotation and Reference System Software

1. Introduction

1.1. Benthic Communities

Benthic habitats are physically different ecological areas found on the seabed of the ocean (Harris and Baker, 2020b). Species in these habitats live on various substrata, ranging from soft sand or mud to bedrock, and make up benthic communities (Harris and Baker, 2020b). Using the definitions from Stroud *et al.* (2015) and Begon *et al.* (2005), a benthic community represents a group of different species populations that are present on the seafloor together in space and time.

Preserving benthic communities is important to ecosystem function. Some benthic species are economically valuable, as they are exploited by fisheries around the world. Crab, lobster, clams, and scallops account for almost 70% of the total value of all commercial fishery landings in Canada (Fisheries and Oceans Canada, 2021a). However, exploitation of single species can destabilize communities and lead to trophic cascade or entire community collapse (Frank *et al.*, 2005). This is because organisms often directly or indirectly interact within communities by providing energy to and controlling other species' populations (Cardinale *et al.*, 2002). These biotic interactions are a key part of a balanced and stable ecosystem which increases resilience against environmental changes and disturbances (Thibaut *et al.*, 2012), sequesters more carbon (Barnes and Sands, 2017), enhances overall ecosystem biomass (Duffy *et al.*, 2016), and buffers against the impacts of climate change (Duffy *et al.*, 2016).

Communities can vary in space and time because spatial and temporal environmental patterns occur hierarchically at various scales (Levin, 1992; Ysebaert *et al.*, 2002). For example, temporally, environments are simultaneously affected by tidal, seasonal, and interannual patterns. There is no single universal scale that is important for all objectives. Instead, to best

characterize communities, observation and analysis scales must match species and processes of interest (Turner and Gardner, 2015).

Since environmental heterogeneity and biological interactions occur on spatial and temporal scales simultaneously there is a general agreement that most communities have a more gradual shift into neighbouring communities rather than being discrete, isolated units (Glemarec, 1973; Wilson and Chiarucci, 2000; Brown *et al.*, 2011). However, to parse out general patterns in characteristic species and their related environmental variables, it is often valuable to statistically delineate and relate discrete communities to environmental variability (Brown *et al.*, 2011).

1.1.1. Spatial Patterns

Benthic organisms are not evenly distributed throughout space. Different communities exhibit their own spatial patterns due to environmental spatial variation, or biological factors (Chang and Marshall, 2016). For example, they can exist in long linear patterns in the intertidal zone where sunlight and oxygen is abundant or in patches to increase fertilization success (Leigh *et al.*, 1987; Downing *et al.*, 1993).

Abiotic environments and their associated biota tend to vary together spatially since species have physiological requirements for specific environmental conditions and can also alter their environments. An example of this is seafloor composition, which is interrelated with the species present in an area. Some organisms (e.g., mussels (Mytilidae)) require hard substrate to attach to, like bedrock and boulders, especially in exposed areas (Gosling, 2021). Other organisms require soft sediment for burrowing (e.g., tube dwelling anemone (Cerianthidae); Frey, 1970). Thus, areas with greater habitat heterogeneity tend to have higher biodiversity because of the increased variety of habitats that suit different species' niches (Zeppilli *et al.*,

2016). Conversely, organisms can also alter the seafloor composition. Corals can attach to rocks and form reefs as they grow, thus altering the morphology of the seafloor (Sorokin, 1995).

Seafloor composition experiences spatial variation, with seafloors geographically close being more similar than those far away, i.e. spatial autocorrelation (Getis, 2008). At a large scale, seafloor composition is influenced by the movement of tectonic plates, which can create canyons and mountain ranges depending on the plate location (Parson and Evans, 2005). At a smaller scale, seafloor composition is controlled by erosion and sedimentation, which vary spatially because of differences in currents, disturbances, tides, distance from the shore, etc. (Earle, 2019). For example, most sand and mud in the ocean originates from rivers and is distributed to the seafloor through waves and currents (Braathen and Brekke, 2020). Sand is only found in small, rare patches in the deep sea, caused by infrequent currents that travel down the continental slope (Braathen and Brekke, 2020). Therefore, seadbeds closer to land have greater proportions of sand and mud in their composition.

Species within communities all present individual abiotic requirements (fundamental niche) (Hutchinson, 1957), and thus do not always vary together. A species' fundamental niche is unique to that species and is based on its physiological requirements (Hutchinson, 1957). For example, the American lobster (*Homarus americanus*) prefers areas with a temperature range of 12 - 18 °C (Crossin *et al.*, 1998) and exhibits physiological stress at temperatures > 22 °C (Dove *et al.*, 2005). Environmental conditions are often interrelated. A classic example is how depth can be a good predictor for species habitat selection since it is connected to temperature, light, and food input. A species realized niche is where an organism is typically found, and is controlled by biotic interactions like competition, search for food, predator avoidance, and mating (Wisz *et al.*, 2013). Spatial requirements vary not only for different species, but also can

differ by sex and life stage. For example, female American lobster generally prefer areas with colder waters and higher salinities than males (Jury *et al.*, 2019).

1.1.2. Temporal Patterns

Seasonality is one temporal scale that has a strong effect on environmental variables and their relationship to communities. Seasonality affects virtually all marine environments, though to varying degrees. Areas of high latitudes present strong seasonal patterns, with abiotic changes such as temperature (Valentine, 1983; Grebmeier *et al.*, 1988; Chauvet *et al.*, 2018), salinity changes from sea ice and freshwater run-off (Valentine, 1983; Chainho *et al.*, 2006; Peck, 2018), sunlight availability (Valentine, 1983; Clarke, 1988; Loeng *et al.*, 2005), and changes in weather patterns (Valentine, 1983; Chauvet *et al.*, 2018). Seasonal patterns can also vary locally due to differing local conditions, how they interact, and external drivers like disturbances, so it is important to understand patterns for specific ecosystems (Cloern and Jassby, 2010). For example, the depth range and timing of algal communities, which provide large influxes of food to benthic communities, vary locally based on local water quality, nutrients, and orientation (Coma *et al.*, 2000).

Phytoplankton blooms are an important seasonal phenomenon that influences the benthos (Zhang *et al.*, 2015). A bloom occurs when phytoplankton reproduces rapidly, leading to a large visible mass in the ocean (Mills, 1989). Phytoplankton are photosynthetic organisms, and blooms are created when specific environmental conditions enable them to reproduce faster than they are dying (Valiela, 2015). By increasing primary productivity considerably, these blooms increase the food availability sequentially for organisms higher in the food web. Globally, 20% of primary production falls to the seafloor which provides short-term food inputs to benthic communities (benthic-pelagic coupling) (Laws *et al.*, 2000).

In the spring, increases in freshwater run-off and surface water temperatures and changes in sea-ice lead to differences in surface and bottom water densities. This density disparity causes thermal and saline stratification in the water column of coastal estuaries which traps the cold mixed layer from the prior winter under it (i.e., the cold intermediate layer) (van Aken, 1986; Petrie *et al.*, 1988; Chubarenko *et al.*, 2017). These stratifications cause nutrients to remain in the euphotic zone, which creates ideal conditions for phytoplankton photosynthesis when coupled with increased sunlight. The thermocline perpetuates these differences until nutrients deplete and surface temperatures cool in the fall, leading to increased mixing and the destruction of the thermocline (Pingree *et al.*, 1976). Seasonal phytoplankton blooms typically occur in two peaks, the first in the spring (described above) and a second smaller bloom in the fall when nutrients from deep water get mixed with surface water previously depleted in the summer (Pepin and Maillet, 2002; Bernier *et al.*, 2018).

Environmental processes are highly influenced by seasonal change, and in response, biological communities also present seasonal patterns (Rosa and Bemvenuti, 2006; Valiela, 2016). Generalist species can survive in a broad range of conditions and consequently are less impacted by seasonally changing conditions (Colossi Brustolin *et al.*, 2019). Species that cannot tolerate a wide range of conditions, or specialist species, must physiologically or behaviourally adapt. Physiological responses to changing conditions can include a variety of mechanisms, such as changes in clutch size, reproduction timing, and, reduced feeding. For example, some benthic suspension feeders exhibit winter dormancy in cold temperate seas due to reduced temperatures but summer dormancy in warm temperate seas due to energy shortage (Gili and Hughes, 1995; Coma *et al.*, 1998, 2000).

For motile organisms, behavioural responses like migration or burrowing are common. Some species migrate due to seasonal abiotic changes in environmental conditions, such as water temperature or food availability, or for spawning purposes (Sackett *et al.*, 2007; Risch *et al.*, 2014; Fairchild *et al.*, 2015). For instance, large numbers of sexually paired snow crabs (*Chionoecetes opilio*) have been observed migrating to shallow depths of about 10-40 m in spring to mate, originating from normal depths of > 100 m (Hooper, 1986; Mullowney *et al.*, 2018). Additionally, rapid responses can be seen by benthic macrofauna in areas with increased organic material, and as a result, megafauna densities are higher during times when food input to the seafloor is greater (e.g., the spring phytoplankton bloom) (Aberle and Witte, 2003; Meyer *et al.*, 2013).

1.1.3. Benthic Commercial Species- Snow Crab

Many species in sub-Arctic benthic ecosystems are economically and ecologically important but have declined in recent years. In 2019, the landings from commercial fishing of benthic species in Atlantic Canada alone were valued at over \$3 billion CAD, 85% of Canada's total commercial landing value (DFO & Economic Analysis and Statistics, 2021).

The snow crab fishery is the largest commercial fishery in Newfoundland and Labrador. It had a landed value of over \$620 million in 2021 (Fisheries and Oceans Canada, pers comm), but little fine-scale quantitative knowledge about snow crab habitat selection is known, as most studies are based on trawl and trap surveys. Snow crab are a stenothermic sub-Arctic species (Mullowney *et al.*, 2014, 2018; Zisserson and Cook, 2017). Dionne et al. (2003) found that juvenile snow crab distribution is largely size and age-dependent. They found youngest juveniles at temperatures near 0°C, with temperature preferences changing to a slightly warmer 1.5°C as they grew. They also found that most juvenile snow crab preferred muddy substrata. They are

typically found at depths between 70 and 500 m and energetically can survive in temperatures below 7°C (Elner 1985; Foyle, O'Dor, and Elner 1989), but are atypically found beyond 3.5°C in the wild (Mullowney *et al.*, 2018). High bottom temperatures are correlated with lower crab abundance (Marcello *et al.*, 2012) and larger crab size (Dawe *et al.*, 2012). Snow crab are highly motile, participating in both an ontogenetic migration downslope and seasonal migrations for mating upslope. They usually mate and molt during the springtime, but primiparous females can mate in the winter (Mullowney *et al.*, 2014). It is generally accepted that snow crabs move seasonally upslope for mating in early spring, but little is known about the extent of these migrations (Mullowney *et al.*, 2018).

It is important to collect baseline information on snow crab abundances and distributions, as future populations are difficult to predict. Climate has a strong impact on snow crab success in early life stages (Marcello *et al.*, 2012; Mullowney *et al.*, 2014; Émond *et al.*, 2015). The North Atlantic Oscillation (NAO) drives large-scale ocean temperature trends throughout atmospheric-surface exchanges in the Northwest Atlantic (Cyr and Galbraith, 2021). However, it is unknown if these long-term oscillations will persist or how they will interact with other changing conditions (Hurrell, 1995). Cooler temperatures are correlated with a lagged increase in snow crab abundance (Boudreau *et al.*, 2011). Though, temperatures have been favourable for the past few years, snow crab populations are smaller than during previous similarly cold regimes, for example in the 1990s when the highest exploitable biomasses were recorded in Newfoundland (Hurrell, 1995; Baker *et al.*, 2021; Cyr and Galbraith, 2021). This discrepancy suggests that there may be a top-down factor regulating these populations like fishing or predation (Fisheries and Oceans Canada, 2019a). Climate change also impacts snow crab populations by causing rising global ocean temperatures and reduced sea ice. Negative impacts on snow crab populations are

already being observed in other snow crab populations (e.g., in Alaska; Fedewa *et al.*, 2020). In Newfoundland and Labrador, bottom temperatures generally increased in recent years (Fisheries and Oceans Canada, 2022). Therefore, rates, extents and directions of snow crab population changes are difficult to predict.

1.1.4. Management

Marine areas' usages are traditionally divided into different sectors (e.g., fishing, recreation, energy, and shipping) whose management and impacts are observed independently of each other. This fragmented approach can lead to inconsistent or conflicting policies and cumulative damage (Salomon and Dross, 2018). There has been a general shift towards more integrated management approaches. Ecosystem-Based Management (EBM) is one approach to managing marine environments, where ecosystems are looked at as whole complex systems instead of single threats or species of interest (McLeod *et al.*, 2005). The first step in EBM is collecting spatial information on the marine area (Cogan *et al.*, 2009). Therefore, accurately mapping benthic communities is an important prerequisite to management practices (Baker and Harris, 2020).

1.2. Mapping Benthic Communities

1.2.1. Creating a Benthic Community Map

Since marine communities are more difficult to characterize than their terrestrial counterparts, the utility of abiotic surrogates is important in benthic ecosystem management (Harris, 2020). Species exhibit particular environmental requirements, so by understanding the spatial patterns of the more easily measured abiotic variables, these abiotic variables can be used as proxies for different biological patterns (McArthur *et al.*, 2010; Brown *et al.*, 2011). Maps describing benthic communities often relate the biota present to the physical environment at

sample locations, then use this to make biological predictions over the full-extent of an area (Brown *et al.*, 2011; O'Brien *et al.*, 2022). These maps can be created at the individual species or community level. Some advantages of benthic community mapping include detecting shared patterns between species and the synthesis of complex ecosystems into interpretable data, which can then be used for management decisions (Ferrier and Guisan, 2006).

Benthic community mapping relies on spatially-continuous environmental data from the seafloor and the water column to use as surrogates to fill in gaps in biological data. The seafloor is characterized using two raw data layers, bathymetry and backscatter, from which secondary layers can be derived. In the last two decades, multibeam echosounders (MBES) have become the tool of choice to map the bathymetry and backscatter of the seafloor (Jakobsson *et al.*, 2016). MBES emit an angular swath from a ship's hull and use the time for the sound to echo off the seabed and return to the system to calculate depth (Brown and Blondel, 2009).

Bathymetry is a measure of seafloor depth and is the underwater equivalent to topography. MBES also use the intensity of the signal (i.e., backscatter or reflectivity) that returns to collect information on the nature of the seabed, higher backscatter is obtained with increasing seafloor hardness and roughness (Hughes Clarke, 2018). This information can help differentiate seafloor substrata based on characteristics, such as sediment grain sizes and heterogeneity.

Other attributes can be derived through these two primary data layers. In the case of bathymetry, these secondary descriptive features (e.g., terrain features) can be extracted to characterize the morphology of the terrain (e.g., slope). Backscatter derivatives can provide information on the textural organization of the seabed. For example, contrast provides information on the local variation in seafloor textures. Many of these attributes are not direct drivers for species habitat selection but are often surrogates for other more direct drivers (Harris,

2020). For example, a slope's angle and direction can impact an area's food input because of sinking detritus transported by currents. These attributes also determine an area's protection from disturbances like storms, which can influence species composition (Aller, 1997; McArthur *et al.*, 2010). However, Stevens and Connolly (2004) found that abiotic surrogates could predict less than 30% of the biotic similarity between sites. This result may partly be due to the variables included (depth, mud fraction, current velocity, distance to a river, distance to the ocean, and fetch) or excluded (e.g., rugosity and slope). Variable selection is a crucial component of the habitat mapping process, with Lecours *et al.* (2016) finding that some combinations of abiotic surrogates could lead to accuracy differences of up to 47% between habitat maps.

Some features of the water column are often difficult to collect; however, CTDs are a common and relatively cost-effective way of collecting basic water column data on conductivity, temperature, depth, and salinity (Baker, 1981). They are often attached to a larger piece of equipment and lowered to the seafloor to collect *in-situ* data. These data can be interpolated to create spatially-continuous predicted layers to be used in benthic community mapping.

As previously discussed, environmental processes and, thus, organisms within benthic communities act at multiple spatial and temporal scales. It is important that community maps are created at the scale most relevant to the species present; however, the appropriate scale is often not known *a priori*, and multiple scales can be relevant simultaneously (Wilson *et al.*, 2007). Traditionally terrain variables have been solely derived at the scale of the primary data later, but more recently, 'multi-scale' analyses have been encouraged (Brown *et al.*, 2011; Lecours *et al.*, 2015). Multiscale analyses calculate data at a range of scales concurrently to ensure relevant scales are captured (Dolan, 2012; Lecours *et al.*, 2015; Misiuk *et al.*, 2021).

Once multi-scale spatially-continuous environmental layers are produced, they are associated to the biota through *in-situ* samples (ground-truthing). Ground-truthing data are physical visualizations of the seabed, often image/video data showing biological communities and sediment characteristics (Brown *et al.*, 2011). Advancements in high-quality underwater video capabilities have made image and video ground-truthing common and more efficient (Durden *et al.*, 2016). Annotations of video data can describe morphospecies present, morphospecies abundances, behaviours, a visual estimation of substrate type, and any other visible features like flora or anthropogenic litter (Durden *et al.*, 2016). Morphospecies are a taxonomic group based on morphology and are useful in video analyses, since definitive species identification is often not possible without biological samples (Howell *et al.*, 2019). Ground-truthing is representative of the area when it accurately captures the heterogeneity of the ecosystem. ‘Spatially-balanced’ sampling ensures areas are not over or under sampled and is a more efficient and accurate representation of the ecosystem than random sampling (Stevens Jr. and Olsen, 2004; Christianson *et al.*, 2016). Representative ground-truthing is important because abiotic processes alone have been found to poorly predict biodiversity patterns, likely due to the role of ecological processes (Stevens Jr. and Olsen, 2004; Fraschetti *et al.*, 2008).

For community data, a common method of modelling the ground-truthing data against the environmental data is through a type of supervised classification, where the biological data are first organized into different classes/communities before building the model (Ferrier and Guisan, 2006; Brown *et al.*, 2011). Under the assumption that the communities are heavily influenced by the abiotic environment, prediction of the communities present in areas that have not been directly measured through ground-truthing can be done. These predictions use the relationships

revealed from the model that was trained on ground-truthing and the environmental variable maps to create spatially-continuous predicted benthic community maps (Brown *et al.*, 2011).

1.2.2. Uses of Benthic Community Maps

Benthic community maps are important for properly managing marine ecosystems because they help provide spatially-explicit accounts of the distribution of marine communities and provide information on the relationships between abiotic variables and biotic communities (Fraschetti *et al.*, 2008). These maps can be used as biological baselines, which are studies that collect information on the biota in an area in its current conditions. They are needed to understand ecosystems and predict future changes, both natural and anthropogenically driven (Fraschetti *et al.*, 2011).

1.3.3. The Issue with Current Practices

Unfortunately, most community maps are built on only one sampling event because many benthic ecosystems are expensive and time-consuming to study, partly due to the vast area of the ocean that still requires mapping (Mayer *et al.*, 2018; Wölfel *et al.*, 2019). Very broad resolution maps describing general seafloor shape can be collected regularly through satellites; however, the average achievable resolution of the seafloor using satellite technology is 8 km, meaning most relevant details are lost (Mayer *et al.*, 2018). Satellite information also does not present information on communities, and it is known that the same broad-scale habitat can host substantially different species at different times (Coma *et al.*, 2000; Fraschetti *et al.*, 2008).

Community mapping of benthic environments rarely incorporates a temporal aspect into its construction and even less consider it at the scale of seasonality (Harris and Baker, 2020a). This is despite the fact that it is known that these environments are not temporally static, especially for mobile organisms (McArthur *et al.*, 2010). A few studies have explored temporal

changes in the production of habitat maps but focused on the acoustic repeatability for creating the environmental layers and on an interannual scale (Rattray *et al.*, 2013; Leon *et al.*, 2020). Zajac *et al.* (2020) built predicted sediment maps and collected biological community information seasonally; however, they did not interpolate the biological data to create benthic community maps. They concluded that some epifaunal communities changed seasonally while others exhibited stability. Radke *et al.* (2011) explored seasonality in habitat maps by building summer and winter maps for infauna on a sandy embayment, and they found that species diversity patterns were different in the two seasons due to temporally changing carbon and redox. Without a temporal aspect like seasonality, most benthic maps are simple snapshots of dynamic ecosystems at one point in time. This lack of temporal coverage can lead to improper management and inappropriate use of areas.

1.3. Approach

The aim of this thesis was to investigate the importance of incorporating ecologically relevant temporal coverage (i.e., seasonal) into investigations on the habitat selection of benthic organisms, at both the levels of community and species. The first objective (community-based) was to assess the level of spatio-temporal changes in the communities and the implications in the production of benthic community maps. I predicted that the habitat maps created in each season will present different biological communities occupying areas of Holyrood caused by individual taxon responses to changing environmental conditions. The second objective (species-based) was to investigate the abiotic factors important in the habitat selection of snow crab and how these may change seasonally. I predicted that while some fine-scale factors that are known to be important to snow crab habitat selection (i.e., temperature) will remain important in all seasons,

the importance of some variables may change seasonally based on seasonal mating requirements or food input.

To explore these objectives, ground-truthing of benthic communities was collected in Holyrood Bay, Conception Bay, Newfoundland and Labrador during four seasons. July is used as a representation of the 'summer' season, November to represent 'fall', February as 'winter', and April as 'spring'. For objective one, four community maps were created using supervised classification methods to create season-specific maps, the communities presented in each map were then qualitatively compared. For objective two, a generalized additive model was created for the presence/absence of snow crab to quantify the importance of the abiotic predictors on snow crab presence.

1.4. Study Site

I conducted my study in the 23.12 km² fjord Holyrood Bay, which lies at the head of Conception Bay (Figure 1). Holyrood Bay reaches depths of 107 m. The average surface water temperature in Holyrood Bay was 4.9°C, with an average high of 14.8°C in August and an average low of -1.3°C in March from 1991 to 2021 (Climate-Data.org, 2022). The average annual precipitation is 1355 mm, with a low of 82 mm in June and a high of 145 mm in December (Climate-Data.org, 2022).

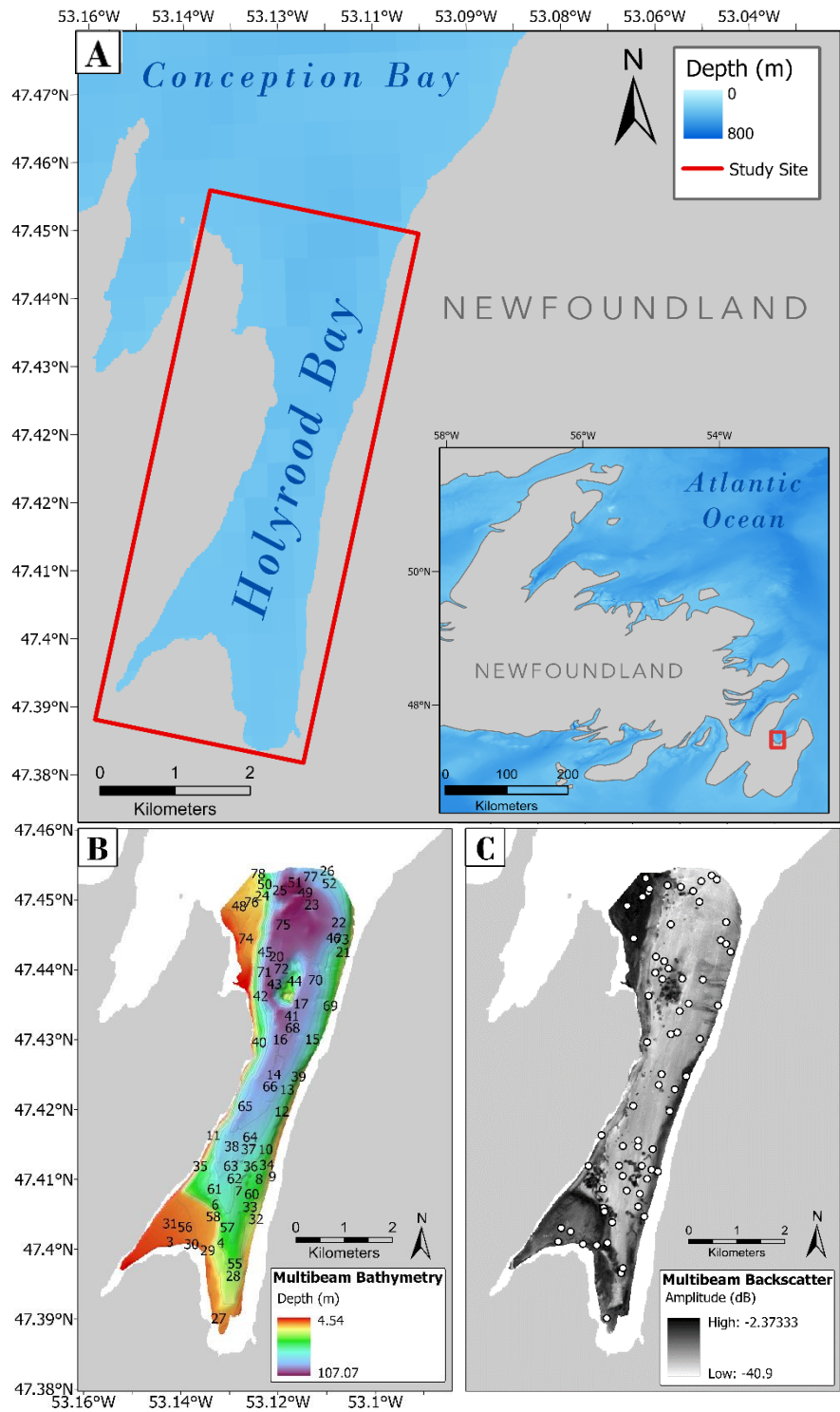


Figure 1. Maps of the study site Holyrood Bay, (A) Denoting its geographical location at the head of Conception Bay in Newfoundland and Labrador, Canada. The red rectangle denotes the extent of the study site. (B-C) The primary continuous data layers used as explanatory variables, bathymetry and backscatter. Numbers on the bathymetry (and associated circles on the backscatter) denote the ground-truthing sites.

Conception Bay is a large (1295 km^2) water body on the southeast shore of the island of Newfoundland, Canada, with a maximum depth of 300 m (de Young and Sanderson, 1995). This bay opens up to the Atlantic Ocean, and is the location of fishing activities targeting American lobster, snow crab, and capelin (*Mallotus villosus*) (Fisheries and Oceans Canada, 2021b, 2021c, 2021d). Conception Bay has weak currents that generally follow a counter-clockwise pattern. Sea ice is a driver of the cold intermediate layer present under the thermocline, which is a primary feature of the benthic thermal regime in this area (Cyr and Galbraith, 2021).

Cold ocean systems at high latitudes, such as that of Conception Bay have strong seasonal variations, which in turn regulate productivity of the ecosystem as a result of phytoplankton blooms (Pomeroy *et al.*, 1991; Shindell *et al.*, 1999). De Young and Sanderson (1995) found that bottom temperatures in Conception Bay were lower, and salinity was higher in the fall than the spring from 1988 to 1991, despite fall months exhibiting increased surface temperatures from the summer. However, the dramatic seasonal changes in sub-Arctic ecosystems can restrict sampling to mainly summer studies (Tian *et al.*, 2003), which has led to the seasonal patterns not being fully understood. For example, winter sampling in Holyrood can be difficult to obtain when pack ice is present.

Snow crab landings in inner and outer Conception Bay have decreased from 1966 metric tons in 2015 to 400 metric tons in 2019, associated with the lowest fishery catch per unit effort in two decades (Fisheries and Oceans Canada, 2016, 2019b). Although the population of large males has increased since this low (573 metric tons in 2021), it is difficult to predict how snow crabs will respond to future anthropogenic and environmental changes (Fisheries and Oceans Canada, 2021d, 2022). Conception Bay is managed by Fisheries and Oceans Canada (DFO) in

crab management unit “6B” (Fisheries and Oceans Canada, 2022). DFO imposes conservation and fishing regulations like catch limits and bycatch measures.

2. Materials and Methods

2.1. Acoustic Survey

Bathymetry and backscatter were collected using a Kongsberg EM710 MBES aboard the vessel *Atlanticat* in 2010. Bathymetry and backscatter data were processed using ‘CARIS HIPS and SIPS v7’ and were exported as 2-m raster grids with UTM projection 22N (Figure 1B,C).

2.2. Environmental Variables

Seabed topography and substrate characteristics are important determinants of (or are indirect surrogates for) the distribution of benthic communities, so a wide variety of terrain attributes were explored as potential community predictors. Seabed topography was described using terrain attributes considered to be potential predictors of benthic communities, which were derived from the bathymetry data. The resolution of the raw environmental layers was reduced to 10 m using the mean cell values to reduce the effect of any potential fine-scale seabed topography changes since acoustic data collection. Seven variables were calculated using the ‘TASSE’ toolbox in ArcGIS Pro (Lecours *et al.*, 2016): aspect, eastness, northness, local mean, local standard deviation, relative difference from the mean value (RDMV), and slope (Table 1 and Appendix A). Lecours *et al.* (2017) found that these variables captured over 70% of the variability in simulated topographic surfaces. Additionally, six other variables were derived from the bathymetry using the ‘*Benthic Terrain Modeler 3.0*’ toolbox (Walbridge *et al.*, 2018) in ArcGIS Pro: bathymetric position index (BPI), surface area to planar area, vector ruggedness measure, curvature, planform curvature, and profile curvature. Derived variables were calculated at multiple spatial scales, recognizing that species are influenced by different scales of terrain

morphology (Levin, 1992; Lecours *et al.*, 2015). The multi-scale approach ‘calculate-average’ was used by calculating a derivative then averaging the results across varying window sizes (Misiuk *et al.*, 2021). Scales were calculated at a gradually increasing range of window sizes to encompass a range of finer-scale and broader-scale features (3 x 3 grid cells, 5 x 5 grid cells, 9 x 9 grid cells, 11 x 11 grid cells, 15 x 15 grid cells, 25 x 25 grid cells), and can be viewed in Table 1 and Appendix A. A few scales were not used for some rasters based on further inspection of the rasters (e.g., 25 grid cells x 25 grid cells for curvature).

Table 1. List of variables used in the analyses, the packages used for their calculation, the range of scales, and a brief description.

Variable	Derivative of	Package	Scales (grid cells)	Description
Raw Bathymetry	NA	NA	1x1	A measurement of seafloor depth, in metres
Raw Backscatter	NA	NA	1x1	The intensity of sound that is reflected by the seafloor, related to seafloor hardness and roughness
Aspect	Bathymetry	TASSE Toolbox in ArcGIS	3x3, 5x5, 9x9, 11x11, 15x15, 25x25	The physical orientation of a slope. It can be further divided into eastness and northness.
Eastness	Bathymetry	TASSE Toolbox in ArcGIS	3x3, 5x5, 9x9, 11x11, 15x15, 25x25	Deviation of the slope’s orientation from true east.
Northness	Bathymetry	TASSE Toolbox in ArcGIS	3x3, 5x5, 9x9, 11x11, 15x15, 25x25	Deviation of the slope’s orientation from true north.

Local Mean	Bathymetry	TASSE Toolbox in ArcGIS	3x3, 5x5, 9x9, 11x11, 15x15, 25x25	A measure of depth. Often more reliable than bathymetry because it filters out noise (Lecours <i>et al.</i> , 2017).
Local Standard Deviation	Bathymetry	TASSE Toolbox in ArcGIS	3x3, 5x5, 9x9, 11x11, 15x15, 25x25	A measure of terrain variability derived from the variation in depth values. A standard deviation of 0 indicates all depths in the window are the same.
Relative Difference from the Mean Value	Bathymetry	TASSE Toolbox in ArcGIS	3x3, 5x5, 9x9, 11x11, 15x15, 25x25	A unitless measure of local topographic position, revealing peaks and depressions.
Slope	Bathymetry	TASSE Toolbox in ArcGIS	3x3, 5x5, 9x9, 11x11, 15x15, 25x25	The steepness of the seafloor using Horn's (1981) algorithm.
Bathymetric Position Index	Bathymetry	BTM Toolbox in ArcGIS	1-5*, 1-9, 1-11, 1- 21, 1-25, 1-40, 20- 50, 15-60, 20-70, 15-80, 20-80, 20- 100	The depth of a referenced location in relation to its surroundings (Wilson <i>et al.</i> , 2007).
Surface Area to Planar Area Ratio	Bathymetry	BTM Toolbox in ArcGIS	3x3, 9x9, 15x15, 21x21	A measure of rugosity, calculated by dividing the contoured surface of a cell by the cell's area (Jenness, 2004).
Vector Ruggedness Measure	Bathymetry	BTM Toolbox in ArcGIS	3x3, 9x9, 21x21, 25x25	A dimensionless measure of terrain roughness, with values ranging from 0 and 1. A value of 0 indicates no variation between neighbouring cells (Hobson, 1972).

Curvature	Bathymetry	SpatialAnalyst Toolbox in ArcGIS	3x3, 9x9, 15x15, 21x21	A second derivative of bathymetry. It can be divided into planform curvature and profile curvature (Zevenbergen and Thorne, 1987).
Planform Curvature	Bathymetry	SpatialAnalyst Toolbox in ArcGIS	3x3, 9x9, 15x15, 21x21	Perpendicular to the original slope, can reveal patterns of flow.
Profile Curvature	Bathymetry	SpatialAnalyst Toolbox in ArcGIS	3x3, 9x9, 15x15, 21x21	Parallel to the original slope, reveals areas of maximum or minimum slope.
GLCM-Contrast	Backscatter	GLCMBasures in R	3x3, 5x5, 9x9, 11x11, 15x15, 21x21	The difference in grey level between adjacent pixels weighted exponentially by the distance from the diagonal of the matrix. a.k.a. sum of squares variance.
GLCM-Dissimilarity	Backscatter	GLCMBasures in R	3x3, 5x5, 9x9, 11x11, 15x15, 21x21	The difference in grey level between adjacent pixels weighted linearly by the distance from the diagonal of the matrix.
GLCM-Homogeneity	Backscatter	GLCMBasures in R	3x3, 5x5, 9x9, 11x11, 15x15, 21x21	The amount of local similarity using the inverse of the contrast weight, values decrease exponentially from the diagonal.
GLCM-Angular Second Moment	Backscatter	GLCMBasures in R	3x3, 5x5, 9x9, 11x11, 15x15, 21x21	A measure of the orderliness of grey levels weighted by the probability value of a

				given grey level outcome as a metric for commonness.
GLCM-Entropy	Backscatter	GLCMTextrures in R	3x3, 5x5, 9x9, 11x11, 15x15, 21x21	The level of spatial organization weighted using the negative probability value. Large values indicating less order (Blondel, 1996).
GLCM-Mean	Backscatter	GLCMTextrures in R	3x3, 5x5, 9x9, 11x11, 15x15, 21x21	Mean of the pixel values weighted by the frequency of the occurrence of the pixel and a specific neighbouring pixel value.
GLCM-Variance	Backscatter	GLCMTextrures in R	3x3, 5x5, 9x9, 11x11, 15x15, 21x21	Variance of the pixel values. Uses combinations of neighbouring pixels to calculate the dispersion around the GLCM mean.
GLCM-Correlation	Backscatter	GLCMTextrures in R	3x3, 5x5, 9x9, 11x11, 15x15, 21x21	The predictability and linearity of neighbouring pixels.
Temperature	NA	Empirical Bayesian Kriging Regression Prediction in ArcGIS	NA	Averaged temperature of a transects in-situ measurements, in degrees Celsius.
Conductivity	NA	Empirical Bayesian Kriging Regression Prediction in ArcGIS	NA	The ability of the water to conduct electricity in milliSiemens per centimeter, calculated by averaging of a

				transects in-situ measurements.
Salinity	Conductivity	Empirical Bayesian Kriging Regression Prediction in ArcGIS	NA	Concentration of salt in the water in practical salinity unit, calculated by averaging a transects in-situ measurements.
Substrate 1	NA	NA	NA	The substrate that covered the most area on a transect, through visual inspection.
Substrate 2	NA	NA	NA	The substrate that covered the second most area on a transect, through visual inspection.

*Inner Diameter- Outer Diameter

Additionally, variables were derived from the backscatter to describe substrate characteristics of the seafloor as potential predictors of benthic communities. A multi-scale (3 x 3 grid cells, 5 x 5 grid cells, 9 x 9 grid cells, 11 x 11 grid cells, 15 x 15 grid cells) textural analysis using grey level co-occurrence matrices (GLCM) was conducted using the ‘*GLCMTextures*’ package in R (Ilich, 2020). GLCMs use the average spatial relationship of pixels to provide a measure of variation in image texture (Blondel, 1996). Eight textural variables were then derived from the GLCM: contrast, dissimilarity, homogeneity, angular second moment, entropy, mean, variance, and correlation (Hall-Beyer, 2017). Definitions and rasters of each variable can be found in Table 1 and Appendix A, respectively. Thirty-two grey levels were used, which is considered a favourable compromise between detection of textures and computational speed (Blondel 1996; Huvenne *et al.* 2002; Leon *et al.* 2020).

Data on temperature ($^{\circ}\text{C}$), conductivity (mS/cm), and salinity (psu) were collected at all 78 sample sites (Sampling protocol described in section 2.3). A Star Oddi DST CTD was used to collect data for two-minute drifts at each site, at an interval of two seconds. Average values of each drift were assigned to the midpoint location of that drift. Malfunctions with the CTD on one day in both winter and spring caused loss of conductivity and salinity data, resulting in 52 data points for these variables. To ensure seasons remained comparable, one day of data from the summer and spring were randomly selected and removed. Empirical Bayesian Kriging Regression Prediction from the '*Geostatistical Analyst*' toolbox (Johnston *et al.*, 2001) in ArcGIS Pro was employed with the raw bathymetry file as the explanatory variable to estimate spatially-continuous maps for temperature, conductivity, and salinity. A smoothed circular neighbourhood with the default smoothing factor of 0.2 was used to reduce the jaggedness of the prediction rasters.

2.3. Ground-Truthing

Ground-truth sampling occurred across four seasons in a single year: July 2020 (summer), October 2020 (fall), January 2021 (winter), and April 2021 (spring). Ground-truthing sites were selected using bathymetry and backscatter layers in a spatially-balanced design. This selects sites within divided ranges of an important environmental variable to ensure the survey area encompassed a broad range of seabed conditions (Strong, 2020). To do this, both layers were segmented into four equal classes (Bathymetry: <27 m, 27-54 m, 55-81 m, >82 m; Backscatter: >-12 dB, -13-(-22 dB), -23-(-32 dB), >-33 dB). Four classes were chosen because it allowed each class to have multiple sites in each sample day, while still being large enough ranges to allow a high level of randomness in site selection. These classes were used in the package '*spsurvey*' (Kincaid *et al.*, 2019) in R 3.6.1 to create a generalized random tessellation

stratified (GRTS) sampling design (Stevens Jr. and Olsen, 2004). This design selected thirteen points from each layer for three sampling days, for a total of 78 ground-truthing sites (26 sites x 3 days). Each season utilized the same 78 sites.

The benthic environment was characterized at each site using underwater video onboard the *D. Cartwright* research vessel. Underwater video was collected using a Sony FDR-X3000 in an ‘in-house’ built housing and frame for the first day of the summer season sampling. This camera had 4K resolution, 30FPS, a 3500 lumen light, and 10 cm scaling lasers. Due to camera malfunction, an alternate camera was used for the remainder of the data collection. The alternate camera was a DeepTrekker DTPod; with a resolution of 1920 x 1080 HD, 30 FPS, a dimmable light with 1000 Lumens, and 2.5 cm scaling lasers. An analysis of similarities (ANOSIM) was conducted between the three sample days in the summer, the first day with the Sony camera and the last two with the DeepTrekker to ensure the change of camera did not cause significant differences in the data collected ($R = -0.037$, $p=0.964$). At each ground-truthing site, the camera (and mounted CTD) was lowered to the seabed for a 2-minute drift. Video was recorded with the camera facing downward while manually held directly above the seabed based on a live video feed. Data from each transect was averaged and aggregated to a single point location (sample site) at the midpoint of the drift. This was performed because precise locational data of the camera was not available and locational inaccuracy tends to influence finer data resolution more than broader data (Hanberry, 2013).

2.4. Video Annotation

Underwater videos were annotated using the Monterey Bay Aquarium Research Institute Video Annotation and Reference System software (VARS). Primary and secondary substrate classes were recorded for each site (Rooper and Zimmermann, 2007). Six different substrate

classes were distinguished in the video: fine sediment, gravel mix, boulders, rhodolith bed, algae mix, and shell hash. Algae mix was considered a 'substrate type' when it obstructed the view of the substrate below. Visible megabenthic organisms larger than 2 cm were identified to the lowest taxonomic level possible and were used to construct a species catalogue (*Appendix B*) (Howell *et al.*, 2019). Since no biological samples were taken to assist in species identification, morphospecies were used when precise identification was not possible. Species counts were converted to densities by dividing each count by the transect area, which was calculated using the lasers and GPS coordinates. Ten sites were removed prior to analyses because they landed outside of the environmental raster boundaries in at least one season. A Michaelis-Menton species accumulation curve was also created for each season to ensure the study area was adequately sampled.

2.5. Community Clustering

Extremely rare species (< 5 observations) and sparsely populated sites (< 3 organisms) were removed from analyses not yet conducted to reduce difficulties in future predictions. Prior to clustering, the data was transformed using a Hellinger transformation because it gives low weights to rare species (Legendre and Gallagher, 2001). Communities were then identified using Unweighted Pair-Group Method with Arithmetic Averages (UPGMA) clustering. UPGMA is an unsupervised agglomerative hierarchical clustering method that uses average linkage and assumes that each cluster accurately represents a sample of the larger population (Legendre and Legendre, 2012). This is a common method to classify samples based on pairwise similarities in ecology (e.g., species composition) (Legendre and Legendre, 2012). The appropriate number of clusters was selected based on silhouette widths, by selecting the number of clusters that had the highest silhouette width while still ensuring that clusters had enough sites to accurately represent

the communities. Silhouette widths aid in determining the optimal number of clusters by measuring the degree of membership of all points, with large values meaning points are clustered well (Borcard *et al.*, 2018). An ANOSIM (Analysis of Similarities) was performed on the clusters within each season to ensure they were statistically different from one another. SIMPER (Similarity Percentages) and IndVal (Indicator Value Index) analyses were used to compare the different clusters within each season (Results in *Appendix C*). Clusters were manually assigned colour identifiers guided by the dominant species in each cluster.

Ordinations were conducted to further describe the changes across seasons by representing the seasonal communities in a more continuous way. This was conducted because discrete communities can often be an over-simplification of ecosystems since species do not always move together (Brown *et al.*, 2011). A two-dimensional, species-based, non-metric multidimensional scaling (NMDS) was performed for individual seasons on the square-root transformed species densities at each site. NMDS is a rank-based approach that produces an ordination based on a dissimilarity matrix (Legendre and Legendre, 2012). A species-based NMDS places species close in distance when they commonly are found together.

2.6. Community Mapping

A random forest model was used in each season to identify which abiotic variables influenced the communities' spatial patterns and build spatially-continuous prediction maps. Random forest is a type of ensemble-based machine learning that can be used to solve classification problems by using many uncorrelated decision trees in a majority vote (Hastie *et al.*, 2009). To ensure trees are uncorrelated, it uses 'bagging' and feature randomness (Breiman, 2001). 'Bagging' entails randomly sampling training data from the original dataset with replacement, so that each decision tree is a random iteration of all possible values (Breiman,

2001). Feature randomness mean that each decision tree uses only a random subset of predictor features. Random Forest is a popular classification method used in benthic habitat mapping and often out-performs other methods (Hasan *et al.*, 2012; Leon *et al.*, 2020).

Feature reduction was completed for the model in each season using the '*Boruta*' package (Kursa *et al.*, 2010) in R. Feature reduction is a robust and repeatable technique to reduce the number of predictor variables used in a statistical model (Chen *et al.*, 2020), which has several desirable outcomes for community mapping. It identifies the most important and uncorrelated variables at the most relevant scales, reducing model overfitting (Salam *et al.*, 2021). A Boruta wrapper was used because it identifies variables that impact communities and decreases variability between random forest runs (Millard and Richardson, 2015; Kumar and Shaikh, 2017). The wrapper creates new variables ('shadow features') by randomly shuffling the values within each variable. Original variables were deemed unimportant if they did not perform better than their shadow features in at least 1% of the iterations (Kursa *et al.*, 2010). Following this, Spearman's rank-order correlation was used to assess pairwise collinearity between variables. If pairs of variables had correlation $|r| > 0.80$, the variables with the lesser impact on the model's accuracy were removed. Previous studies have used 0.8 as a threshold since Random Forest can keep performance integrity with some degree of collinearity (Porskamp *et al.*, 2018).

Sites were classified using random forest with 10,000 trees, the number of variables at each split was selected for each model independently using 'leave-one-out' cross-validation. 'Leave-one-out' cross-validation is an effective method for small sample sizes because it does not require withholding a large portion of the dataset (Legendre and Legendre, 2012). This method removes a single sample, and the model is trained on all other samples (Webb *et al.*, 2011). The

value of the withheld data point is predicted, and this is repeated n times, corresponding to the total number of samples, to produce error matrices.

The kappa coefficient and overall accuracy were calculated to quantify the strength of the predictive ability of the model. The kappa coefficient measures agreement between the classification and the reference data, and accounts for chance agreement (Cohen, 1960). Overall accuracy measures the total number of correctly classified sites. Predictor variable importance was assessed by the mean decrease in accuracy of the model when such variable was removed. The random forest model was then used to predict the cluster values for the rest of the continuous dataset to produce spatially-continuous maps.

2.7. Modelling Snow Crab Presence

To investigate the important predictors of small-scale habitat selection of the commercially important species, snow crab, and how these relationships changed seasonally, a binomial generalized additive model (GAM) was employed using the '*mcgv*' package in R. Generalized additive models are commonly used models to explain non-linear relationships by applying smoothing factors to the co-variates (Wood, 2017).

In this model, the presence and absence of snow crab at each site (265 sites with all seasons merged) was modelled against the derived variables (covariates) mentioned in the previous section. For each covariate, a global smoother and season-specific smoothers were produced; the latter was created using 'by-factor smooth' interactions with season. Season-specific smoothers allowed the relationship between the covariates and snow crab presence to differ between seasons (Pedersen *et al.*, 2019). First-order penalties were applied to smoothers with the 'by-variable' interactions to reduce collinearity between the global smoothers and the season-specific smoothers (Pedersen *et al.*, 2019). Restricted maximum likelihood was used as

the smoothness selection method because it has shown to lead to unbiased predictions of the model coefficients and smoothing parameters (Wood, 2011).

A model diagnostic check was performed to ensure that no assumptions of the model were violated. The '*DHARMA*' package (Hartig, 2022) was used to conduct residual diagnostics and check for spatial and temporal autocorrelation. The model was also checked for concurvity to ensure over-fitting did not occur. Concurvity occurs when the smoother of one co-variate can be reproduced by one or multiple other covariates (Pedersen *et al.*, 2019). Covariates presenting concurvity were removed from the model until all covariates had a 'worst case' concurvity estimate less than 0.8 (Ross, 2019).

3. Results

3.1. Species Accumulation Curves

Species accumulation curves for each season neared plateau, indicating that the area had been adequately sampled. In total, 61 morphospecies were observed in Holyrood Bay (Figure 2A). The species richness was highest in the spring, with 50 morphospecies observed; this contrasted with 47 morphospecies in fall and winter, and 43 in the summer (Figure 2B). Overall species density was highest in summer and lowest in winter (Table 2). The most commonly observed species was brown psolus sea cucumber, *Psolus phantapus*, despite being present at relatively low densities in the fall and winter. The average transect length was 26.80 m. There was an average of 14 observations of anthropogenic trash per season, which included glass bottles, aluminum cans, rope, a tire, and a plastic bag.

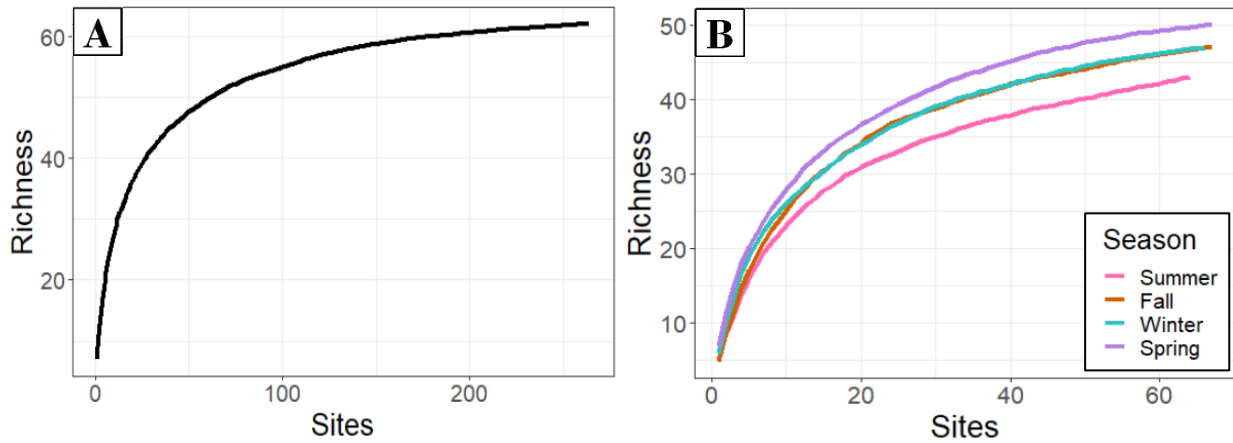


Figure 2. Species accumulation curves for Holyrood Bay sampled from July 2020 to April 2021 for (A) all seasons combined and (B) each season independently.

Table 2. Total density of organisms and individual species densities of taxa of interest, of the sampled sites in Holyrood Bay in all seasons.

	Summer	Fall	Winter	Spring
Organism Density	5.779 m^{-2}	2.242 m^{-2}	0.714 m^{-2}	2.495 m^{-2}
<i>Psolus phantapus</i>	2.955 m^{-2}	0.007 m^{-2}	0.017 m^{-2}	1.606 m^{-2}
<i>Pachycerianthus borealis</i>	0.121 m^{-2}	0.047 m^{-2}	0.118 m^{-2}	0.156 m^{-2}
<i>Ophiuroidea spp.</i>	1.450 m^{-2}	1.182 m^{-2}	0.359 m^{-2}	0.212 m^{-2}
<i>Echinarachnius parma</i>	0.107 m^{-2}	0.006 m^{-2}	0.002 m^{-2}	0.225 m^{-2}
<i>Strongylocentrotus droebachensis</i>	0.518 m^{-2}	0.356 m^{-2}	0.097 m^{-2}	0.133 m^{-2}
<i>Chionoecetes opilio</i>	0.019 m^{-2}	0.010 m^{-2}	0.005 m^{-2}	0.003 m^{-2}

3.2. Community Clusters

The number of communities varied across seasons, with a total of eight different communities identified (Figure 3). Five significantly different communities were observed in the summer and spring, while four were observed in the fall, and two in the winter (Figure 4). The ‘red’ community was dominated by stars and common sand dollars (*Echinarachnius parma*) and the ‘orange’ community was dominated by green sea urchins. These clusters merged in some

seasons to make ‘brown’ which was dominated by stars and green sea urchins. The ‘yellow’ cluster was dominated by brittle stars (*Ophiuroidea* spp.) and the ‘blue’ cluster was dominated by sea cucumber. In some seasons the yellow and blue clusters merged to make the ‘green’ cluster which was dominated by brittle stars and sea cucumbers. The purple cluster was dominated by decapods and the grey cluster was an aggregation of flatfish.

NMDS graphs depicted how morphospecies distances changed throughout the seasons.

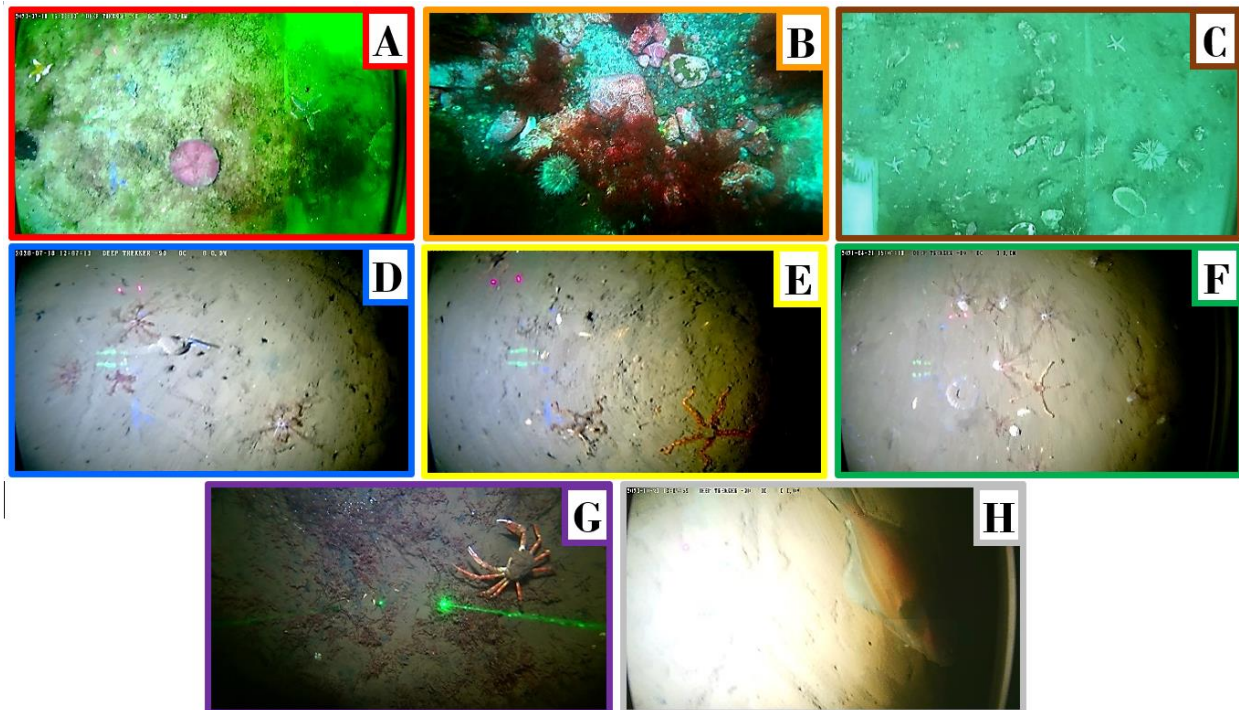


Figure 3. Photos documenting examples of each community observed throughout the seasons, based on Unweighted Pair-Group Method with Arithmetic Averages (UPGMA) hierarchical clustering of Holyrood Bay site observations from July 2020- April 2021. The communities are: (A) star and sand dollar dominated, (B) urchin dominated, (C) star and urchin dominated, (D) sea cucumber dominated, (E) brittle star dominated, (F) sea cucumber and brittle star dominated, (G) decapod dominated, and (H) flatfish dominated.

All season-specific NMDSs had adequate stress levels (< 0.18) at two dimensions and non-metric R^2 values of 0.969 –0.973. Detailed descriptions of seasonal changes in the communities are provided below and depicted in Figure 5.

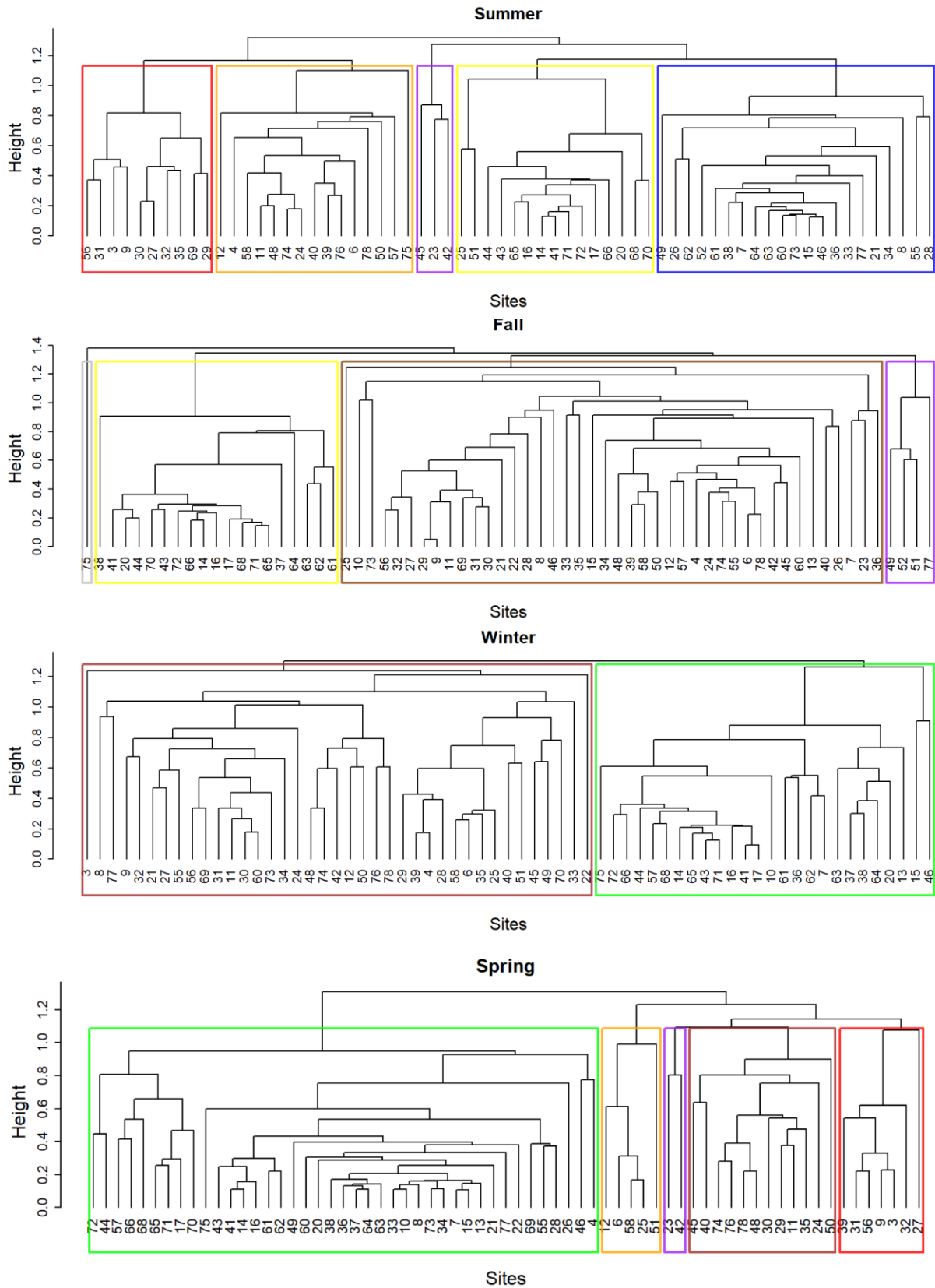


Figure 4. UPGMA hierarchical clustering of all sites across the four seasons in Holyrood Bay. (Summer ($n=64$), Fall ($n=66$), Winter ($n=65$), and Spring ($n=67$)). Coloured rectangles denote the cluster grouping for each season.

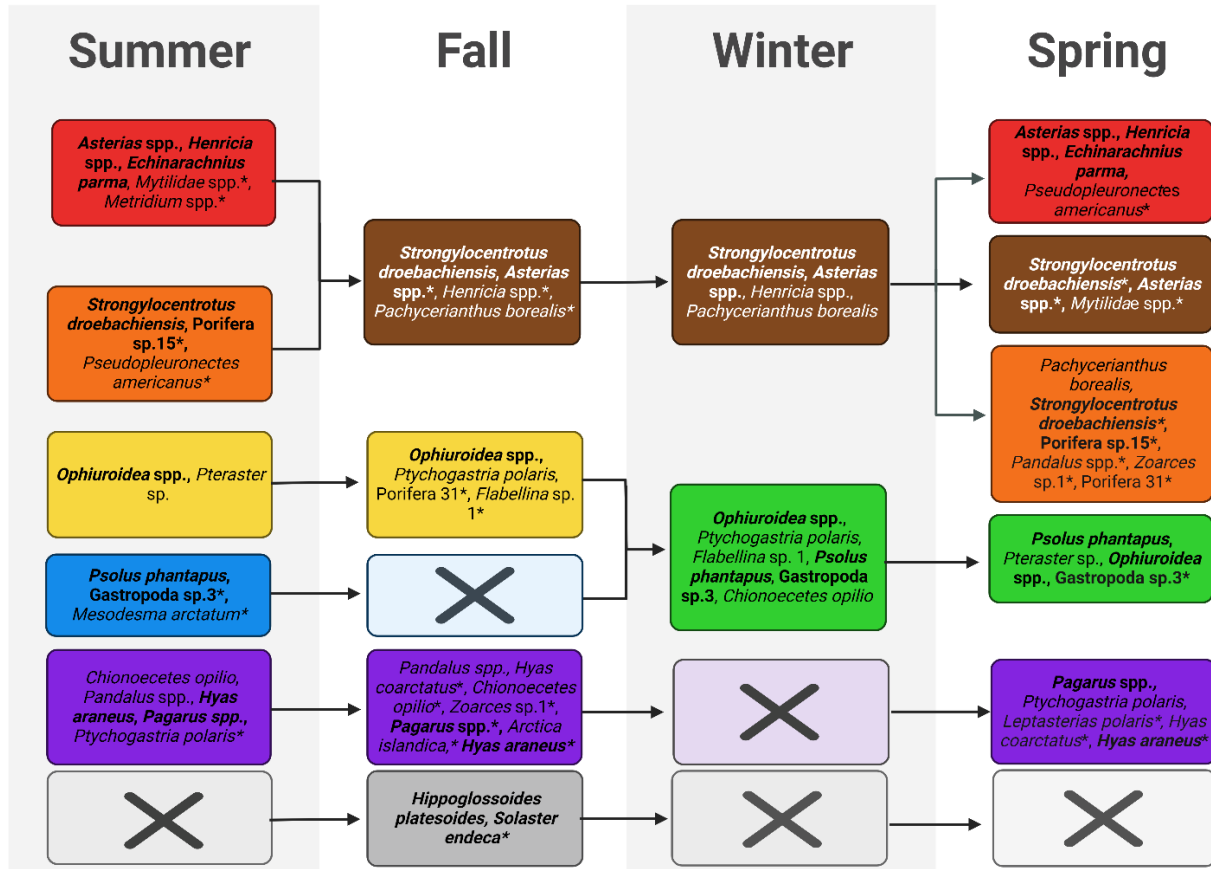
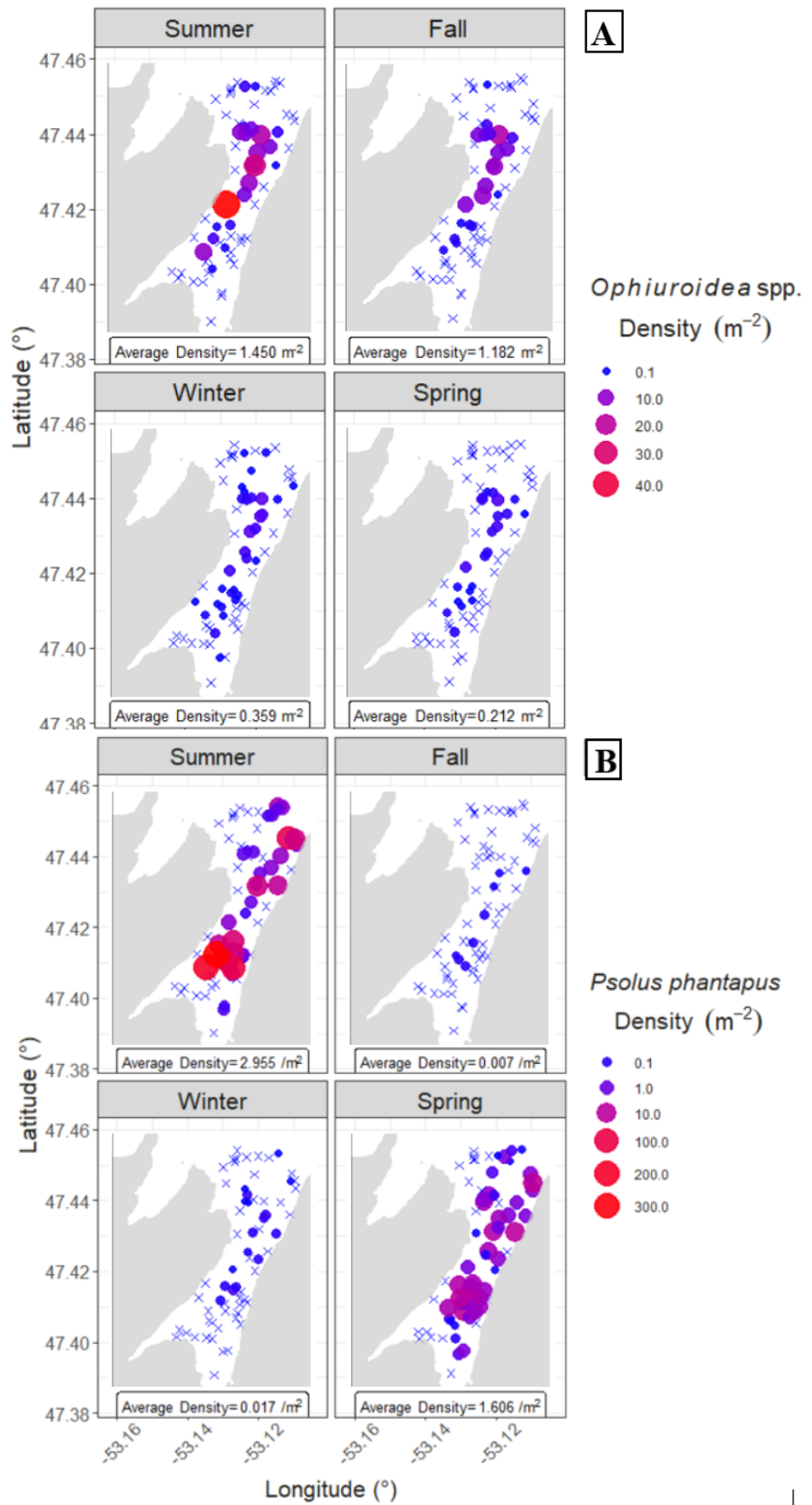
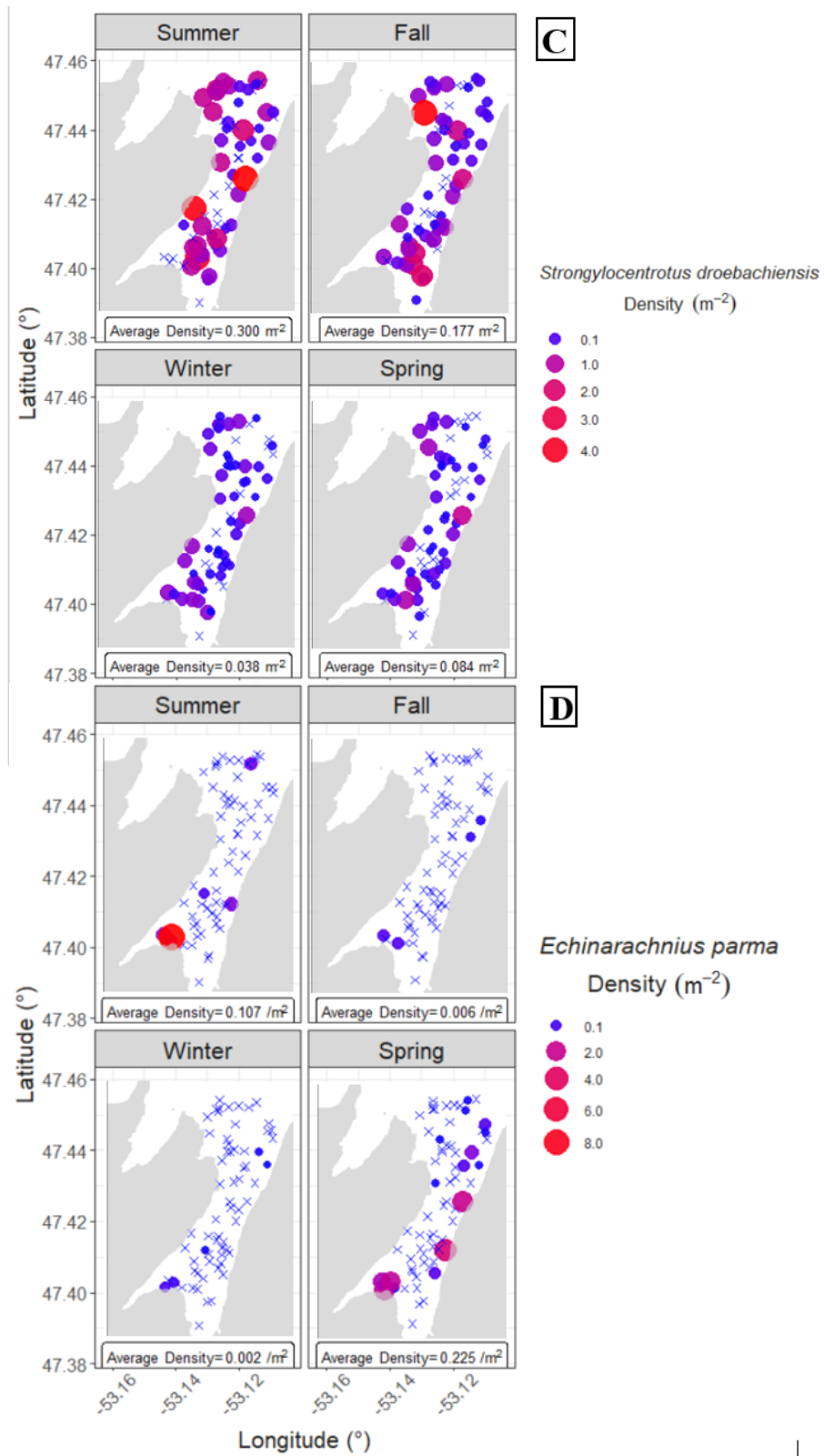


Figure 5. A flow chart depicting the change in important taxa for each cluster throughout the seasons. Bolded taxa are the defining taxa for each cluster. Asterisks denote that a taxa was not an indicator taxa but still significantly contributed to the difference between clusters (using SIMPER). Numbered taxa represent morphospecies names. X's denote when a cluster was not present in a season. (Created with BioRender.com).

3.3. Description of Clusters and their Seasonal Change

The yellow cluster was present in the summer and fall seasons, with high predicted superficialities in fall. The dominant organism in these areas, the brittle star, was observed in all four seasons with high abundances (>1500/season) but were observed at lower densities in the winter and spring (Figure 6A). The yellow cluster had additional indicator taxa; wrinkled stars (*Pteraster* sp.) in the summer and jellies (*Ptychogastria polaris*) in the fall. Both species were the most common within the yellow cluster in all seasons when present but varied in densities and importance.





*Figure 6. Bubble map of (A) Brittle stars (*Ophiuroidea spp.*), (B) Brown psolus (*Psolus phantapus*), (C) Green sea urchin (*Strongylocentrotus droebachiensis*), and (D) Common sand dollar (*Echinarachnius parma*) densities at sample sites in Holyrood Bay in all four seasons. The average density of each morphospecies for the total area observed is at the bottom of each plot. The maps use a UTM projection in zone 22N. X's denote absence of the morphospecies at a site.*

The dominant species of the blue cluster, brown psolus, was most observed species in the summer and spring seasons, with total densities of 2.95 m^{-2} and 1.61 m^{-2} , respectively (Figure 6B). The density of brown psolus declined to near zero ($< 0.01 \text{ m}^{-2}$) in the fall, resulting in the absence of both the blue and the green clusters. This species density remained low in the winter at 0.02 m^{-2} ; however, this cluster had both brittle stars and brown psolus as indicator taxa, therefore was combined with the yellow cluster to create a green cluster.

The green cluster was formed by the merging of the yellow and blue clusters. It was present in the winter and spring and had three important morphospecies: brittle stars, brown psolus, and a species of sea snail (*Gastropoda sp. 3*). When separate, the high densities of brittle stars in the yellow cluster and brown psolus in the blue cluster accounted for 86% of their total difference ($p < 0.001$). This was consistent with the results of the NMDS (Figure 7); with these morphospecies physically closer in the winter and the spring, as opposed to the summer.

The brown cluster was present in the fall, winter, and spring, and was categorized by the presence of blood stars (*Henricia spp.*), common stars (*Asterias spp.*), and green sea urchin (*Strongylocentrotus droebachiensis*). It spanned most of the exterior of the sample area in fall and winter. During the summer and spring, the brown cluster was differentiated into two distinct clusters, red and orange. In the spring, the red cluster, orange cluster, and mixed brown cluster were all present. A driver of the separation of this cluster was the increase in densities and movement of green sea urchins in the summer (Figure 6C). The increase in density of the

common sand dollar, an indicator species for the red cluster, in the summer (0.12 m^{-2}) and spring (0.22 m^{-2}), also significantly contributed to the separation (Figure 6D). This species was not present in any orange sites. Densities of the common sand dollar were low in fall (0.006 m^{-2}) and winter (0.002 m^{-2}), which enabled the merging of the red and orange clusters.

When separate, the main differences between the red and orange clusters were the high density of green sea urchins in the orange cluster and the high densities of common stars, blood stars, and the common sand dollar in the red cluster. These species collectively accounted for 89% of the differences between these two clusters in the summer ($p < 0.001$), and 95% of the difference in the spring ($p < 0.05$). The merging and separation of these species throughout the seasons were evident in the NMDS plots (Figure 7).

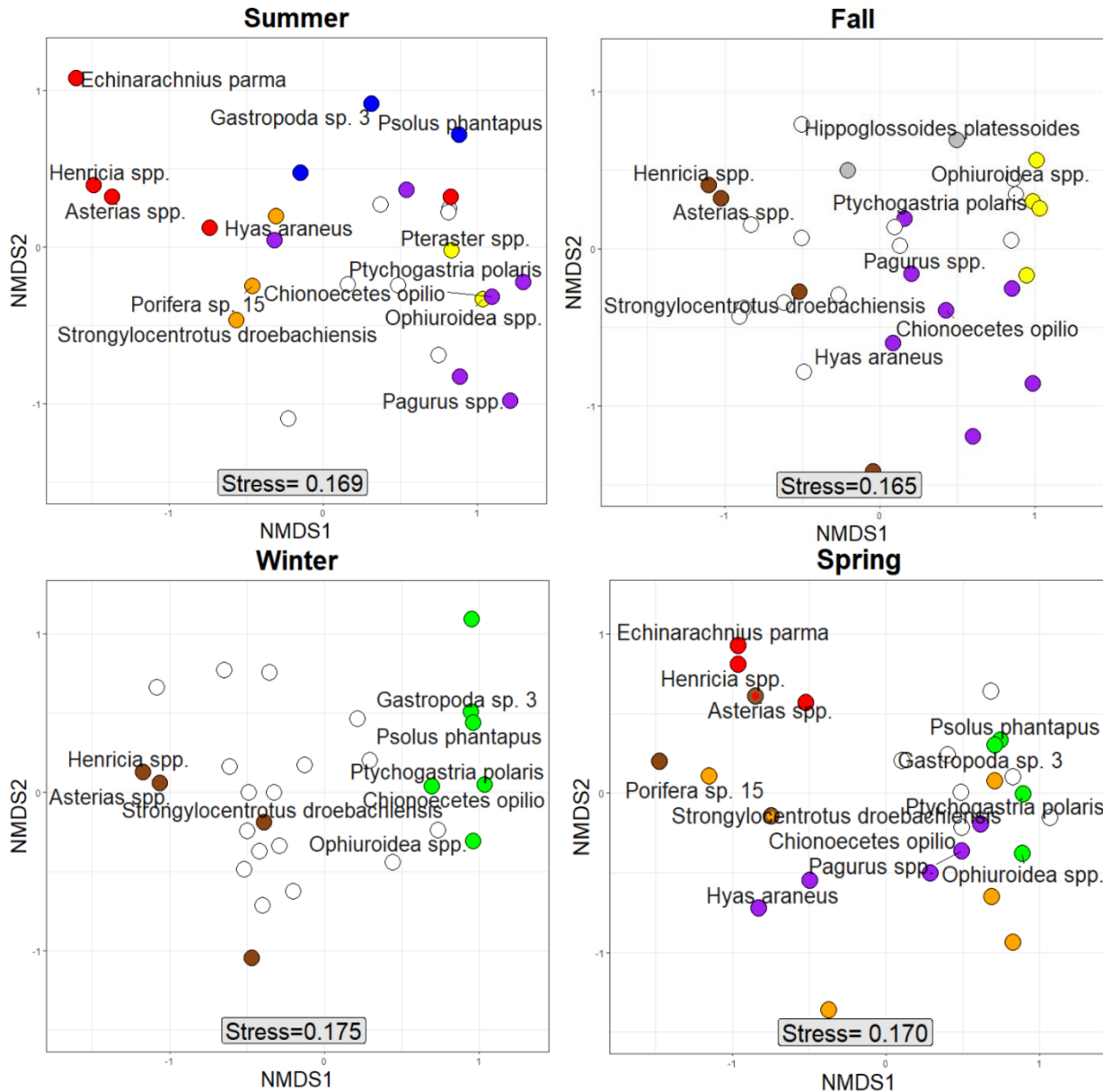


Figure 7. Non-metric dimensional scaling plots of the morphospecies present in each season. The coloured points represent the important taxa for the corresponding cluster in that season, with points with two colours being dominant in two different clusters in a season. Labels represent species that were further discussed in this study.

The rare purple cluster was observed in the summer (n=3), fall (n=4), and spring (n=2).

Hermit crabs (*Pagurus* spp.) and Atlantic toad crab (*Hyas araneus*) were considered the defining morphospecies for this cluster because in all seasons they both were indicator species or

significantly contributed to the difference from other clusters. There were no purple sites in the winter. The presence of the purple cluster was possibly masked by the larger green cluster in the winter. This is apparent because snow crab and jellies were indicator species for the green cluster in the winter, whereas in all other seasons both morphospecies were exclusively associated with the purple cluster.

In the fall, a single site (site 75) had a small but unique aggregation of American plaice (*Hippoglossoides platesoides*), which formed a new cluster. This observation was removed from future analyses.

3.4. Variables Influencing Clusters

In the seasons that the green cluster was present, it had low GLCM mean values, suggesting a soft substrate (Figure 8 A, E, F). The green cluster (brittle star and sea cucumber dominated) was present at areas with low temperatures and depths, with medians of 0.35 °C and 75.05 m, respectively. When the green cluster was separated into the yellow (brittle star dominated) and blue (sea cucumber dominated) clusters in the summer, there were a few abiotic differences. The yellow cluster was found at the deepest sites, with an average median depth of 90 m, while the blue cluster was found in moderate depths of 65 m. The yellow cluster also had lower temperatures, higher salinity and lower BPI than the blue cluster. Both clusters had soft substrata with low GLCM mean values. The main reason for the separation of green into yellow and blue was a reduction in the depth range of high densities of the brown psolus from spring to summer, which reduced the overlap between this species' depth range and that of 'Brittle stars' (Figure 9).

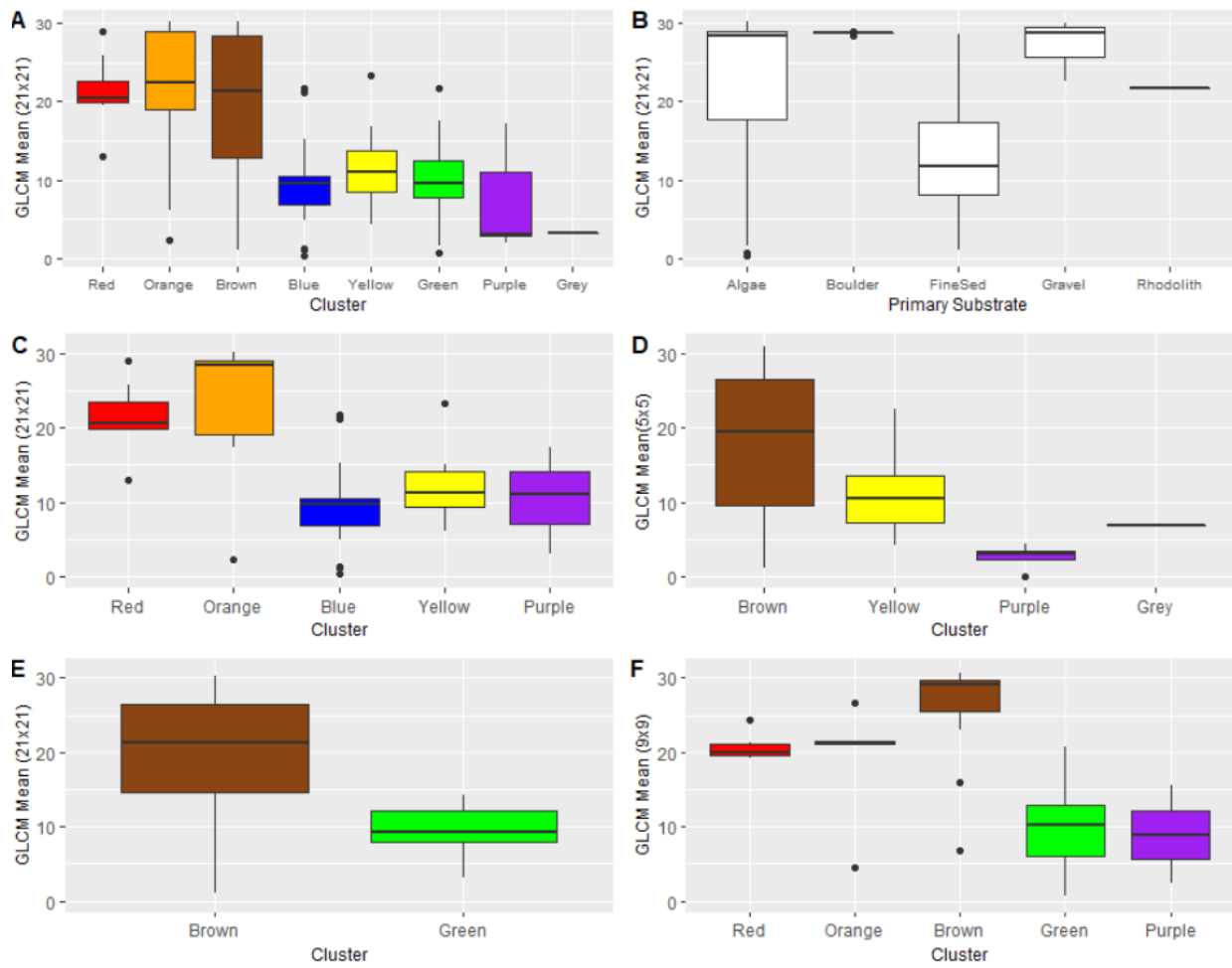


Figure 8. Boxplots of broad-scale GLCM Mean (21x21). (A) Comparing the GLCM Mean values of the different clusters (all seasons merged), and (B) Comparing the GLCM mean value of the primary substrata that were recorded at each site. Algae occurred across a range of seafloor hardness and were only used as a 'substrate' when it obscured all view of the substrate. (D-F) The most important scale of GLCM Mean by cluster for each of the seasons

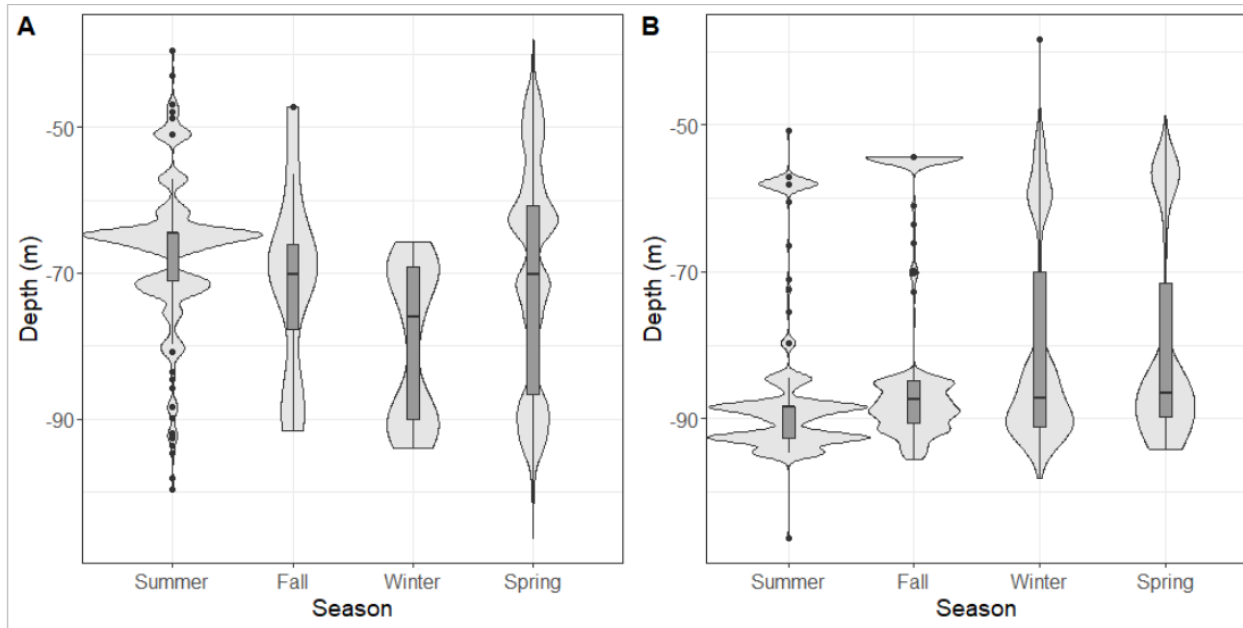


Figure 9. Violin plots of the (A) Brown psolus (*Psolus phantapus*) and (B) Brittle stars (*Ophiuroidea spp.*) abundances by depth, binned by season.

The brown cluster (star and urchin dominated) was created by merging the two shallower clusters, red (star and sand dollar dominated) and orange (urchin dominated), in the fall and winter. When the red and orange clusters were not present, the brown cluster had the shallowest median depths by over 35 m, the hardest seafloor, the highest temperatures, the highest BPI values, and the steepest slopes. The brown cluster also had the largest ranges in variables; likely due to the joining of the red and orange clusters. The substrata most often observed in this cluster were algae, boulders, and gravel.

The orange cluster was found at median depths of 30 and 55 m in the two seasons when it was present (summer and spring). It also had high GLCM mean values and higher than average slopes. The one abiotic variable that changed for this cluster was BPI, having the highest value in the summer and one of the lowest when this cluster returned in the spring (Figure 10 A, D). One

driver in the joining of the red and orange clusters in the fall and winter was the change in observation of green sea urchins from deeper to shallower sites (Figure 11). They were observed at the deepest locations in the summer season (20.4 –106.4 m) and were absent from the five shallowest sites sampled. In the fall and winter, the observed depth distribution of green sea urchin was shallower (18.0 –95.6 m and 14.9 –106.4 m) and encompassed even the shallowest sites. In the spring, only one of the shallowest sample sites did not observe green sea urchins (sea urchin distribution: 17.5 m –100.3 m). The small orange cluster in the spring ($n=5$) could have represented the start of the movement back to deeper depths.

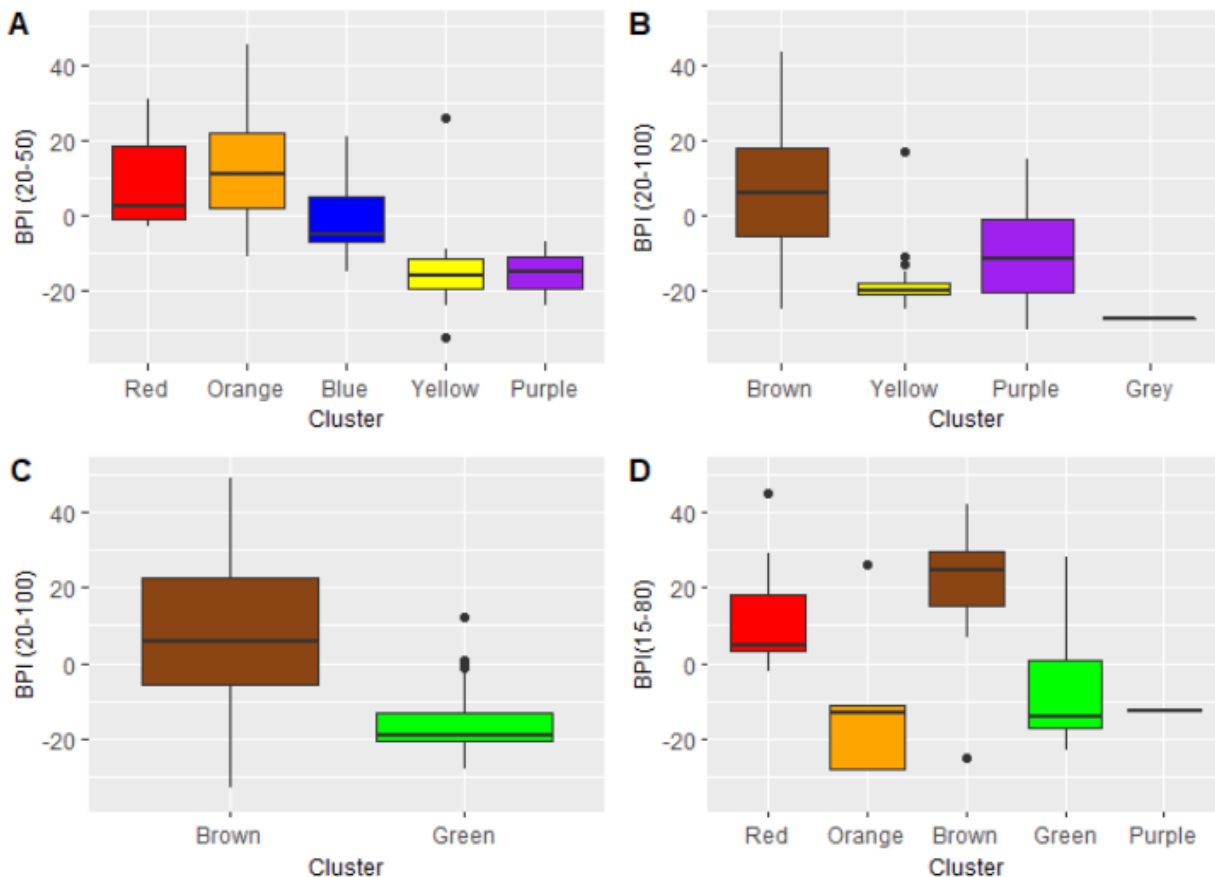


Figure 10. Boxplots of Bathymetric Position Index (BPI) by the cluster for each of the seasons (A) Summer, (B) Fall, (C) Winter, and (D) Spring.

The red cluster occurred at slightly shallower depths than the orange cluster, with a median depth of ~20 m. It had BPI values close to zero, meaning it broadly occurred on flat areas without any peaks or depressions. This cluster was characterized by fine sediment and gravel and had a common presence of algae and few boulders. Despite the red cluster having slightly lower median GLCM mean values (less hard) than the orange cluster, it still was among the highest of all the sites (red GLCM mean median value of > 20). The red cluster consistently had the lowest salinities and highest temperatures.

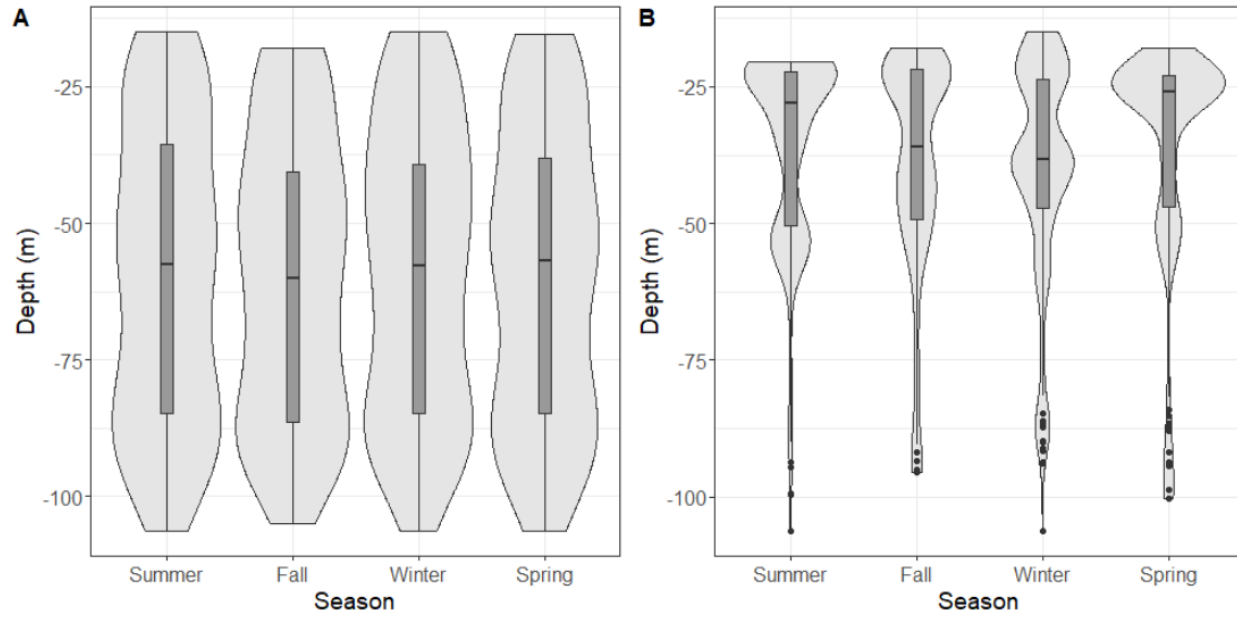


Figure 11. Violin plots and associated boxplots of (A) overall sampling density, and (B) green sea urchin (*Strongylocentrotus droebachiensis*) abundance, by depth.

The purple cluster (decapod dominated) was found in deep areas with low temperatures and high salinities and consisted of mostly mobile species. It was variable in most environmental variables and specific location. Median depths generally remained the same at $90\text{ m} \pm < 2\text{ m}$, but GLCM mean for this cluster varied from 10.98 in the summer to 3.06 in the fall. All the purple

sites observed in the spring were also purple in the summer, however, there was no overlap between the purple sites in the fall.

3.5. Spatially-Continuous Community Maps and Variable Importance

Random forest modelling showed good accuracies when training separate models for each season (75–94%) (Table 3), and spatially-continuous prediction maps showed that each community varied in space across seasons (Figure 12). Many variables were intercorrelated and therefore were removed from the final model. The importance of variables, and therefore the final variables selected for the random forest models, changed across the seasons despite many of these variables being static (Table 3), likely representing the changing requirements of individual species. For example, the directions of terrain slopes did not change between seasons, but directionality was not important in distinguishing between communities in the fall.

Table 3. Model performance statistics and important non-correlated variables and their associated scales for the final random forest models. Variables are listed in their order of importance determined using VarImp.

	Summer	Fall	Winter	Spring
Overall Accuracy	75%	86%	94%	87%
Kappa	0.67	0.70	0.87	0.76
Important Variables	Temperature BPI (20-50) GLCM mean (21x21) Salinity Eastness (25x25) Slope (3x3)	BPI (20-100) Temperature GLCM mean (5x5) Slope (5x5) RDMV (5x5)	Temperature GLCM mean (21x21) BPI (20-100) Northness (25x25) Northness (11x11) Slope (5x5)	GLCM mean (9x9) Eastness (25x25) Temperature BPI (15-80) GLCM Entropy (21x21)

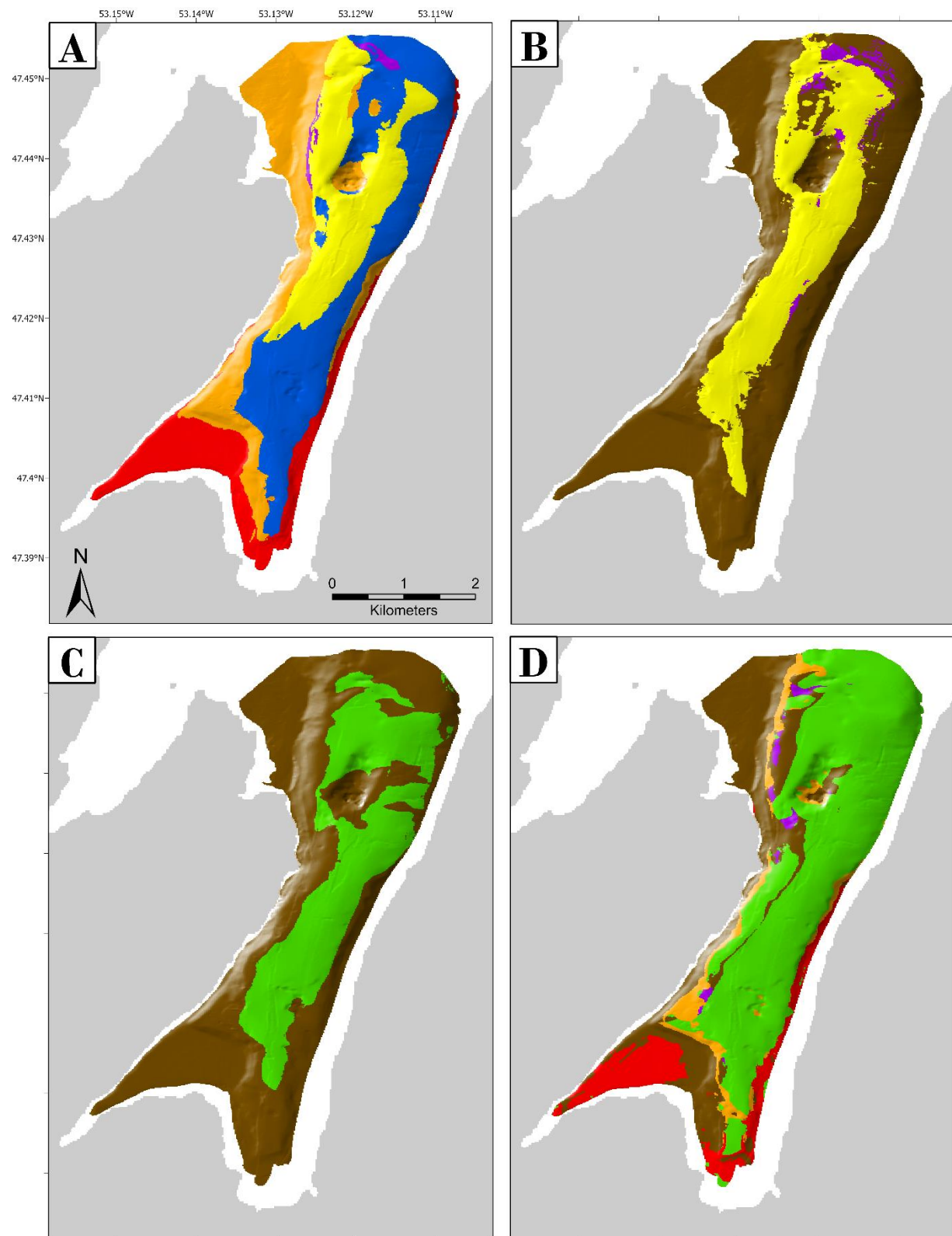


Figure 12. Maps showing the predicted spatial coverage of each community as predicted by the random forest models for all four seasons in Holyrood Bay A) summer 2020, B) fall 2020, C) winter 2021, and D) spring 2021. See Figure 5 for community descriptions.

The only variables that were important for distinguishing clusters in all four final models (corresponding to each season) were GLCM mean, temperature, and BPI. All spatial scales of GLCM mean were important in every season; however, the most important scale varied. GLCM mean is a proxy for the hardness, therefore it provides information on seafloor substrate. Models had > 60% mean decreases in accuracy when this variable was removed. GLCM mean divided the clusters into hard and soft substrata; with red, orange, and brown considered hard (median GLCM mean values of > 15) and blue, yellow, green, purple, and grey considered soft (median GLCM mean values of < 15) (Figure 8A). GLCM mean values for each cluster remained relatively consistent across the seasons, with most species consistently found on their respective substrate. Figure 8B illustrates the close relationship between GLCM mean and *in-situ* primary substrate classifications. Algae and fine sediment had ambiguous relationships with GLCM mean, possibly caused by their ability to occur on top of substrate of varying hardness. It was not possible to observe this with the video data alone; thus, GLCM mean was a better measure of seafloor type and was kept in the model. GLCM mean was also correlated with the raw backscatter, which was removed from the final models because GLCM mean reduced noise and consistently outperformed the raw backscatter.

Temperature was important for differentiating the clusters in every season (Figure 13). Models had a mean degree decrease in accuracy of >90% when temperature was removed. Temperature was correlated with and outperformed mean depth, raw bathymetry, salinity, and conductivity. Spatial patterns of bottom temperatures in Holyrood Bay remained consistent throughout the year, with shallow inland areas being the warmest. However, they varied in magnitude across the seasons; summer had the largest range in temperatures (-1.10 – 9.10°C) and

spring had the smallest ($0.19 - 1.92^{\circ}\text{C}$). In summer, the relationship between temperature and salinity was below the correlation threshold, so both were included in the final model.

BPI was important for distinguishing between the clusters in all seasons. BPI described peaks and depressions. The yellow and purple cluster were consistently found in depressions, while the red and brown cluster were consistently found on peaks (Figure 10). The mean decrease in accuracy when this variable was excluded from the model was $> 60\%$. Multiple scales of BPI were important in the model in each season, thus only the best performing scale was kept.

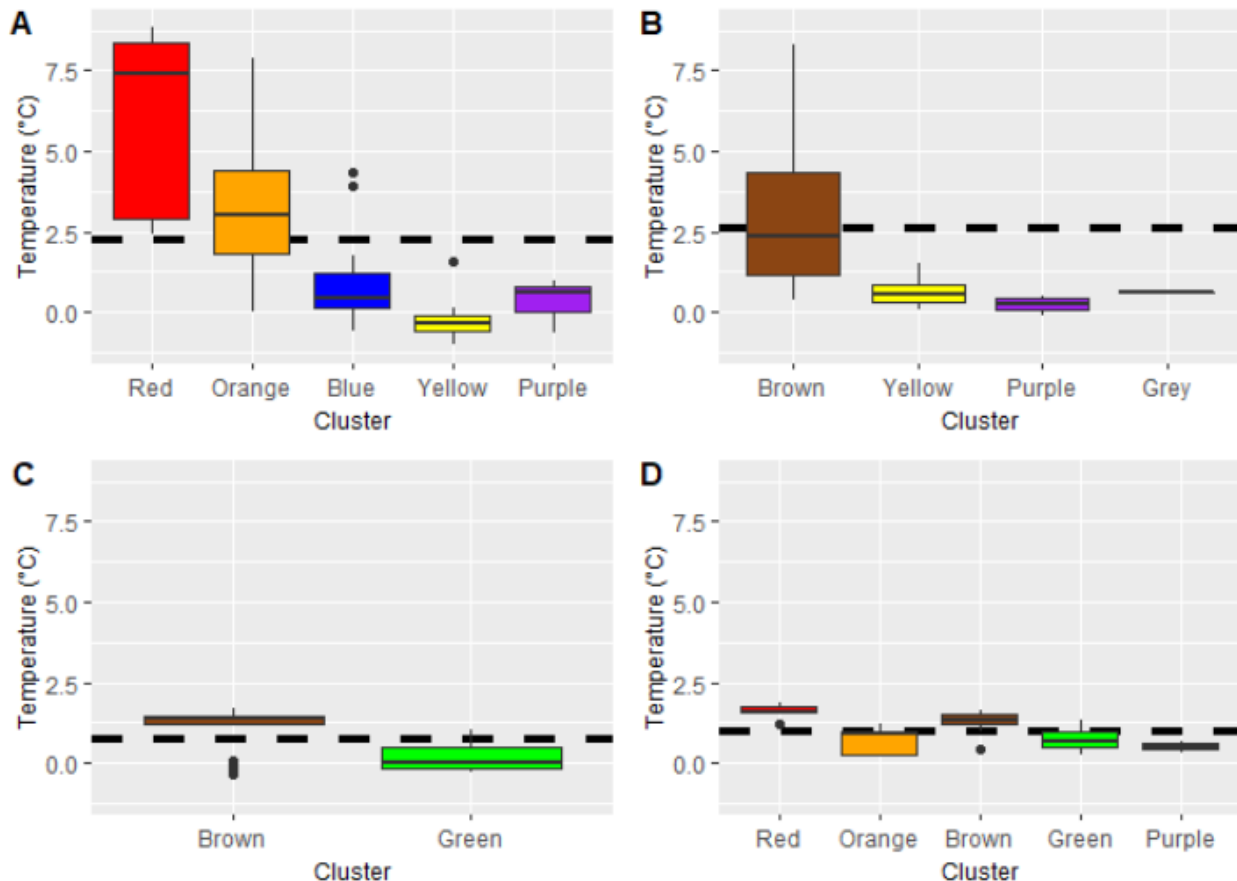


Figure 13. Boxplots of temperature by the cluster for each of the seasons (A) Summer, (B) Fall, (C) Winter, and (D) Spring. The dashed lines denotes the mean temperature of the study area (2.23°C in summer, 2.62°C in fall, 0.70°C in winter, and 0.94°C in spring).

3.6. Variables Driving Snow Crab Presence

A GAM model was built to explore the relationship between environmental variables and the presence of snow crab and how these relationships changed seasonally. Due to low densities of snow crab observed in the study area (Table 2), density data were condensed to presence-absence for the model. The number of sites with snow crab present varied slightly by season; they were present at 17, 15, 16, and 13 sites in the summer, fall, winter, and summer, respectively (Figure 14). Site 45 in the summer had a considerably higher density than any other site in any season ($5.50 \text{ snow crab m}^{-2}$). The model had an explained deviance of 22.2% (Table 4), with temperature ($p < 0.001$), slope ($p < 0.01$), and GLCM mean significantly influencing the probability of snow crab presence. The model predicted a baseline chance of snow crab presence of 12% (Intercept) with all other covariates at their average values. The probability of snow crab presence decreased with global temperature and increased with global slope (Figure 15). When temperatures were at the lowest observed values (-1.0°C), the probability of snow crab presence was at a high of 70%, which decreased down to 0% at temperatures $>4.0^{\circ}\text{C}$. Inversely, at a slope of zero, the probability of their presence was 10%, which increased up to a probability of 33% at a slope of 15. GLCM mean did not affect snow crab presence in the summer and fall and had minimal effects in the spring. The relationship between snow crab presence and GLCM mean exhibited quadratic effects in the winter and spring, with peaks at 7 (35% probability of presence) and 18 (15% probability of presence), respectively. However, winter was the only season where this relationship was significant ($p < 0.05$).

Snow crab was present at shallower depths in the fall and spring seasons (Figure 16). However, post hoc tests of the model with depth smoothers instead of temperature did not perform as well as my final model.

Table 4. Summary of the model output describing the parametric and smoothed terms of the snow crab Presence/Absence Generalized Additive Model.

Parametric Term	Estimate	Std. Error	Z Value	P-Value
(Intercept)	-1.942	0.461	-4.209	<0.01
SeasonFall	0.499	0.505	0.988	0.323
SeasonWinter	-0.519	0.537	-0.967	0.334
SeasonSpring	-0.201	0.483	-0.416	0.678
Smoothed Term	edf	Ref df	Chi. sq	P-value
s(GLCM mean (3x3)):	5.642 x10 ⁻⁵	8	0.000	0.812
Summer				
s(GLCM mean (3x3)): Fall	7.596 x10 ⁻¹	8	0.970	0.253
s(GLCM mean (3x3)):	2.984	8	6.949	<0.05
Winter				
s(GLCM mean (3x3)):	1.171	8	1.486	0.258
Spring				
s(temperature)	1.000	1	17.772	<0.001
s(slope (25x25))	1.000	1	7.230	<0.01

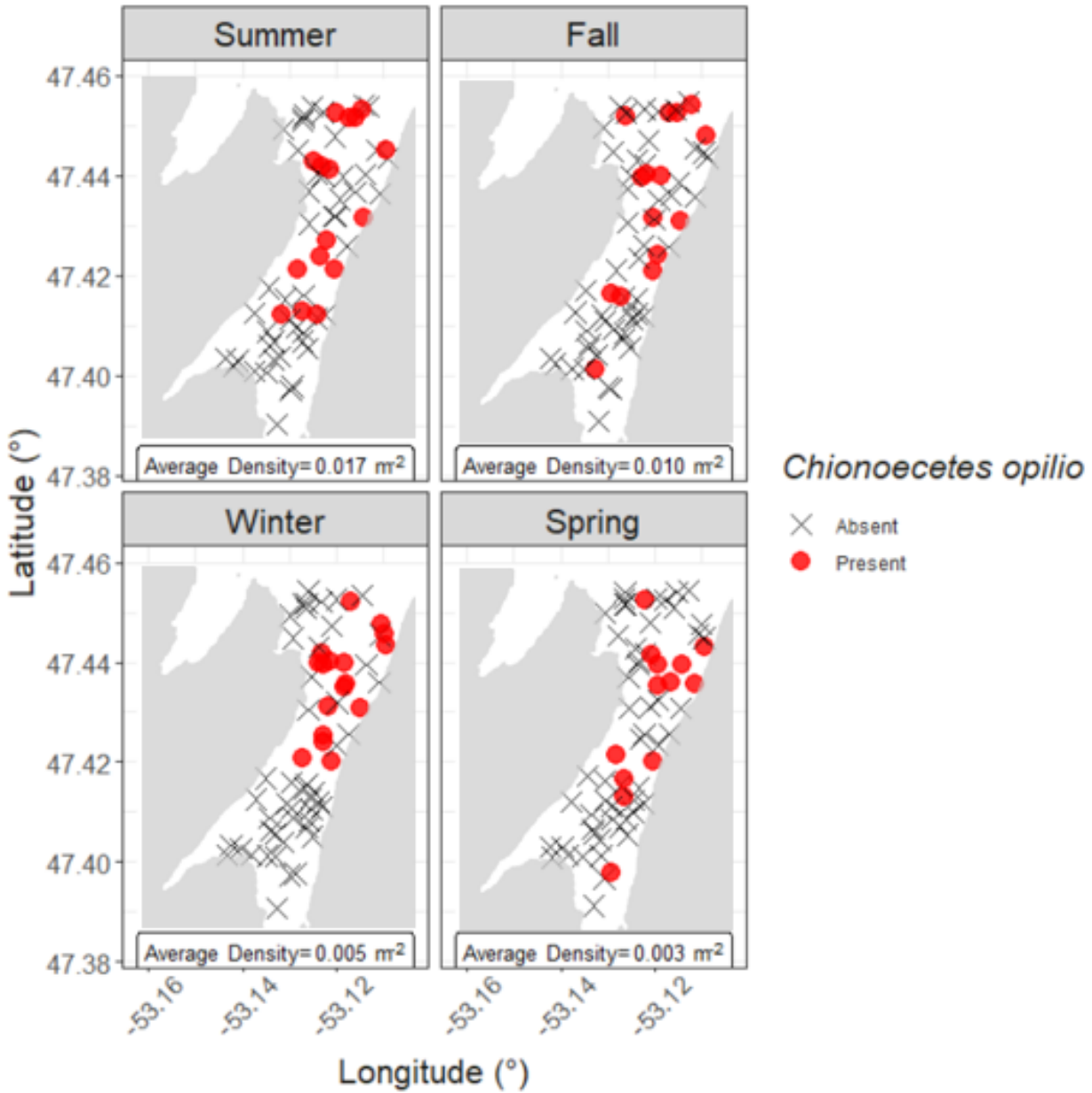


Figure 14. Presence/Absence map of snow crab (*Chionoecetes opilio*) at sample sites in Holyrood Bay across the four seasons. The maps use a UTM projection in zone 22N.

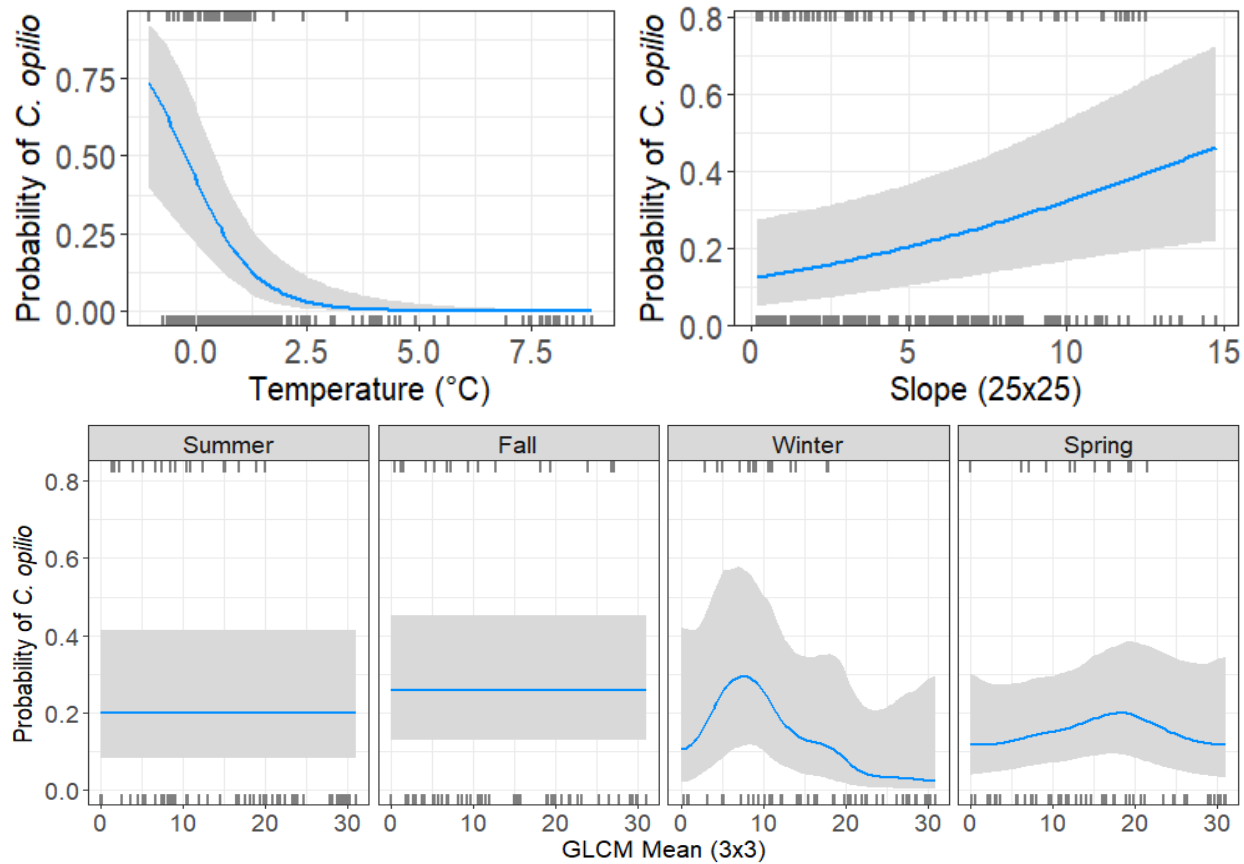
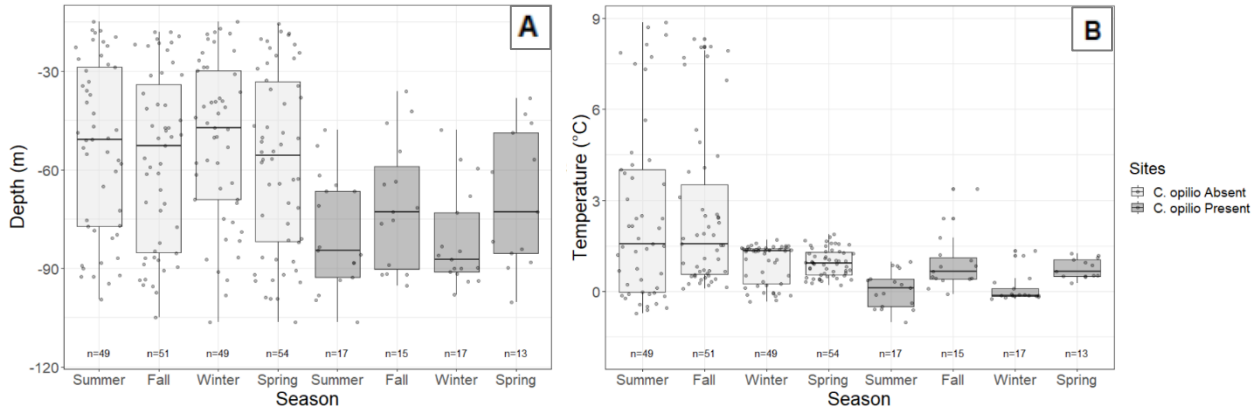


Figure 15. Partial-effects plots of the smoother relationships from the snow crab (*Chionoecetes opilio*) binomial GAM model converted to the probability scale with the model intercept, and the intercept uncertainty added to the smooth uncertainty. Significant covariates (A) global temperature, (B) global slope (25x25), and (C) GLCM Mean (3x3) by season are illustrated. Hashes on the x-axis denote the presence or absence of snow crab from in-situ data collected in Holyrood Bay from 2020-2021, which was used to inform the model.



*Figure 16. Boxplots of the (A) depths and (B) temperatures of the study sites sampled in Holyrood Bay with snow crabs (*Chionoecetes opilio*) absent (light grey), and with snow crabs present (dark grey) across the four seasons from July 2020 to April 2021.*

4. Discussion

4.1. Overview

The present study shows that community mapping can produce different maps of the same physical area when groundtruthing is collected in different seasons. Map differences were due to density and locational changes of individual species, driven by changes in their ecological requirements and the area's environmental characteristics. Overall organism density decreased from over five organisms per metre squared in the summer to less than one in the winter. This was primarily driven by the widespread disappearance of the brown psolus in the fall and winter. Other notable changes in the fall and winter included the reduction of the common sand dollar by two orders of magnitude and the increase in green sea urchin densities in shallower sites. Fine-scale habitat preference of the commercially important snow crab was driven by temperature, slope, and in the winter, seafloor hardness.

4.2. Abiotic Patterns

Temporal changes in community distributions and abundances can be partly attributed to the large seasonal variation that occurs in cold ocean systems (Shindell *et al.*, 1999). Many abiotic and oceanographic variables that are documented as important drivers of the distribution of benthic species are intrinsically linked to each other (e.g., temperature, depth, and salinity) (Clarke and Green, 1988). In Conception Bay, stratification begins in late spring and reaches a maximum in August and September (Tian *et al.*, 2003). Convection mixing starts in October, leading to a homogenous water column in the winter. Bottom temperature patterns observed followed this stratification cycle, with the largest temperature range in summer and the smallest temperature range in spring. This narrow range of bottom temperatures in the spring was likely the cause of the decreased importance of temperature in the model that season. Additionally, abundant snow precipitations during winter (Climate-Data.org, 2022), followed by melting in the spring, contributed to the lowest salinities in the spring. The weakened relationship between temperature and salinity in the summer was likely due to the lack of vertical mixing caused by the thermocline. Decreased precipitation (Climate-Data.org, 2022), increased evaporation, and lack of vertical mixing lead to shallow waters with high salinity due to evaporation and deeper waters with low salinity (Tian *et al.*, 2003).

The most important terrain variables in spatially distinguishing between the communities within each season were GLCM mean, temperature, and BPI. Terrain variables do not change seasonally but their explanatory importance still varied across seasons. For example, eastness of slopes was only important in the spring and summer. The direction of a slope is important for suspension feeders who rely on currents for food input (Gage and Tyler, 1991; Wilson *et al.*, 2007). Currents in Conception Bay are weak and vary spatially based on the topography but tend

to follow a counter-clockwise pattern (de Young and Sanderson, 1995). Hence, suspension feeders on west-facing slopes in Conception Bay may receive an increased food supply, especially in the spring during the phytoplankton bloom. This could have been a driver of habitat selection for the suspension feeder brown psolus, found mostly on west-facing slopes. The importance of eastness was only apparent in spring and summer, the seasons when this species was almost exclusively observed.

The ‘best’ scale for variables in the random forest often performed only moderately better than other scales. The fine-scale variations of slope and the broad-scale variations of directionality (eastness and northness) were favoured in the models irrelevant of season. Slope is likely important at a fine-scale because fine-scale slope affects sedimentation and the types of substrata available to organism (e.g., steep wall for attaching to vs. flat sandy area for burrowing). BPI and GLCM mean were important at varying scales throughout the seasons. Broad-scale BPI performed better in the model when there were fewer clusters (fall and winter), likely because at that level the main distinction between communities was between the shallower area with hard substrate and larger objects (e.g. boulders) and the deep, sandy flat bottom of the fjord.

The most recent acoustic data available for this study were from 2010; consequently, it is possible that the seafloor morphology changed slightly since collection. However, with the bathymetry gridded to 10 x 10 m resolution, it is unlikely that depths have changed enough in 10 years to alter pixel values. Since all four seasonal maps were built on the same environmental layers, this would not affect the patterns of biological change that are visible across the seasons.

Although food input can significantly influence benthic communities, I was unable to measure this variable directly. However, temperature can be a proxy because increasing water

temperatures is the primary driver of phytoplankton productivity (i.e., blooms) (Trombetta *et al.*, 2019). A connected study in 2021 found that as temperatures warmed in the spring, the spring phytoplankton bloom peaked mid-April and again in mid-May (Command *et al.*, 2022). This coincides with historical data in Conception Bay, where the biomass of the spring phytoplankton bloom peaked in April (Redden, 1994; Choe *et al.*, 2003). This phytoplankton bloom would have led to a large increase in seasonal food input to my study site, since in Conception Bay an estimated 56% of spring primary productivity is deposited on the seafloor (Thompson *et al.*, 2008). The higher food input to my study area from the spring bloom was likely an important cause of the species richness peak in the spring.

4.3. Biotic Patterns

4.3.1. Community-Level

There is often a link between benthic communities and the increased food inputs from seasonal blooms. This can be observed as large, rapid responses in macrobenthic abundance, biomass, and species richness following phytoplankton blooms (Austen *et al.*, 1991; Zhang *et al.*, 2015). I observed the response in species richness to be faster than organism density, which peaked in spring and summer, respectively. The nature and timing of responses by different benthic feeding groups can vary (Zhang *et al.*, 2015; Lessin *et al.*, 2019). A study in Conception Bay observed the maximum copepod abundance to be lagged three weeks from the peak of the spring bloom. Additionally, consumers of these copepods (*Parasagitta elegans*) had a lag of an additional three weeks before their maximum abundance (Choe *et al.*, 2003). Compared to historical spring blooms in Conception Bay, my spring data collection (April 21-25, 2021) was likely too early to reflect the impact of increased food input on overall density. However, it captured the impact of transient species (e.g., *Zoarces americanus*) on species richness.

Other habitat mapping studies in Newfoundland have found biological communities similar to those observed in this study. One study conducted in Conception Bay characterized the biological community on the bay's northeast coast between June and October (Novaczek *et al.*, 2017). They identified three distinct communities; one dominated by green sea urchins, one dominated by brittle stars, and one dominated by snow crab. These communities are consistent with what I observed in Holyrood Bay in the fall: the brown cluster (dominated by urchins), the yellow cluster (dominated by brittle stars), and the purple cluster (dominated by decapods). Studies in other bays across Newfoundland, specifically Newman Sound (Proudfoot *et al.*, 2020) and Placentia Bay (Nemani, 2022), also documented brittle star dominated (consistent with my yellow cluster), common sand dollar dominated (consistent with my red cluster), and green sea urchin dominated (consistent with my orange cluster) communities. The latter study also observed a shrimp dominated community (consistent with my purple cluster). While they have similarities to the communities I observed, they do not capture the dynamic seasonal aspect of the ecosystems. The ground-truthing in Placentia Bay occurred partially in August and in November, with no observations of the brown psolus. It is difficult to know whether the variations between bays are true differences, or from missing temporal coverage.

It is generally accepted that most communities gradually shift into others, rather than acting as discrete units (Brown *et al.*, 2011). Temporally, this gradual shift was apparent in the present study in the spring, when the brown cluster (star and urchin dominated) was beginning to return to separate orange (urchin dominated) and red (star and sand dollar dominated) clusters, but still appeared as brown in some areas. Spatially, it also explains why there is some overlap in species between different clusters. This was likely a cause of some of the moderate accuracies in random forest models (75% overall accuracy in the summer).

4.3.2. Species Driving Community Change

Not all species would be expected to respond similarly to seasonal changes in their environment (Buhl-Mortensen *et al.*, 2012). Generalist species can tolerate a broader range of conditions (Colossi Brustolin *et al.*, 2019). In contrast, specialist species must use behavioural mechanisms (e.g., migrating, or burrowing) or life history adaptations (e.g., reduced feeding, timed reproduction, and short life span) to survive in areas where conditions are not always optimal.

The decrease in brown psolus densities by three orders of magnitude from summer to fall suggest that they are specialists. Brown psolus is a mobile, suspension-feeding (Nesis, 1965) sea cucumber that inhabits depths of 10-400 m (Mortensen, 1927; Nesis, 1965). It has been documented on the North and Northeast Newfoundland shelf on fine sediment between June-September (Nesis, 1965) and in the fall on the east coast of Newfoundland (Mercier and Hamel, 2010). This species was found at the most sites in the spring (69% of sites) but had highest densities in the summer (2.955 m^{-2}). Brown psolus free-spawns in mid-April, likely coinciding with increased food inputs, followed by a pelagic larval stage of ≥ 58 days (Mercier and Hamel, 2010), which could explain the lagged increase in densities after the bloom. The Holyrood Subsea Observatory (February 2021-June 2021) stationed at a depth of 85 m in the bay observed only one brown psolus in June, down from a maximum of 259 m^{-2} (Command *et al.*, 2022). The difference in summer densities of this species between the Subsea Observatory and my observations is likely an artefact of their reduced depth distribution (from a median of 70 m, IQR=26, in the spring to 65 m, IQR= 6, in summer). The reduced depth distribution of the brown psolus could be caused by less food reaching deeper habitats late in the season (Harris, 2020).

The reason behind the reduction in densities of the brown psolus in the fall and winter is unknown and so is the mechanism used to survive suboptimal conditions. The brown psolus may remain in Holyrood Bay under the sediment until conditions are favourable, or they may migrate to other areas; both behaviours have been documented in other sea cucumber species (Choe, 1963; Jordan, 1972; Yingst, 1976; Bulteel *et al.*, 1992; Hamel and Mercier, 1996; Mercier *et al.*, 2000; Fraser *et al.*, 2004; Yamana *et al.*, 2009; Domínguez-Godino and González-Wangüemert, 2020). It is unlikely that the disappearance is caused by the die-off of this organism as most sea cucumber species are slow growing and live for > 8 years (Fish, 1967; Hamel and Mercier, 1996; Sun *et al.*, 2019; Ramírez-González *et al.*, 2020). A study in eastern Canada on the orange-footed sea cucumber (*Cucumaria frondosa*) documented a sudden movement at sexual maturity from shallow to deep water in early fall when the temperature decreased rapidly (Hamel and Mercier, 1996). If brown psolus shares a similar strategy to the orange-footed sea cucumber, the disappearance could be explained by movement outside of Holyrood Inlet to areas deeper than its maximum depth of 100 m. Nevertheless, in the Subsea Observatory video footages, that records 5 minutes every hour, there was no observable movement of this species on top of the sediment (Command, pers comm). This instead supports the idea that brown psolus over-winter below the sediment similar to *Heterocucumis steineni* (Fraser *et al.*, 2004). This cycle would likely be controlled by food input as many other suspension-feeding sea cucumber species cease feeding from October to early spring (Engstrom, 1982; Hamel and Mercier, 1998; Singh *et al.*, 1999; Fraser *et al.*, 2004). This feeding cessation is not related to temperature, but instead day length and chloropigment concentrations (Singh *et al.*, 1999; Fraser *et al.*, 2004), which likely explains why I did not observe high densities in the fall when benthic temperatures were the highest.

The grouping of shallow-water clusters (red and orange to brown) in the fall and winter was partially caused by green sea urchins moving to shallower areas in these seasons. The green sea urchin is a highly abundant species that mainly consumes macroalgae but will consume animal prey when available, making them generalists (Lyons and Scheibling, 2007). Large green sea urchins are often found in aggregations that can travel up to 3 m/day in search of food (Garnick 1978; Dumont et al. 2004). Macroalgae are found in higher abundances during the summer and decrease in abundance with depth (Pascelli *et al.*, 2013; Ojeda *et al.*, 2019). The search for food during periods of decreased abundance/ depth distributions of macroalgae could have driven this species' movement. Another major seasonal cause for the movement of this species is aggregation for breeding (Miller and Mann, 1973). Aggregations occur seasonally for breeding in spring (April) and fall (November), since fertilization is dependent on spatial and temporal coordination of gamete release (Miller and Mann, 1973). One site in the fall had abnormally high green sea urchin densities (4.68 m^{-2}); however, it is difficult to know if this was a breeding aggregation since two other sites with densities of $> 4 \text{ m}^{-2}$ were also observed in the summer.

The reduction of common sand dollar densities in the fall and winter also affected the grouping of the shallow clusters (red and orange). The common sand dollar is a mobile organism that lives in various conditions and greatly impacts other macrobenthic populations (Stanley and James, 1971; Richardson *et al.*, 1983). Their distribution is predominantly determined by topography, current regime, and grain size, while depth, tidal cycle, salinity, and temperature do not significantly impact their distribution (Stanley and James, 1971). I observed this sand dollar in clusters with high GLCM mean values (associated with harder substrate), which represented shallow patches of fine sediment surrounded by rock structures. It is unknown why the common

sand dollar had lower densities during the fall and winter since they have been documented to be tolerant of large seasonal variations (Stanley and James, 1971). It could be explained by a biological mechanism, such as predation or predation avoidance (fish, sea stars, sea urchins) (Himmelman and Steele, 1971; Brown, 1983). Since green sea urchins moved to shallower regions in the fall and winter, it is possible that the common sand dollar also moved shallower (out of my study area) as a means of predator avoidance, or they were consumed.

4.3.3. Snow Crab Fine-Scale Habitat Preferences

These results suggested that snow crabs were not randomly distributed throughout Holyrood Bay, with spatial distribution influenced by temperature, substrate, and slope. Patchy spatial distributions of snow crab have been documented previously (Miller, 1975; Conan and Maynard, 1987; Comeau *et al.*, 1998) and are thought to be related to substrate preferences and intraspecific factors more than depth (Comeau *et al.*, 1998). Substrate hardness was one of the main abiotic variables influencing snow crab presence, and the only variable whose relationship to their presence changed seasonally. Snow crab are predominantly found in deep muddy habitats (Conan *et al.*, 1996); however, annually, large crabs migrate to shallower gravelly locations in the spring (Comeau et al. 1998; Conan et al. 1996; Hooper 1986; Mullowney et al. 2018). These movements are believed to be related to density and temperature-dependent influence on reproduction and growth. It is thought that competitive exclusion drives couples, inferior males, and pre-moult crabs upslope to less favourable habitats because snow crab are polyandrous, and to avoid cannibalism during moult (Comeau et al. 1991). At the same time, low water temperatures in the spring allow spatial ranges of snow crab to expand into shallower water (Comeau et al. 1991; Conan et al. 1996). As the thermocline develops, organisms move downslope again (Conan *et al.*, 1996). Primiparous mating occurs in the winter, with migration

in late fall (Lovrich et al. 1995; Mullowney et al. 2018; Sainte-Marie et al. 1999). Snow crab were present at sites with softer substrata in the winter and harder substrata in the spring, though substrate hardness was only significant in the winter. This seasonal movement did not produce signals in all seasons, likely due to four confounding factors. Firstly, Comeau et al. (1991) documented that not all mating couples migrate upslope (Comeau *et al.*, 1991). Secondly, seasonal migration behaviour differs between sexes, with females acting sedentary and often remaining in shallow water after mating (Ernst et al. 2005; Lovrich et al. 1995; Mullowney et al. 2018; Sainte-Marie et al. 1999). Drop camera video limited the view of organisms to overhead, which made identification of sex impossible. Thirdly, small immature crabs of both sexes reside on shallow rocky bottoms (Dawe and Colbourne, 2002) for their early benthic stages in September (Conan *et al.*, 1996) until their ontogenetic migration, where they migrate to deep, muddy habitats (Ernst et al. 2005; Mullowney et al. 2018). Fourth, there were small sample sizes of observed snow crab in this study area in all seasons.

Temperature was found to be important and negatively correlated with the presence of snow crab. The temperature range observed (-1.0 –4°C) aligns with documented temperature preferences of this species (-1.5 –4°C) (Dawe and Colbourne, 2002). This species has been documented moving to remain within its optimal temperature range (Conan *et al.*, 1996). The linearity of the relationship was likely because the lowest temperature recorded in the study area (-1.1 °C) was within the tolerated range of snow crab.

Less is documented in the literature about the influence of slope on snow crab's habitat selection. Cote et al. (2019) found that juvenile snow crabs that were relocated to flat muddy habitats promptly returned to their preferred slope habitats. I observed a positive association between slope and snow crab presence, and this relationship did not change seasonally. This

contradicts Conan *et al.* (1996), who stated that most snow crabs are found in deep, flat, muddy habitats. This difference can likely be attributed to the fact that fine-scale associations were able to be captured by this study that may be obscured by larger-scale studies (e.g., trawl, trap, species distribution modelling) and the varying life-stage preferences of snow crabs. Since my study site only goes to a maximum depth of 100 m, I only captured the upper limit of this species' niche. This species has been reported travelling an average of 54 to 72 km for the average ontogenetic migration and 25 km for the average seasonal migration in small inshore bays (Mullowney *et al.*, 2018). Therefore, it is likely that many of the organisms I observed are juveniles or have seasonally moved upslope.

4.4. Broader Implications

The seasonal change I observed in this study is not unique to sub-Arctic areas. Seasonal change in environmental conditions and the response of communities occur in virtually all benthic environments (Coma *et al.*, 2000; Clarke *et al.*, 2008; Kim Juniper *et al.*, 2013; Chauvet *et al.*, 2018). Areas closer to the equator may be affected by seasonality to a lesser degree; however, seasonal monsoonal disturbances can impact salinities, temperatures, and vertical mixing (Alongi, 1990; Dalia Susan *et al.*, 2014; Zheng *et al.*, 2017). Offshore there are significant seasonal variations in currents, large-scale wind forcings, and shelf circulation (Loder *et al.*, 1998). It is also well documented that most of the food input to deep-sea benthic communities comes from seasonal fluxes of organic matter falling from euphotic zones (Grebmeier *et al.*, 1988; Iken *et al.*, 2001; Clarke *et al.*, 2008; Tamelander *et al.*, 2008). Hence, a static 'snapshot' of benthic communities cannot accurately represent this dynamism. This work demonstrated community maps can look vastly different across season. Entire species can be

missed or misrepresented since the same physical habitat can host different species depending on the season (Fraschetti *et al.*, 2008).

Quality of ground-truthing methods was identified as one of the most influential methodological variables that can impact the accuracy and repeatability of habitat maps (Strong, 2020). This error analysis by Strong focused on spatial replication and distribution issues, but this error should be extended to temporal replication. In benthic community mapping research, the need for temporal coverage is often overlooked or mentioned as an afterthought, but rarely are steps taken to address this issue (Harris and Baker, 2020a). The error of overlooking temporal ground-truthing replication is especially important in community mapping since the potential inaccuracies of biological classes are higher than that of physical classes (Strong, 2020).

In a review of 53 habitat mapping case studies (Harris and Baker, 2020) 42% of analyzed maps were intended to be a part of longitudinal monitoring programs, and of the instances that were 'one-off' maps, 63% reported that their benthic map would form a baseline for monitoring future changes. Baseline community maps can inform decisions on the zoning of anthropogenic activities, locating areas of potential biodiversity importance, 'Marine Protected Area' creation and management, and for fisheries activities like minimizing bycatch and assessing stocks (Brown *et al.*, 2012). They can also be used to monitor the effects of climate change on benthic communities, which will need to adapt to changing seasonality, temperatures, precipitation pattern, and increased severity of storms. However, large uncertainty in habitat maps, like those caused by the lack of temporal coverage, can confound other temporal changes and render monitoring useless (Fraschetti *et al.*, 2008; Frost *et al.*, 2014; Strong, 2020). Caution should be placed on previous baseline maps that do not have temporal coverage since they can only

describe the season that was actually ground-truthed, and any maps compared must be ground-truthed in the same season. Therefore, understanding and describing temporal dynamics is just as important for effective benthic management as spatial dynamics and must be incorporated into future benthic community mapping studies.

5. Conclusions and Future Directions

5.1. Key Findings

The present study's key finding is the demonstrated importance to include spatio-temporal variation in the production of benthic community maps. The maps produced in this thesis ranged from 2 to 5 different communities in Holyrood depending on the season, with no single community being present in all four seasons. Notable changes in the community compositions between the seasonal maps coincided with distribution changes at the species level. One cluster disappeared in the fall, following the widespread reduction in brown psolus sea cucumber. This cluster then merged with a previously distinct cluster characterized by brittle stars in the winter and spring, corresponding with the shifted depth distribution of brown psolus sea cucumbers (although still at low densities in the winter) to deeper water. Two shallower separate clusters merged in the fall and winter which represented two changes at the species-level; the reduction in common sand dollars, and the shift in distribution of green sea urchins to shallower water in the fall and winter. In the spring, this cluster partly separated again, likely showing a gradual shift back to separate clusters in the summer. If ground-truthing occurred in this area in only one of these seasons, the distribution, and densities of these three species, and thus the overall communities present, would have been misleading.

The secondary key finding in the study was that fine-scale habitat selection of snow crab was impacted by temperature, slope, and substrate hardness (GLCM mean). Probability of snow crab presence had a negative relationship to temperature, and a positive relationship with slope. In the winter, the probability of this species' presence was higher on soft substrata, in the spring it was higher on harder substrata, with substrate hardness having no effect in the summer and fall. Understanding what influences snow crab habitat selection is crucial to protecting their populations and ensuring that fishing efforts remain sustainable.

5.2. Recommendations

It is essential that future benthic community mapping encompasses both spatial and temporal variability in order to accurately represent the dynamic nature of these ecosystems. Without accurate representation, entire species can be missed or misrepresented, leading to poor management and the possible extirpation of species. Ground-truthing data should be collected seasonally to capture natural variability in communities and associated habitats. If this is not possible, maps can only be used to describe the study area in the season studied, and this limitation should be clearly stated. Considerations of the purpose of a study, and the ecology of species present in the area (if available), can help inform decisions on ground-truthing timing to describe benthic communities. Biodiversity monitoring is often seasonally limited in coverage thus only capturing species present in a particular season. Including better temporal coverage would allow for a more complete picture of the biodiversity and thus better fine-scale monitoring.

Future studies should explore the influence and possibly confounding impacts of other relevant temporal scales to community maps. It may be beneficial to explore how seasonal patterns in community maps also change inter-annually by collecting multiple years of seasonal

data. Inter-annual repetition would also help confirm that these changes were in fact a factor of changing seasons. It is possible that ‘seasonal’ is not the key ecological scale acting on communities in this study and that the changes observed were differences cause by an unexplored scale or random fluctuations. If the patterns observed were not due to seasonal change but were a representation of random fluctuations, that would in itself justify the need for temporal coverage in all ground-truthing endeavours.

References

- Aberle, N. and Witte, U. (2003) 'Deep-sea macrofauna exposed to a simulated sedimentation event in the abyssal NE Atlantic: In situ pulse-chase experiments using ^{13}C -labelled phytodetritus', *Marine Ecology Progress Series*, 251, pp. 37–47.
doi:10.3354/meps251037.
- van Aken, H.M. (1986) 'The onset of seasonal stratification in shelf seas due to differential advection in the presence of a salinity gradient', *Continental Shelf Research*, 5(4), pp. 475–485. doi:10.1016/0278-4343(86)90071-3.
- Aller, J.Y. (1997) 'Benthic community response to temporal and spatial gradients in physical disturbance within a deep-sea western boundary region', *Deep Sea Research Part I: Oceanographic Research Papers*, 44(1), pp. 39–69. doi:10.1016/S0967-0637(96)00092-1.
- Alongi, D.M. (1990) 'The ecology of Tropical Soft-Bottom Benthic Ecosystems', *Oceanography and Marine Biology: An Annual Review*, 28, pp. 381–396.
- Austen, M.C., Buchanan, J.B., Hunt, H.G., Josefson, A.B. and Kendall, M.A. (1991) 'Comparison of long-term trends in benthic and pelagic communities of the North Sea', *Journal of the Marine Biological Association of the United Kingdom*, 71(1), pp. 179–190.
doi:10.1017/S0025315400037498.
- Baker, D.J.J. (1981) 'Ocean instruments and experiment design', in *Evolution of Physical Oceanography*, pp. 396–433.
- Baker, E.K. and Harris, P.T. (2020) 'Habitat mapping and marine management', in *Seafloor*

geomorphology as benthic habitat: GeoHab atlas of seafloor geomorphic features and benthic habitat. 2nd edn. London: Elsevier, pp. 17–34. doi:10.1016/B978-0-12-385140-6.00002-5.

Baker, K., Mullowney, D., Pederson, E., Coffey, W., Cyr, F. and Belanger, D. (2021) *An assessment of Newfoundland and Labrador snow crab (*Chionoecetes opilio*) in 2018.* St.John's.

Barnes, D.K.A. and Sands, C.J. (2017) ‘Functional group diversity is key to Southern Ocean benthic carbon pathways’, *PLOS ONE*, 12(6), p. e0179735. doi:10.1371/journal.pone.0179735.

Begon, M., Townsend, C.R. and Harper, J.L. (2005) *Ecology: From individuals to ecosystems.* 4th edn, *Blackwell Publishing*. 4th edn. Wiley-Blackwell.

Bernier, R.Y., Jamieson, R.E. and Moore, A.M. (2018) ‘State of the Atlantic Ocean synthesis report’, *Canadian Technical Report of Fisheries and Aquatic Sciences*, 3167.

Blondel, P. (1996) ‘Segmentation of the Mid-Atlantic Ridge south of the Azores, based on acoustic classification of TOBI data’, *Geological Society Special Publication*, 118, pp. 17–28. doi:10.1144/GSL.SP.1996.118.01.02.

Borcard, D., Gillet, F. and Legendre, P. (2018) *Numerical ecology with R.* 2nd edn. Springer. doi:10.1007/978-1-4419-7976-6.

Boudreau, S.A., Anderson, S.C. and Worm, B. (2011) ‘Top-down interactions and temperature control of snow crab abundance in the northwest Atlantic Ocean’, *Marine Ecology Progress Series*, 429, pp. 169–183. doi:10.3354/MEPS09081.

Braathen, A. and Brekke, H. (2020) ‘Characterizing the Seabed: a Geoscience Perspective’, in *The Law of the Seabed*. Brill Nijhoff, pp. 21–35. doi:10.1163/9789004391567_003.

Breiman, L. (2001) ‘Random forests’, *Machine Learning*, 45(1), pp. 5–32.
doi:10.1023/A:1010933404324.

Brown, C.J. and Blondel, P. (2009) ‘Developments in the application of multibeam sonar backscatter for seafloor habitat mapping’, *Applied Acoustics*, 70(10), pp. 1242–1247.
doi:10.1016/J.APACOUST.2008.08.004.

Brown, C.J., Sameoto, J.A. and Smith, S.J. (2012) ‘Multiple methods, maps, and management applications: Purpose made seafloor maps in support of ocean management’, *Journal of Sea Research*, 72, pp. 1–13. doi:10.1016/J.SEARES.2012.04.009.

Brown, C.J., Smith, S.J., Lawton, P. and Anderson, J.T. (2011) ‘Benthic habitat mapping: A review of progress towards improved understanding of the spatial ecology of the seafloor using acoustic techniques’, *Estuarine, Coastal and Shelf Science*, 92(3), pp. 502–520.
doi:10.1016/j.ecss.2011.02.007.

Brown, C.L. (1983) ‘Substrate Preference and Test Morphology of a Sand Dollar (*Echinorachnius parma*) Population in the Gulf of Maine’, *Beta Beta Beta Biological Society*, 54(4), pp. 246–254.

Buhl-Mortensen, L., Buhl-Mortensen, P., Dolan, M.F.J., Dannheim, J., Bellec, V. and Holte, B. (2012) ‘Habitat complexity and bottom fauna composition at different scales on the continental shelf and slope of northern Norway’, *Hydrobiologia*, 685(1), pp. 191–219.
doi:10.1007/s10750-011-0988-6.

Bulteel, P., Jangoux, M. and Coulon, P. (1992) 'Biometry, bathymetric distribution, and reproductive cycle of the holothuroid *Holothuria tubulosa* (Echinodermata) from Mediterranean Sea grass beds', *Marine Ecology*, 13(1), pp. 53–62. doi:10.1111/J.1439-0485.1992.TB00339.X.

Cardinale, B.J., Palmer, M.A. and Collins, S.L. (2002) 'Species diversity enhances ecosystem functioning through interspecific facilitation', *Nature*, 415(6870), pp. 426–429. doi:10.1038/415426a.

Chainho, P. et al. (2006) 'Seasonal and spatial patterns of distribution of subtidal benthic invertebrate communities in the Mondego River, Portugal-a poikilohaline estuary', *Hydrobiologia*, 555, pp. 59–74. doi:10.1007/s10750-005-1132-2.

Chang, C.Y. and Marshall, D.J. (2016) 'Spatial pattern of distribution of marine invertebrates within a subtidal community: do communities vary more among patches or plots?', *Ecology and Evolution*, 6(22), pp. 8330–8337. doi:10.1002/ECE3.2462.

Chauvet, P., Metaxas, A., Hay, A.E. and Matabos, M. (2018) 'Annual and seasonal dynamics of deep-sea megafaunal epibenthic communities in Barkley Canyon (British Columbia, Canada): A response to climatology, surface productivity and benthic boundary layer variation', *Progress in Oceanography*, 169, pp. 89–105. doi:10.1016/j.pocean.2018.04.002.

Chen, R.-C., Dewi, C., Huang, S.-W. and Caraka, R.E. (2020) 'Selecting critical features for data classification based on machine learning methods', *Journal of Big Data*, 7(1), pp. 1–26. doi:10.1186/S40537-020-00327-4.

Choe, N., Deibel, D., Thompson, R.J., Lee, S.H. and Bushell, V.K. (2003) 'Seasonal variation in

the biochemical composition of the chaetognath *Parasagitta elegans* from the hyperbenthic zone of Conception Bay, Newfoundland', *Marine Ecology Progress Series*, 251, pp. 191–200. doi:10.3354/MEPS251191.

Choe, S. (1963) *Biology of the Japanese common sea cucumber, Stichopus japonicus (Selenka)*. Pusan National University.

Christianson, D.S., Kaufman, C.G. and Freckleton, R. (2016) 'Effects of sample design and landscape features on a measure of environmental heterogeneity', *Methods in Ecology and Evolution*, 7(7), pp. 770–782. doi:10.1111/2041-210X.12539.

Chubarenko, I.P. *et al.* (2017) 'Spring thermocline formation in the coastal zone of the southeastern Baltic Sea based on field data in 2010–2013', *Oceanology*, 57(5), pp. 632–638. doi:10.1134/S000143701705006X.

Clarke, A. (1988) 'Seasonality in the antarctic marine environment', *Comparative Biochemistry and Physiology Part B: Comparative Biochemistry*, 90(3), pp. 461–473. doi:10.1016/0305-0491(88)90285-4.

Clarke, A., Meredith, M.P., Wallace, M.I., Brandon, M.A. and Thomas, D.N. (2008) 'Seasonal and interannual variability in temperature, chlorophyll and macronutrients in northern Marguerite Bay, Antarctica', *Deep Sea Research*, 2(55), pp. 1988–2006. doi:10.1016/j.dsr2.2008.04.035.

Clarke, K. and Green, R. (1988) 'Statistical design and analysis for a "biological effects" study', *Marine Ecology Progress Series*, 46, pp. 213–226. doi:10.3354/MEPS046213.

Climate-Data.org (2022) *Holyrood climate: Average temperature, weather by month, Holyrood*

water temperature. Available at: <https://en.climate-data.org/north-america/canada/newfoundland-and-labrador/holyrood-46266/> (Accessed: 1 September 2022).

Cloern, J.E. and Jassby, A.D. (2010) ‘Patterns and scales of phytoplankton variability in estuarine-coastal ecosystems’, *Estuaries and Coasts*, 33, pp. 230–241.
doi:10.1007/s12237-009-9195-3.

Cogan, C.B., Todd, B.J., Lawton, P. and Noji, T.T. (2009) ‘The role of marine habitat mapping in ecosystem-based management’, *ICES Journal of Marine Science*, 66(9), pp. 2033–2042. doi:10.1093/icesjms/fsp214.

Cohen, J. (1960) ‘A coefficient of agreement for nominal scales’, *Educational and Psychological Measurement*, 20(1). doi:10.1177/001316446002000104.

Colossi Brustolin, M., Nagelkerken, I., Moitinho Ferreira, C., Urs Goldenberg, S., Ullah, H. and Fonseca, G. (2019) ‘Future ocean climate homogenizes communities across habitats through diversity loss and rise of generalist species’, *Global Change Biology*, 25(10), pp. 3539–3548. doi:10.1111/gcb.14745.

Coma, R., Ribes, M., Gili, J.M. and Zabala, M. (1998) ‘An energetic approach to the study of life-history traits of two modular colonial benthic invertebrates’, *Marine Ecology Progress Series*, 162, pp. 89–103. doi:10.3354/MEPS162089.

Coma, R., Ribes, M., Gili, J.M. and Zabala, M. (2000) ‘Seasonality in coastal benthic ecosystems’, *Trends in Ecology & Evolution*, 15(11), pp. 448–453. doi:10.1016/S0169-5347(00)01970-4.

- Comeau, M., Conan, G.Y., Maynou, F., Robichaud, G., Therriault, J.-C. and Starr, M. (1998) ‘Growth, spatial distribution, and abundance of benthic stages of the snow crab (*Chionoecetes opilio*) in Bonne Bay, Newfoundland, Canada’, *Canadian Journal of Fisheries and Aquatic Sciences*, 55(1), pp. 262–279. doi:10.1139/cjfas-55-1-262.
- Comeau, M., Conan, Y., Robichaud, G. and Jones, A. (1991) *Life history patterns and population fluctuations of snow crab (*Chionoecetes opilio*) in the fiord of Bonne Bay on the west coast of Newfoundland, Canada - from 1983 to 1990*, Canadian Technical Report of Fisheries and Aquatic Sciences. Department of Fisheries and Oceans.
- Command, R., McKenzie, C.H., De Leo, F.C. and Robert, K. (2022) ‘A first look at the megabenthic community response to the spring phytoplankton bloom using the new Holyrood Underwater Observatory in Conception Bay, NL [Conference presentation]’, in *Ocean Sciences Meeting*.
- Conan, G.Y. and Maynard, D.R. (1987) ‘Estimates of snow crab (*Chionoecetes opilio*) abundance by underwater television-a method for population studies on benthic fisheries resources’, *Journal of Applied Ichthyology*, 3(4), pp. 158–165. doi:10.1111/J.1439-0426.1987.TB00536.X.
- Conan, G.Y., Starr, M., Comeau, M., Therriault, J.-C., Maynou, I., Hernandez, F.X. and Robichaud, G. (1996) ‘Life history strategies, recruitment fluctuations, and management of the Bonne Bay fjord Atlantic snow crab (*Chionoecetes opilio*)’, in *Proceedings of the international symposium on biology, management, and economics of crabs from high latitude habitats*. Alaska Sea Grant College Program Report, pp. 96–102.
- Cote, D., Nicolas, J.-M., Whoriskey, F., Cook, A.M., Broome, J., Regular, P.M. and Baker, D.

(2019) ‘Characterizing snow crab (*Chionoecetes opilio*) movements in the Sydney Bight (Nova Scotia, Canada): a collaborative approach using multiscale acoustic telemetry’, *Canadian Journal of Fisheries and Aquatic Sciences*, 76(2), pp. 334–346. doi:10.1139/cjfas-2017-0472.

Crossin, G.T., Al-Ayoub, S.A., Jury, S.H., Howell, W.H. and Watson, W.H. (1998) ‘Behavioral thermoregulation in the American lobster *Homarus americanus*.’, *Journal of Experimental Biology*, 201(3), pp. 365–374. doi:10.1242/jeb.201.3.365.

Cyr, F. and Galbraith, P.S. (2021) ‘A climate index for the Newfoundland and Labrador shelf’, *Earth System Science Data*, 13(5), pp. 1807–1828. doi:10.5194/ESSD-13-1807-2021.

Dalia Susan, V., Satheesh Kumar, P. and Pillai, N.G.K. (2014) ‘Biodiversity and seasonal variation of benthic macrofauna in Minicoy Island, Lakshadweep, India’, *Acta Oceanologica Sinica*, 33(10), pp. 58–73. doi:10.1007/S13131-014-0541-3.

Dawe, E.G. and Colbourne, E.B. (2002) ‘Distribution and demography of snow crab (*Chionoecetes opilio*) males on the Newfoundland and Labrador shelf [Conference paper]’, *Crabs in Cold Water Regions*, pp. 577–594. doi:10.4027/CCWRBME.2002.42.

Dawe, E.G., Mullowney, D.R., Moriyasu, M. and Wade, E. (2012) ‘Effects of temperature on size-at-terminal molt and molting frequency in snow crab *Chionoecetes opilio* from two Canadian Atlantic ecosystems’, *Marine Ecology Progress Series*, 469, pp. 279–296. doi:10.3354/meps09793.

Dionne, M., Sainte-Marie, B., Bourget, E. and Gilbert, D. (2003) ‘Distribution and habitat selection of early benthic stages of snow crab *Chionoecetes opilio*’, *Marine Ecology Progress Series*, 259, pp. 117–128. doi:10.3354/meps259117.

Dolan, M.F.J. (2012) *Calculation of slope angle from bathymetry data using GIS - effects of computation algorithms, data resolution and analysis scale*. Trondheim, Norway.

Domínguez-Godino, J.A. and González-Wangüemert, M. (2020) 'Habitat associations and seasonal abundance patterns of the sea cucumber *Holothuria arguinensis* at Ria Formosa coastal lagoon (south Portugal)', *Aquatic Ecology*, 54(1), pp. 337–354.
doi:10.1007/S10452-020-09746-0.

Dove, A.D.M., Allam, B., Powers, J.J. and Sokolowski, M.S. (2005) 'A prolonged thermal stress experiment on the American lobster, *Homarus americanus*', *Journal of Shellfish Research*, 24(3), pp. 761–765. doi:10.2983/0730-8000(2005)24[761:APTSEO]2.0.CO;2.

Downing, J.A., Perusse, M. and Harvey, H. (1993) 'Spatial aggregation, body size, and reproductive success in the freshwater mussel *Elliptio complanata*', *Journal of the North American Benthological Society*, 12(2), pp. 148–156. doi:10.2307/1467344.

Duffy, J.E., Lefcheck, J.S., Stuart-Smith, R.D., Navarrete, S.A. and Edgar, G.J. (2016) 'Biodiversity enhances reef fish biomass and resistance to climate change', *Proceedings of the National Academy of Sciences of the United States of America*, 113(22), pp. 6230–6235. doi:10.1073/pnas.1524465113.

Dumont, C., Himmelman, J.H. and Russell, M.P. (2004) 'Size-specific movement of green sea urchins *Strongylocentrotus droebachiensis* on urchin barrens in eastern Canada', *Marine Ecology Progress Series*, 276(1), pp. 93–101. doi:10.3354/MEPS276093.

Durden, J.M. *et al.* (2016) 'Perspectives in visual imaging for marine biology and ecology: From acquisition to understanding', in *Oceanography and Marine Biology*. 1st edn. Boca Raton, FL: CRC Press, pp. 1–72.

- Earle, S. (2019) ‘Sea-floor sediments’, in *Physical geology*. 2nd edn.
- Émond, K., Sainte-Marie, B., Galbraith, P.S. and Bêty, J. (2015) ‘Top-down vs. bottom-up drivers of recruitment in a key marine invertebrate: Investigating early life stages of snow crab’, *ICES Journal of Marine Science*, 72(5), pp. 1336–1348.
doi:10.1093/ICESJMS/FSU240.
- Engstrom, N.A. (1982) ‘Brooding behaviour and reproductive biology of a subtidal Puget Sound sea cucumber *Cucumaria lubrica* (Clark, 1901) (Echinodermata: Holothuroidea)’, in *International Echinoderms Conference*, pp. 447–450.
- Ernst, B., Orensanz, J.M. (Lobo) and Armstrong, D.A. (2005) ‘Spatial dynamics of female snow crab (*Chionoecetes opilio*) in the eastern Bering Sea’, *Canadian Journal of Fisheries and Aquatic Sciences*, 62, pp. 250–268. doi:10.1139/F04-201.
- Fairchild, E.A., Tallack, S., Elzey, S.P. and Armstrong, M.P. (2015) ‘Spring feeding of Atlantic wolffish (*Anarhichas lupus*) on Stellwagen Bank, Massachusetts’, *Fishery Bulletin*, 113(2), pp. 191–201. doi:10.7755/FB.113.2.7.
- Fedewa, E.J., Jackson, T.M., Richar, J.I., Gardner, J.L. and Litzow, M.A. (2020) ‘Recent shifts in northern Bering Sea snow crab (*Chionoecetes opilio*) size structure and the potential role of climate-mediated range contraction’, *Deep Sea Research Part II: Topical Studies in Oceanography*, 181–182, p. 104878. doi:10.1016/j.dsr2.2020.104878.
- Ferrier, S. and Guisan, A. (2006) ‘Spatial modelling of biodiversity at the community level’, *Journal of Applied Ecology*, 43(3), pp. 393–404. doi:10.1111/j.1365-2664.2006.01149.x.
- Fish, J.D. (1967) ‘The biology of *Cucumaria elongata* (Echinodermata: Holothuroidea)’, *Journal*

of the Marine Biological Association of the United Kingdom, 47(1), pp. 129–144.
doi:10.1017/S0025315400033622.

Fisheries and Oceans Canada (2016) *Species quota report- snow crab, Newfoundland and Labrador region.*

Fisheries and Oceans Canada (2019a) *Assessment of Newfoundland and Labrador (Divisions 2HJ3KLNOP4R) snow crab, Canadian Science Advisory Secretariat Science Advisory Report.*

Fisheries and Oceans Canada (2019b) *Species quota report- snow crab, Newfoundland and Labrador region.*

Fisheries and Oceans Canada (2021a) *2020 Value of Atlantic and Pacific coast commercial landings, by province.* Ottawa.

Fisheries and Oceans Canada (2021b) *Species quota report- capelin, Newfoundland and Labrador region.* Available at: https://www.inter.dfo-mpo.gc.ca/publications/reports_rapports/Capelin_Capelan_2021_eng.htm (Accessed: 15 June 2022).

Fisheries and Oceans Canada (2021c) *Species quota report- lobster, Newfoundland and Labrador region.* Available at: https://www.inter.dfo-mpo.gc.ca/publications/reports_rapports/Lobster_Homard_2021_eng.htm (Accessed: 15 June 2022).

Fisheries and Oceans Canada (2021d) *Species quota report- snow crab, Newfoundland and Labrador region.* Available at: https://www.inter.dfo-mpo.gc.ca/publications/reports_rapports/SnowCrab_2021_eng.htm (Accessed: 15 June 2022).

mpo.gc.ca/publications/reports_rapports/Crab_Crabe_2021_eng.htm (Accessed: 15 June 2022).

Fisheries and Oceans Canada (2022) *Science advisory report: Assessment of Newfoundland and Labrador (divisions 2HJ3KLNOP4R) snow crab.* St.John's.

Fisheries and Oceans Canada and Economic Analysis and Statistics (2021) *Canada's Fisheries: Fast Facts 2020.*

Foyle, T.P., O'Dor, R.K. and Elner, R.W. (1989) 'Energetically defining the thermal limits of the snow crab', *Journal of Experimental Biology*, 145(1), pp. 371–393.
doi:10.1242/jeb.145.1.371.

Frank, K.T., Petrie, B., Choi, J.S. and Leggett, W.C. (2005) 'Trophic cascades in a formerly cod-dominated ecosystem', *Science*, 308(5728), pp. 1621–1623.
doi:10.1126/SCIENCE.1113075/SUPPL_FILE/FRANK.SOM.PDF.

Fraschetti, S., Claudet, J. and Grorud-Colvert, K. (2011) 'Management-Transitioning from a single-sector management to ecosystem-based management: what can marine protected areas offer?', in *Marine Protected Areas: A Multidisciplinary Approach*. Cambridge University Press, pp. 11–34.

Fraschetti, S., Terlizzi, A. and Boero, F. (2008) 'How many habitats are there in the sea (and where)?', *Journal of Experimental Marine Biology and Ecology*, 366(1), pp. 109–115.
doi:10.1016/J.JEMBE.2008.07.015.

Fraser, K.P.P., Peck, L.S. and Clarke, A. (2004) 'Protein synthesis, RNA concentrations, nitrogen excretion, and metabolism vary seasonally in the antarctic holothurian

Heterocucumis steineni (Ludwig 1898)', *Physiological and Biochemical Zoology*, 77(4), pp. 556–569. doi:10.1086/420949/ASSET/IMAGES/LARGE/FG6.JPG.

Frey, R.W. (1970) 'The Lebensspuren of Some Common Marine Invertebrates near Beaufort, North Carolina. II. Anemone Burrows', *Journal of paleontology*, 44(2), pp. 308–311.

Frost, M., Sanderson, W.G., Vina-Herbon, C. and Lowe, R.J. (2014) *The potential use of mapped extent and distribution of habitats as indicators of Good Environmental Status (GES)*. doi:10.13140/RG.2.1.1199.0881.

Gage, J.D. and Tyler, P.A. (1991) *Deep-sea biology : a natural history of organisms at the deep-seafloor*, Cambridge University Press. Cambridge, England: Cambridge University Press.

Garnick, E. (1978) 'Behavioral ecology of *Strongylocentrotus droebachiensis* (Muller) (Echinodermata: echinoidea). Aggregating behavior and chemotaxis', *Source: Oecologia*, 37(1), pp. 77–84.

Getis, A. (2008) 'A history of the concept of spatial autocorrelation: A geographer's perspective', *Geographical Analysis*, 40(3), pp. 297–309. doi:10.1111/J.1538-4632.2008.00727.X.

Gili, J. and Hughes, R.G. (1995) 'The ecology of marine benthic hydroids', *Oceanography and Marine Biology: an Annual Review*, 33, pp. 351–426.

Glemarec, M. (1973) 'The benthic communities of the European North Atlantic continental shelf', in *Oceanography and Marine Biology: an Annual Review*, pp. 263–289.

Gosling, E.M. (2021) *Marine mussels : ecology, physiology, genetics and culture*. John Wiley

and Sons.

Grebmeier, J.M., McRoy, C.P. and Feder, H.M. (1988) ‘Pelagic-benthic coupling on the shelf of the northern Bering and Chukchi Seas. I. Food supply source and benthic biomass’, *Marine Ecology Progress Series*, 48, pp. 57–67.

Hall-Beyer, M. (2017) *GLCM Texture Tutorial v3.0*.

Hamel, J.-F. and Mercier, A. (1996) ‘Early development, settlement, growth, and spatial distribution of the sea cucumber *Cucumaria frondosa* (Echinodermata: Holothuroidea)’, *Canadian Journal of Fisheries and Aquatic Sciences*, 53, pp. 253–271. doi:10.1139/f95-186.

Hamel, J.-F. and Mercier, A. (1998) ‘Diet and feeding behaviour of the sea cucumber *Cucumaria frondosa* in the St. Lawrence estuary, eastern Canada’, *Canadian Journal of Zoology*, 76(6), pp. 1194–1198. doi:10.1139/CJZ-76-6-1194.

Hanberry, B.B. (2013) ‘Finer grain size increases effects of error and changes influence of environmental predictors on species distribution models’, *Ecological Informatics*, 15, pp. 8–13. doi:10.1016/j.ecoinf.2013.02.003.

Harris, P.T. (2020) ‘Surrogacy’, in *Seafloor Geomorphology as Benthic Habitat*. 2nd edn. Elsevier Inc., pp. 97–114. doi:10.1371/journal.pone.0179735.

Harris, P.T. and Baker, E.K. (2020a) ‘GeoHab Atlas of seafloor geomorphic features and benthic habitats - synthesis and lessons learned’, in *Seafloor Geomorphology as Benthic Habitat*. 2nd edn. Elsevier, pp. 969–987.

Harris, P.T. and Baker, E.K. (2020b) ‘Why map benthic habitats?’, in *Seafloor geomorphology*

as benthic habitat: GeoHab atlas of seafloor geomorphic features and benthic habitats.
2nd edn. Elsevier Inc., pp. 3–16.

Hartig, F. (2022) ‘DHARMA: Residual diagnostics for hierarchical (Multi-level / mixed) regression models. R package version 0.4.5.’

Hasan, R.C., Ierodiaconou, D. and Monk, J. (2012) ‘Evaluation of four supervised learning methods for benthic habitat mapping using backscatter from multi-beam sonar’, *Remote Sensing*, 4(11), pp. 3427–3443. doi:10.3390/RS4113427.

Hastie, T., Tibshirani, R. and Friedman, J. (2009) ‘Random Forests’, in *The Elements of Statistical Learning Data Mining, Inference, and Prediction*. 2nd edn. New York: Springer, pp. 587–604.

Himmelman, J.H. and Steele, D.H. (1971) ‘Foods and predators of the green sea urchin *Strongylocentrotus droebachiensis* in Newfoundland waters’, *Marine Biology*, 9(4), pp. 315–322. doi:10.1007/BF00372825.

Hobson, R.D. (1972) ‘Surface roughness in topography: quantitative approach’, in *Spatial Analysis in Geomorphology*, pp. 221–245.

Hooper, R.G. (1986) ‘A spring breeding migration of the snow crab, *Chionoecetes opilio* (O. Fabr.), into shallow water in Newfoundland’, *Crustaceana*, 50(3), pp. 257–264. doi:10.1163/156854086X00287.

Howell, K.L. *et al.* (2019) ‘A framework for the development of a global standardised marine taxon reference image database (SMarTaR-ID) to support image-based analyses’. doi:10.1371/journal.pone.0218904.

Hughes Clarke, J.E. (2018) 'Multibeam echosounders', in *Submarine Geomorphology*. Springer Geology, pp. 25–41. doi:10.1007/978-3-319-57852-1_3.

Hurrell, J.W. (1995) 'Decadal trends in the North Atlantic oscillation: Regional temperatures and precipitation', *Science*, 269(5224), pp. 676–679. doi:10.1126/science.269.5224.676.

Hutchinson, G.E. (1957) 'Concluding remarks', *Cold Spring Harbor Symposia on Quantitative Biology*, 22, pp. 415–427.

Huvenne, V.A.I., Blondel, P. and Henriet, J.P. (2002) 'Textural analyses of sidescan sonar imagery from two mound provinces in the Porcupine Seabight', *Marine Geology*, 189(3–4), pp. 323–341. doi:10.1016/S0025-3227(02)00420-6.

Iken, K., Brey, T., Wand, U., Voigt, J. and Junghans, P. (2001) 'Food web structure of the benthic community at the Porcupine Abyssal Plain (NE Atlantic): A stable isotope analysis', *Progress in Oceanography*, 50(1–4), pp. 383–405. doi:10.1016/S0079-6611(01)00062-3.

Ilich, A.R. (2020) 'GLCMTexels.' doi:10.5281/zenodo.4310187.

Jakobsson, M. et al. (2016) 'Mapping submarine glacial landforms using acoustic methods', *Memoirs - Geological Society of London*, 46(1), pp. 17–40. doi:10.1144/M46.182.

Jenness, J.S. (2004) 'Calculating landscape surface area from digital elevation models', *Wildlife Society Bulletin*, 32(3), pp. 829–839. doi:10.2193/0091-7648(2004)032[0829:CLSAFD]2.0.CO;2.

Johnston, K., Ver Hoef, J.M., Krivoruchko, K. and Lucas, N. (2001) *ArcGIS ® 9 Using ArcGIS ® Geostatistical Analyst*. New York.

Jordan, A.J. (1972) *On the ecology and behavior of Cucumaria frondosa (Echinodermata: Holothuroidea) at Lamoine Beach, Maine*. University of Maine.

Jury, S.H., Pugh, T.L., Henninger, H., Carloni, J.T. and Watson, W.H. (2019) ‘Patterns and possible causes of skewed sex ratios in American lobster (*Homarus americanus*) populations’, *Invertebrate Reproduction and Development*, 63(3), pp. 189–199. doi:10.1080/07924259.2019.1595184.

Kim Juniper, S., Matabos, M., Mihá, S., Ajayamohan, R.S., Gervais, F. and Bui, A.O. V (2013) ‘A year in Barkley Canyon: A time-series observatory study of mid-slope benthos and habitat dynamics using the NEPTUNE Canada network’, *Deep-Sea Research II*, 92, pp. 114–123. doi:10.1016/j.dsr2.2013.03.038.

Kincaid, T.M., Olsen, A.R. and Weber, M.H. (2019) ‘spsurvey: Spatial survey design and analysis’. R package.

Kumar, S.S. and Shaikh, T. (2017) ‘Empirical evaluation of the performance of feature selection approaches on random forest’, in *International Conference on Computer and Applications, ICCA*. Institute of Electrical and Electronics Engineers Inc., pp. 227–231. doi:10.1109/COMAPP.2017.8079769.

Kursa, M.B., Jankowski, A. and Rudnicki, W.R. (2010) ‘Boruta - A system for feature selection’, *Fundamenta Informaticae*, 101(4), pp. 271–285. doi:10.3233/FI-2010-288.

Laws, E.A., Falkowski, P.G., Smith, W.O., Ducklow, H. and McCarthy, J.J. (2000) ‘Temperature effects on export production in the open ocean’, *Global Biogeochemical Cycles*, 14(4), pp. 1231–1246. doi:10.1029/1999GB001229.

- Lecours, V., Brown, C.J., Devillers, R., Lucieer, V.L. and Edinger, E.N. (2016) ‘Comparing selections of environmental variables for ecological studies: A focus on terrain attributes’, *PLoS ONE*, 11(12), pp. 1–18. doi:10.1371/journal.pone.0167128.
- Lecours, V., Devillers, R., Schneider, D.C., Lucieer, V.L., Brown, C.J. and Edinger, E.N. (2015) ‘Spatial scale and geographic context in benthic habitat mapping: Review and future directions’, *Marine Ecology Progress Series*, 535, pp. 259–284. doi:10.3354/meps11378.
- Lecours, V., Devillers, R., Simms, A.E., Lucieer, V.L. and Brown, C.J. (2017) ‘Towards a framework for terrain attribute selection in environmental studies’, *Environmental Modelling and Software*, 89, pp. 19–30. doi:10.1016/j.envsoft.2016.11.027.
- Legendre, P. and Gallagher, E.D. (2001) ‘Ecologically meaningful transformations for ordination of species data’, *Oecologia*, 129(2), pp. 271–280. doi:10.1007/S004420100716.
- Legendre, P. and Legendre, L. (2012) *Numerical ecology. Developments in environmental modeling*, Elsevier.
- Leigh, E.G.J., Paine, R.T., Quinn, J.F. and Suchanek, T.H. (1987) ‘Wave energy and intertidal productivity’, *Proceedings of the National Academy of Sciences*, 84(5), pp. 1314–1318. doi:10.1073/PNAS.84.5.1314.
- Leon, A.Z., Huvenne, V.A.I., Benoist, N.M.A., Ferguson, M., Bett, B.J. and Wynn, R.B. (2020) ‘Assessing the repeatability of automated seafloor classification algorithms, with application in marine protected area monitoring’, *Remote Sensing*, 12(10), p. 1572. doi:10.3390/rs12101572.
- Lessin, G., Bruggeman, J., McNeill, C.L. and Widdicombe, S. (2019) ‘Time scales of benthic

macrofaunal response to pelagic production differ between major feeding groups’, *Frontiers in Marine Science*, 6, pp. 1–12. doi:10.3389/fmars.2019.00015.

Levin, S.A. (1992) ‘The problem of pattern and scale in ecology’, *Ecology*, 73(6), pp. 1943–1967. doi:10.2307/1941447.

Loder, J.W., Petrie, B. and Gawarkiewicz, G. (1998) ‘Climate change in the northwest Atlantic’, in Robinson, Allan, R. and Brink, K.H. (eds) *The sea*. John Wiley & Sons, Inc., pp. 105–133.

Loeng, H. *et al.* (2005) ‘Marine systems’, in *Arctic climate impact assessment report*. Cambridge University Press, pp. 453–538.

Lovrich, G.A., Sainte-Marie, B. and Smith, B.D. (1995) ‘Depth distribution and seasonal movements of Chionoecetes opilio (Brachyura: Majidae) in Baie Sainte-Marguerite, Gulf of Saint Lawrence’, *Canadian Journal of Zoology*, 73(9), pp. 1712–1726. doi:10.1139/Z95-203.

Lyons, D.A. and Scheibling, R.E. (2007) ‘Effect of dietary history and algal traits on feeding rate and food preference in the green sea urchin *Strongylocentrotus droebachiensis*’, *Journal of Experimental Marine Biology and Ecology*, 349, pp. 194–204. doi:10.1016/j.jembe.2007.05.012.

Marcello, L.A., Mueter, F.J., Dawe, E.G. and Moriyasu, M. (2012) ‘Effects of temperature and gadid predation on snow crab recruitment: Comparisons between the Bering Sea and Atlantic Canada’, *Marine Ecology Progress Series*, 469, pp. 249–261. doi:10.3354/meps09766.

Mayer, L. *et al.* (2018) ‘The Nippon Foundation—GEBCO Seabed 2030 Project: The Quest to See the World’s Oceans Completely Mapped by 2030’, *Geosciences*, 8(2), p. 63. doi:10.3390/geosciences8020063.

McArthur, M.A. *et al.* (2010) ‘On the use of abiotic surrogates to describe marine benthic biodiversity’, *Estuarine, Coastal and Shelf Science*, 88(1), pp. 21–32. doi:10.1016/j.ecss.2010.03.003.

McLeod, K.L., Lubchenco, J., Palumbi, S.R. and Rosenberg, A.A. (2005) *Scientific Consensus Statement on Marine Ecosystem-Based Management*.

Mercier, A., Battaglene, S.C. and Hamel, J.F. (2000) ‘Periodic movement, recruitment and size-related distribution of the sea cucumber *Holothuria scabra* in Solomon Islands’, *Hydrobiologia*, 440, pp. 81–100. doi:10.1023/A:1004121818691.

Mercier, A. and Hamel, J.F. (2010) ‘Synchronized breeding events in sympatric marine invertebrates: Role of behavior and fine temporal windows in maintaining reproductive isolation’, *Behavioral Ecology and Sociobiology*, 64(11), pp. 1749–1765. doi:10.1007/S00265-010-0987-Z.

Meyer, K.S., Bergmann, M. and Soltwedel, T. (2013) ‘Interannual variation in the epibenthic megafauna at the shallowest station of the HAUSGARTEN observatory (79 N, 6 E)’, *Biogeosciences*, 10, pp. 3479–3492. doi:10.5194/bg-10-3479-2013.

Millard, K. and Richardson, M. (2015) ‘On the importance of training data sample selection in random forest image classification: A case study in peatland ecosystem mapping’, *Remote Sensing*, 7(7), pp. 8489–8515. doi:10.3390/rs70708489.

Miller, R.J. (1975) 'Density of the commercial spider crab, *Chionoecetes opilio*, and calibration of effective area fished per trap using bottom photography', *Journal of the Fisheries Research Board of Canada*, 32(6), pp. 761–768. doi:10.1139/F75-099.

Miller, R.J. and Mann, K.H. (1973) 'Ecological energetics of the seaweed zone in a marine bay on the Atlantic coast of Canada. III. Energy transformations by sea urchins', *Marine Biology*, 18, pp. 99–114.

Mills, E.L. (1989) *Biological oceanography: an early history, 1870-1960*. Cornell University Press.

Misiuk, B., Lecours, V., Dolan, M.F.J. and Robert, K. (2021) 'Evaluating the suitability of multi-scale terrain attribute calculation approaches for seabed mapping applications', *Marine Geodesy*, 44(4), pp. 327–385. doi:10.1080/01490419.2021.1925789.

Mortensen, T.H. (1927) 'Holothurioidea', in *Handbook of the Echinoderms of the British Isles*. Humphrey Milford Oxford University Press, pp. 414–416.

Mullowney, D., Morris, C., Dawe, E., Zagorsky, I. and Goryanova, S. (2018) 'Dynamics of snow crab (*Chionoecetes opilio*) movement and migration along the Newfoundland and Labrador and Eastern Barents Sea continental shelves', *Reviews in Fish Biology and Fisheries*, 28, pp. 435–459. doi:10.1007/s11160-017-9513-y.

Mullowney, D.R.J., Dawe, E.G., Colbourne, E.B. and Rose, G.A. (2014) 'A review of factors contributing to the decline of Newfoundland and Labrador snow crab (*Chionoecetes opilio*)', *Reviews in Fish Biology and Fisheries*, 24, pp. 639–657. doi:10.1007/s11160-014-9349-7.

Nemani, S. (2022) *A species- and traits-based approach to predictive mapping of the distribution and diversity of costal benthic assemblages*. Memorial University of Newfoundland and Labrador.

Nesis, K. (1965) ‘Bioebenoses and biomass of benthos of the Newfoundland-Labrador region’, *Fisheries Research Board of Canada Translation Series No. 1375*, 57, pp. 453–489.

Novaczek, E., Devillers, R., Edinger, E. and Mello, L. (2017) ‘High-resolution seafloor mapping to describe coastal denning habitat of a Canadian species at risk: Atlantic wolffish (*Anarhichas lupus*)’, *Canadian Journal of Fisheries and Aquatic Sciences*, 74(12), pp. 2073–2084. doi:10.1139/cjfas-2016-0414.

O’Brien, J.M., Stanley, R.R.E., Jeffery, N.W., Heaslip, S.G., DiBacco, C. and Wang, Z. (2022) ‘Modeling demersal fish and benthic invertebrate assemblages in support of marine conservation planning’, *Ecological Applications*, 32(3). doi:10.1002/EAP.2546.

Ojeda, J., Marambio, J., Rosenfeld, S., Contador, T., Rozzi, R. and Mansilla, A. (2019) ‘Seasonal changes of macroalgae assemblages on the rocky shores of the Cape Horn biosphere reserve, sub-Antarctic channels, Chile’, *Aquatic Botany*, 157, pp. 33–41. doi:10.1016/J.AQUABOT.2019.06.001.

Parson, L.M. and Evans, A.J. (2005) ‘Seafloor topography and tectonic elements of the Western Indian Ocean’, *Philosophical Transactions of the Royal Society A: Mathematical, Physical and Engineering Sciences*, 363(1826), pp. 15–24. doi:10.1098/RSTA.2004.1472.

Pascelli, C. *et al.* (2013) ‘Seasonal and depth-driven changes in rhodolith bed structure and associated macroalgae off Arvoredo island (southeastern Brazil)’, *Aquatic Botany*, 111,

pp. 62–65. doi:10.1016/J.AQUABOT.2013.05.009.

Peck, L.S. (2018) ‘Antarctic marine biodiversity: Adaptations, environments and responses to change’, in *Oceanography and Marine Biology: An Annual Review*. 1st edn, pp. 105–236.

Pedersen, E.J., Miller, D.L., Simpson, G.L. and Ross, N. (2019) ‘Hierarchical generalized additive models in ecology: An introduction with mgcv’, *PeerJ*, 2019(5). doi:10.7717/peerj.6876.

Pepin, P. and Maillet, G. (2002) *Biological and chemical oceanographic conditions on the Newfoundland shelf during 2001 with comparisons with earlier observations*. Ottawa.

Petrie, B., Akenhead, S., Lazier, J. and Loder, J. (1988) ‘The cold intermediate layer on the Labrador and Northeast Newfoundland Shelves, 1978-1986’, *NAFO Scientific Council Studies*, 12, p. 5769.

Pingree, R.D., Holligan, P.M., Mardell, G.T. and Head, R.N. (1976) ‘The influence of physical stability on spring, summer and autumn phytoplankton blooms in the Celtic Sea’, *Journal of the Marine Biological Association of the United Kingdom*, 56(4), pp. 845–873. doi:10.1017/S0025315400020919.

Pomeroy, L.R., Wiebe, W.J., Deibel, D., Thompson, R.J., Rowe, G.T. and Pakulski, J.D. (1991) ‘Bacterial responses to temperature and substrate concentration during the Newfoundland spring bloom’, *Marine Ecology Progress Series*, 75, pp. 143–159. doi:10.3354/meps075143.

Porskamp, P., Rattray, A., Young, M. and Ierodiaconou, D. (2018) ‘Multiscale and Hierarchical

Classification for Benthic Habitat Mapping', *Geosciences*, 8(4), p. 119.

doi:10.3390/GEOSCIENCES8040119.

Proudfoot, B., Devillers, R., Brown, C.J., Edinger, E. and Copeland, A. (2020) 'Seafloor mapping to support conservation planning in an ecologically unique fjord in Newfoundland and Labrador, Canada', *Journal of Coastal Conservation*, 24(3). doi:10.1007/S11852-020-00746-8.

Radke, L.C. *et al.* (2011) 'Including biogeochemical factors and a temporal component in benthic habitat maps: Influences on infaunal diversity in a temperate embayment', *Marine and Freshwater Research*, 62(12), pp. 1432–1448. doi:10.1071/MF11110.

Ramírez-González, J., Moity, N., Andrade-Vera, S. and Mackliff, H.R. (2020) 'Estimation of age and growth and mortality parameters of the sea cucumber *Isostichopus fuscus* (Ludwig, 1875) and implications for the management of its fishery in the Galapagos Marine Reserve', *Aquaculture and Fisheries*, 5(5), pp. 245–252. doi:10.1016/J-AAF.2020.01.002.

Rattray, A., Ierodiaconou, D., Monk, J., Versace, V.L. and Laurenson, L.J.B. (2013) 'Detecting patterns of change in benthic habitats by acoustic remote sensing', *Marine Ecology Progress Series*, 477, pp. 1–13. doi:10.3354/meps10264.

Redden, A.M. (1994) *Grazer-mediated chloropigment degradation and the vertical flux of spring bloom production in Conception Bay, Newfoundland*. Memorial University of Newfoundland and Labrador.

Richardson, M.D., Tietjen, J.H. and Ray, R.I. (1983) *Environmental support for project WEAP (Weapons environmental acoustic program), east of Montauk Point, New York, 7-28 May*

1982.

Risch, D. *et al.* (2014) ‘Seasonal migrations of North Atlantic minke whales: Novel insights from large-scale passive acoustic monitoring networks’, *Movement Ecology*, 2(24). doi:10.1186/s40462-014-0024-3.

Rooper, C.N. and Zimmermann, M. (2007) ‘A bottom-up methodology for integrating underwater video and acoustic mapping for seafloor substrate classification’, *Continental Shelf Research*, 27, pp. 947–957. doi:10.1016/j.csr.2006.12.006.

Rosa, L.C. and Bemvenuti, C.E. (2006) ‘Temporal variability of the estuarine macrofauna of the Patos Lagoon, Brazil’, *Revista de Biología Marina y Oceanografía*, 41(1), pp. 1–9. doi:10.4067/S0718-19572006000100003.

Ross, N. (2019) ‘Generalized additive models in R: A free interactive course’, p. online.

Sackett, D.K., Able, K.W. and Grothues, T.M. (2007) ‘Dynamics of summer flounder, *Paralichthys dentatus*, seasonal migrations based on ultrasonic telemetry’, *Estuarine, Coastal and Shelf Science*, 74(1–2), pp. 119–130. doi:10.1016/j.ecss.2007.03.027.

Sainte-Marie, B., Urbani, N., Sevigny, J.-M., Hazel, F. and Kuhnlein, U. (1999) ‘Multiple choice criteria and the dynamics of assortative mating during the first breeding season of female snow crab *Chionoecetes opilio* (Brachyura, Majidae)’, *Marine Ecology Progress Series*, 181, pp. 141–153.

Salam, M.A., Azar, A.T., Elgendi, M.S. and Fouad, K.M. (2021) ‘The effect of different dimensionality reduction techniques on machine learning overfitting problem’, *International Journal of Advanced Computer Science and Applications*, 12(4), pp. 641–

655. doi:10.14569/IJACSA.2021.0120480.

Salomon, M. and Dross, M. (2018) ‘Integrating sectoral ocean policies’, in *Handbook on marine environment protection*. Springer International Publishing, pp. 919–931.
doi:10.1007/978-3-319-60156-4_49.

Shindell, D.T., Miller, R.L., Schmidt, G.A. and Pandolfo, L. (1999) ‘Simulation of recent northern winter climate trends by greenhouse-gas forcing’, *Nature*, 399(6735), pp. 452–455. doi:10.1038/20905.

Singh, R., MacDonald, B.A., Thomas, M.L.H. and Lawton, P. (1999) ‘Patterns of seasonal and tidal feeding activity in the dendrochirote sea cucumber *Cucumaria frondosa* (Echinodermata: Holothuroidea) in the Bay of Fundy, Canada’, *Marine Ecology Progress Series*, 187, pp. 133–145. doi:10.3354/MEPS187133.

Sorokin, Y.I. (1995) *Coral Reef Ecology*. Berlin, Heidelberg: Springer Berlin Heidelberg (Ecological Studies). doi:10.1007/978-3-642-80046-7.

Stanley, D.J. and James, N.P. (1971) *Distribution of Echinorachnius parma (Lamarck) and associated fauna on Sable Island Bank, southeast Canada, Smithsonian contributions to the earth sciences*. doi:10.5479/si.00810274.6.1.

Stevens Jr., D.L. and Olsen, A.R. (2004) ‘Spatially balanced sampling of natural resources’, *Journal of the American Statistical Association*, 99, pp. 262–278.
doi:10.1198/016214504000000250.

Stevens, T. and Connolly, R.M. (2004) ‘Testing the utility of abiotic surrogates for marine habitat mapping at scales relevant to management’, *Biological Conservation*, 119(3), pp.

351–362. doi:10.1016/j.biocon.2003.12.001.

Strong, J.A. (2020) ‘An error analysis of marine habitat mapping methods and prioritised work packages required to reduce errors and improve consistency’, *Estuarine, Coastal and Shelf Science*, 240, p. 106684. doi:10.1016/j.ecss.2020.106684.

Stroud, J.T., Bush, M.R., Ladd, M.C., Nowicki, R.J., Shantz, A.A. and Sweatman, J. (2015) ‘Is a community still a community? Reviewing definitions of key terms in community ecology’, *Ecology and Evolution*, 5(21), pp. 4757–4765. doi:10.1002/ECE3.1651.

Sun, J., Hamel, J.F., Gianasi, B.L. and Mercier, A. (2019) ‘Age determination in echinoderms: First evidence of annual growth rings in holothuroids’, *Proceedings of the Royal Society B: Biological Sciences*, 286(1906). doi:10.1098/rspb.2019.0858.

Tamelander, T., Reigstad, M., Hop, H., Carroll, M.L. and Wassmann, P. (2008) ‘Pelagic and sympagic contribution of organic matter to zooplankton and vertical export in the Barents Sea marginal ice zone’, *Deep-Sea Research Part II: Topical Studies in Oceanography*, 55(20), pp. 2330–2339. doi:10.1016/J.DSR2.2008.05.019.

Thibaut, L.M., Connolly, S.R., Sweatman, H.P.A. and Aronson, R.B. (2012) ‘Diversity and stability of herbivorous fishes on coral reefs’, *Ecology*, 93(4), pp. 891–901. doi:10.1890/11-1753.1.

Thompson, R.J., Deibel, D., Redden, A.M. and McKenzie, C.H. (2008) ‘Vertical flux and fate of particulate matter in a Newfoundland fjord at sub-zero water temperatures during spring’, *Marine Ecology Progress Series*, 357, pp. 33–49. doi:10.3354/MEPS07277.

Tian, R.C., Deibel, D., Thompson, R.J. and Rivkin, R.B. (2003) ‘Modeling of climate forcing on

a cold-ocean ecosystem, Conception Bay, Newfoundland', *Marine Ecology Progress Series*, 262, pp. 1–17. doi:10.3354/meps262001.

Trombetta, T., Vidussi, F., Mas, S., Parin, D., Simier, M. and Mostajir, B. (2019) 'Water temperature drives phytoplankton blooms in coastal waters', *PLOS ONE*, 14(4). doi:10.1371/JOURNAL.PONE.0214933.

Turner, M.G. and Gardner, R.H. (2015) 'Introduction to Landscape Ecology and Scale', in *Landscape Ecology in Theory and Practice Pattern and Process*. New York: Springer, pp. 1–32.

Valentine, J.W. (1983) 'Seasonality: effects in marine benthic communities.', in *Biotic interactions in recent and fossil benthic communities*. New York: Spring Science and Business Media, pp. 121–156. doi:10.1007/978-1-4757-0740-3_3.

Valiela, I. (2015) 'Temporal structure: Perturbation, colonization, succession', in *Marine Ecological Processes*. 3rd edn. Springer, pp. 437–465.

Valiela, I. (2016) *Marine ecological processes*, *Marine Ecological Processes*. doi:10.1007/978-0-387-79070-1.

Walbridge, S., Slocum, N., Pobuda, M. and Wright, D.J. (2018) 'Unified geomorphological analysis workflows with benthic terrain modeler', *Geosciences 2018, Vol. 8, Page 94*, 8(3), p. 94. doi:10.3390/GEOSCIENCES8030094.

Webb, G.I. *et al.* (2011) 'Leave-One-Out Cross-Validation', *Encyclopedia of Machine Learning*. Springer, Boston, MA. doi:10.1007/978-0-387-30164-8_469.

Wilson, J.B. and Chiarucci, A. (2000) 'Do plant communities exist? Evidence from scaling-up

local species-area relations to the regional level', *Journal of Vegetation Science*, 11(5), pp. 773–775. doi:10.2307/3236582.

Wilson, M.F.J., O'Connell, B., Brown, C., Guinan, J.C. and Grehan, A.J. (2007) *Multiscale terrain analysis of multibeam bathymetry data for habitat mapping on the continental slope*, *Marine Geodesy*. doi:10.1080/01490410701295962.

Wisz, M.S. et al. (2013) 'The role of biotic interactions in shaping distributions and realised assemblages of species: implications for species distribution modelling', *Biological Reviews*, 88(1), pp. 15–30. doi:10.1111/J.1469-185X.2012.00235.X.

Wölfel, A.-C. et al. (2019) 'Seafloor mapping – the challenge of a truly global ocean bathymetry', *Frontiers in Marine Science*, 6, p. 283. doi:10.3389/fmars.2019.00283.

Wood, S.N. (2011) 'Fast stable restricted maximum likelihood and marginal likelihood estimation of semiparametric generalized linear models', *Journal of the Royal Statistical Society: Series B (Statistical Methodology)*, 73(1), pp. 3–36. doi:10.1111/J.1467-9868.2010.00749.X.

Wood, S.N. (2017) *Generalized additive models: An introduction with R*. 2nd edn. New York: CRC Press. doi:10.1201/9781315370279/GENERALIZED-ADDITIONAL-MODELS-SIMON-WOOD.

Yamana, Y., Hamano, T. and Goshima, S. (2009) 'Seasonal distribution pattern of adult sea cucumber Apostichopus japonicus (Stichopodidae) in Yoshimi Bay, western Yamaguchi Prefecture, Japan', *Fisheries Science*, 75(3), pp. 585–591. doi:10.1007/S12562-009-0076-2.

Yingst, J.Y. (1976) 'The utilization of organic matter in shallow marine sediments by an epibenthic deposit-feeding holothurian', *Journal of Experimental Marine Biology and Ecology*, 23(1), pp. 55–69. doi:10.1016/0022-0981(76)90085-X.

de Young, B. and Sanderson, B. (1995) 'The circulation and hydrography of Conception Bay, Newfoundland', *Atmosphere - Ocean*, 33(1), pp. 135–162. doi:10.1080/07055900.1995.9649528.

Ysebaert, T., Meire, P., Herman, P.M.J. and Verbeek, H. (2002) 'Macrofaunal species response surfaces along estuarine gradients: Prediction by logistic regression', *Marine Ecology Progress Series*, 225, pp. 79–95. doi:10.3354/MEPS225079.

Zajac, R.N., Stefaniak, L.M., Babb, I., Conroy, C.W., Penna, S., Chadi, D. and Auster, P.J. (2020) 'An integrated seafloor habitat map to inform marine spatial planning and management: a case study from Long Island Sound (Northwest Atlantic)', in *Seafloor Geomorphology as Benthic Habitat*. Elsevier, pp. 199–217. doi:10.1016/B978-0-12-814960-7.00010-5.

Zeppilli, D., Pusceddu, A., Trincardi, F. and Danovaro, R. (2016) 'Seafloor heterogeneity influences the biodiversity–ecosystem functioning relationships in the deep sea', *Scientific Reports*, 6, pp. 1–12. doi:10.1038/srep26352.

Zevenbergen, L.W. and Thorne, C.R. (1987) 'Quantitative analysis of land surface topography', *Earth Surface Processes and Landforms*, 12(1), pp. 47–56. doi:10.1002/ESP.3290120107.

Zhang, Q., Warwick, R.M., McNeill, C.L., Widdicombe, C.E., Sheehan, A. and Widdicombe, S. (2015) 'An unusually large phytoplankton spring bloom drives rapid changes in benthic

diversity and ecosystem function', *Progress in Oceanography*, 137, pp. 533–545.
doi:10.1016/J.POCEAN.2015.04.029.

Zheng, B., Li, Y., Li, J., Shu, F. and He, J. (2017) 'Impact of tropical cyclones on the evolution of the monsoon-driven upwelling system in the coastal waters of the northern South China Sea', *Ocean Dynamics*, 68(2), pp. 223–237. doi:10.1007/S10236-017-1126-4.

Zisserson, B. and Cook, A. (2017) 'Impact of bottom water temperature change on the southernmost snow crab fishery in the Atlantic Ocean', *Fisheries Research*, 195, pp. 12–18. doi:10.1016/j.fishres.2017.06.009.

Appendix A – Rasters of Environmental Variables

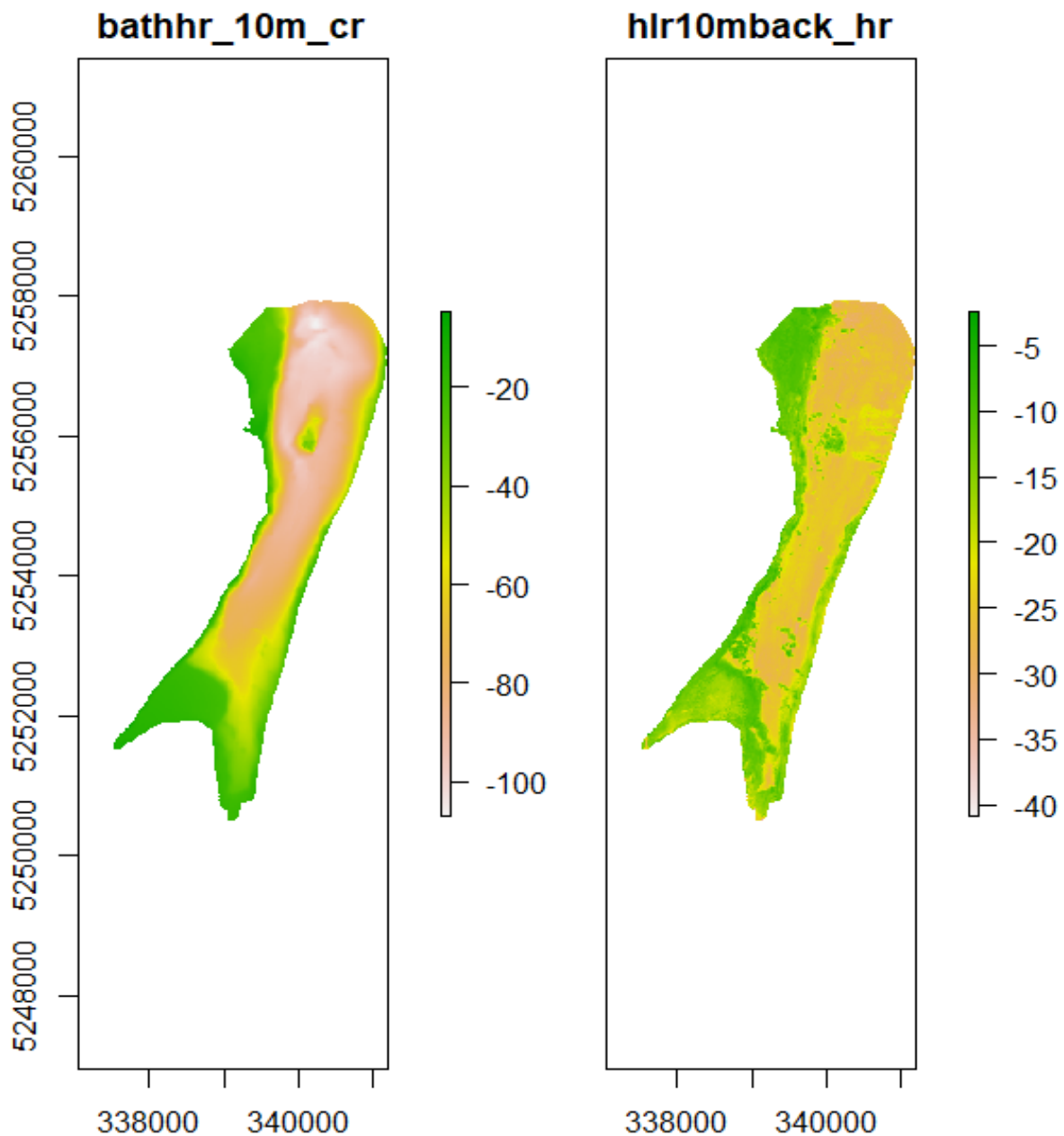


Figure A-1. Raster of the study site, Holyrood Bay, with raw data overlaid; (A) bathymetry and (B) backscatter. The data is gridded at 10m x 10m using projection UTM 22N.

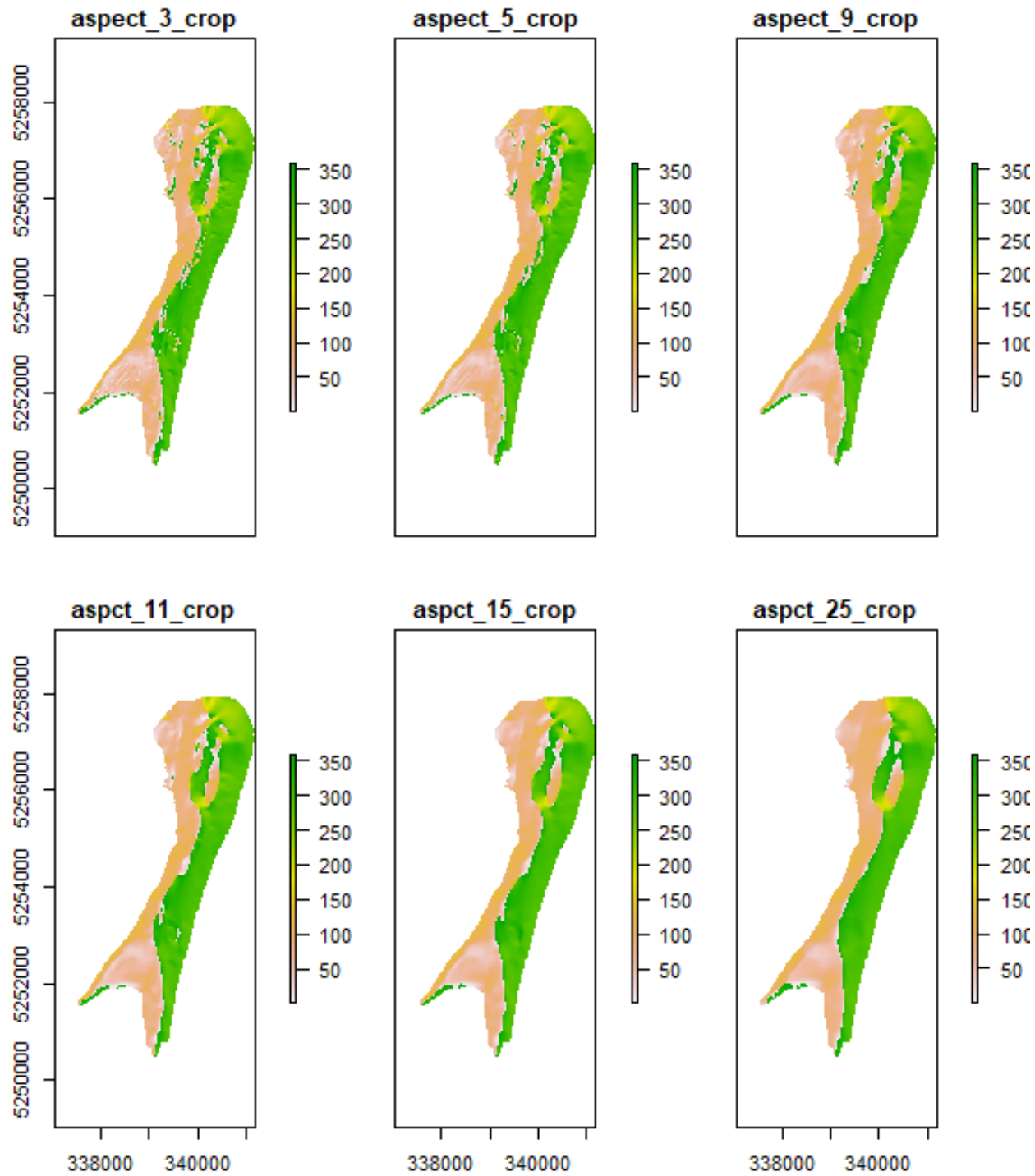


Figure A-2. Raster of the study site, Holyrood Bay, with derived Aspect overlayed, calculated at multiple scales; (A) 3 x 3 window, (B) 5 x 5 window, (C) 9 x 9 window, (D) 11 x 11 window, (E) 15 x 15 window, and (F) 25 x 25 window. The data is gridded at 10m x 10m using projection UTM 22N.

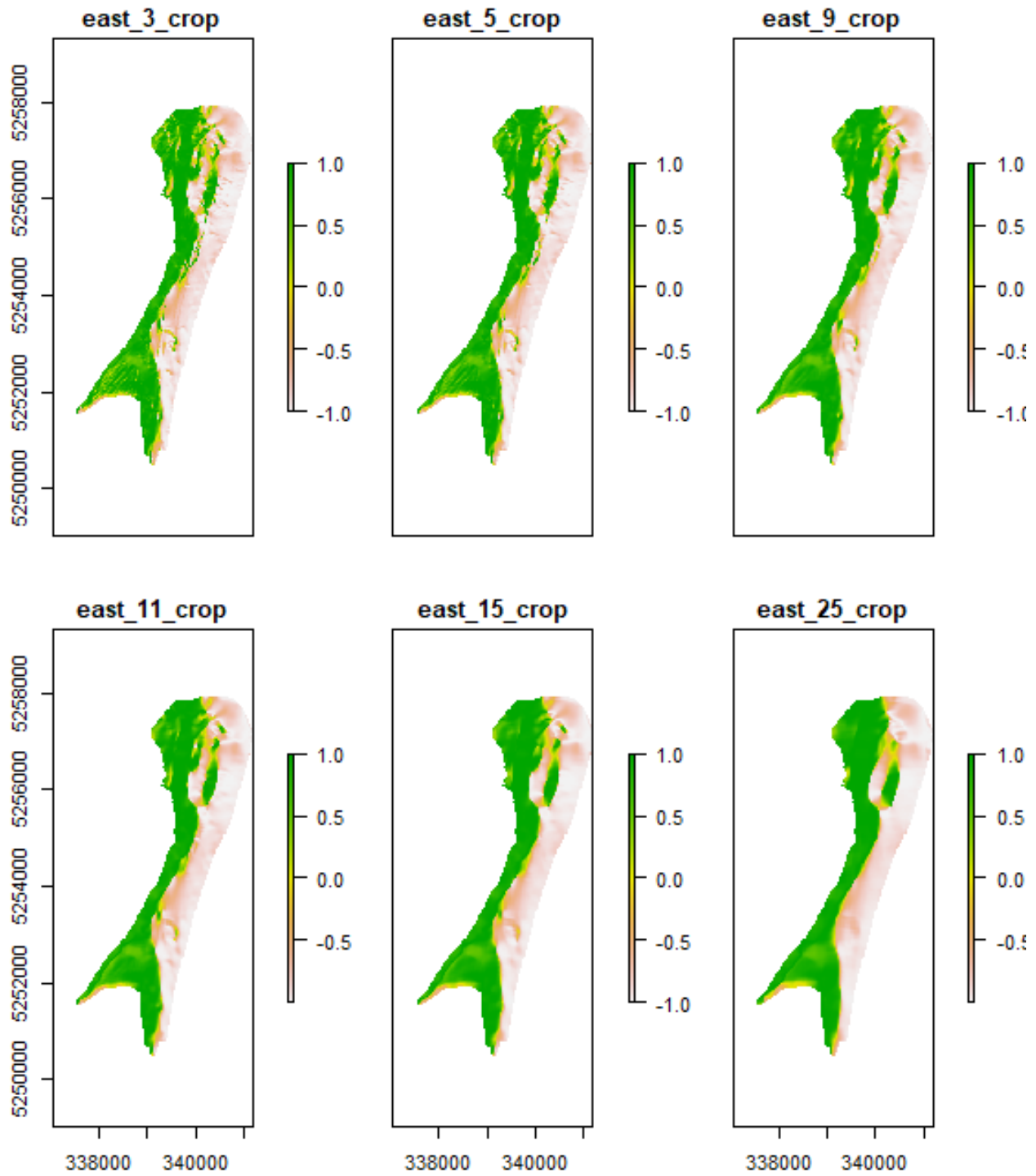


Figure A-3. Raster of the study site, Holyrood Bay, with derived Eastness overlayed, calculated at multiple scales; (A) 3 x 3 window, (B) 5 x 5 window, (C) 9 x 9 window, (D) 11 x 11 window, (E) 15 x 15 window, and (F) 25 x 25 window. The data is gridded at 10m x 10m using projection UTM 22N.

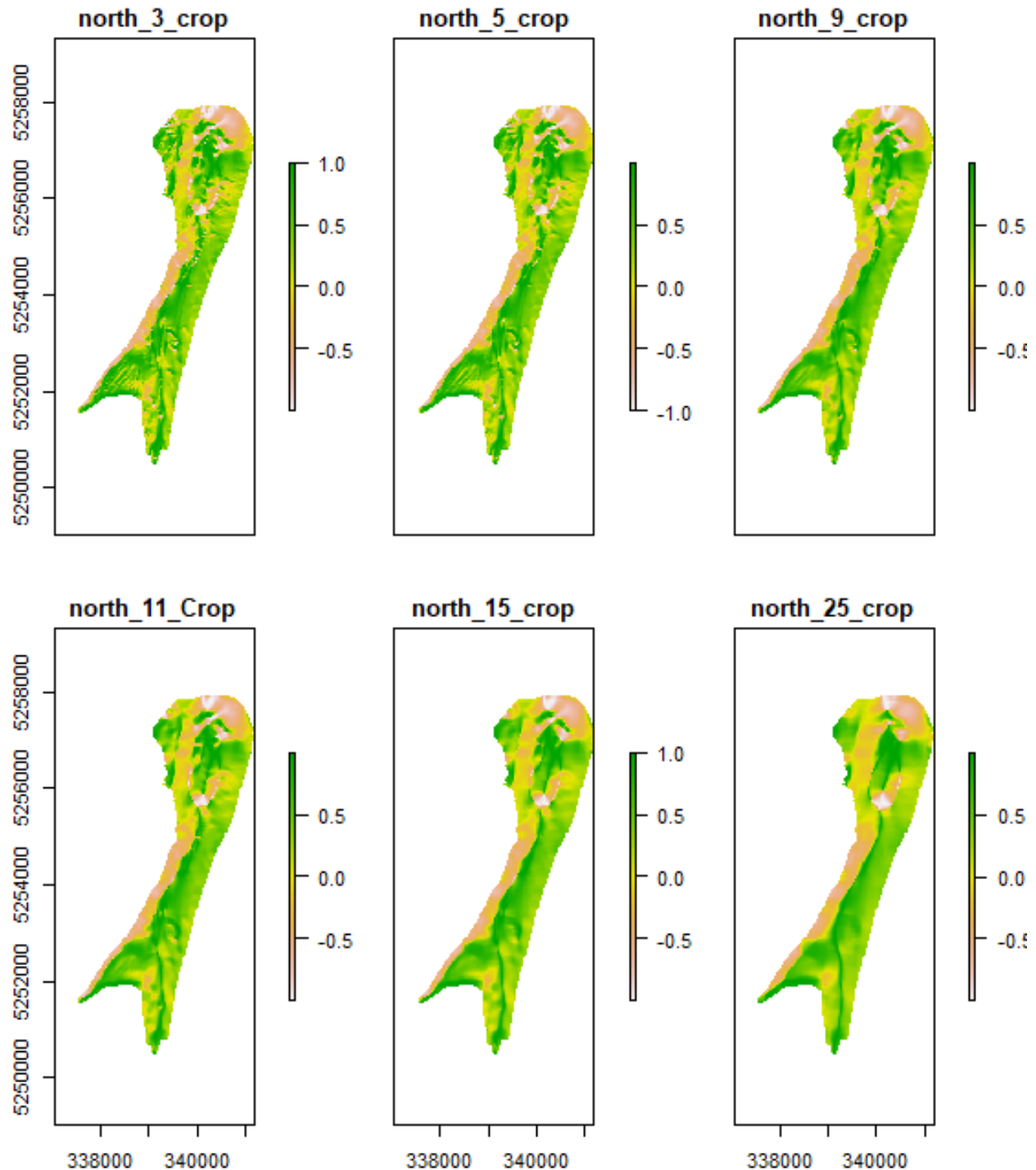


Figure A-4. Raster of the study site, Holyrood Bay, with derived Northness overlayed, calculated at multiple scales; (A) 3 x 3 window, (B) 5 x 5 window, (C) 9 x 9 window, (D) 11 x 11 window, (E) 15 x 15 window, and (F) 25 x 25 window. The data is gridded at 10m x 10m using projection UTM 22N.

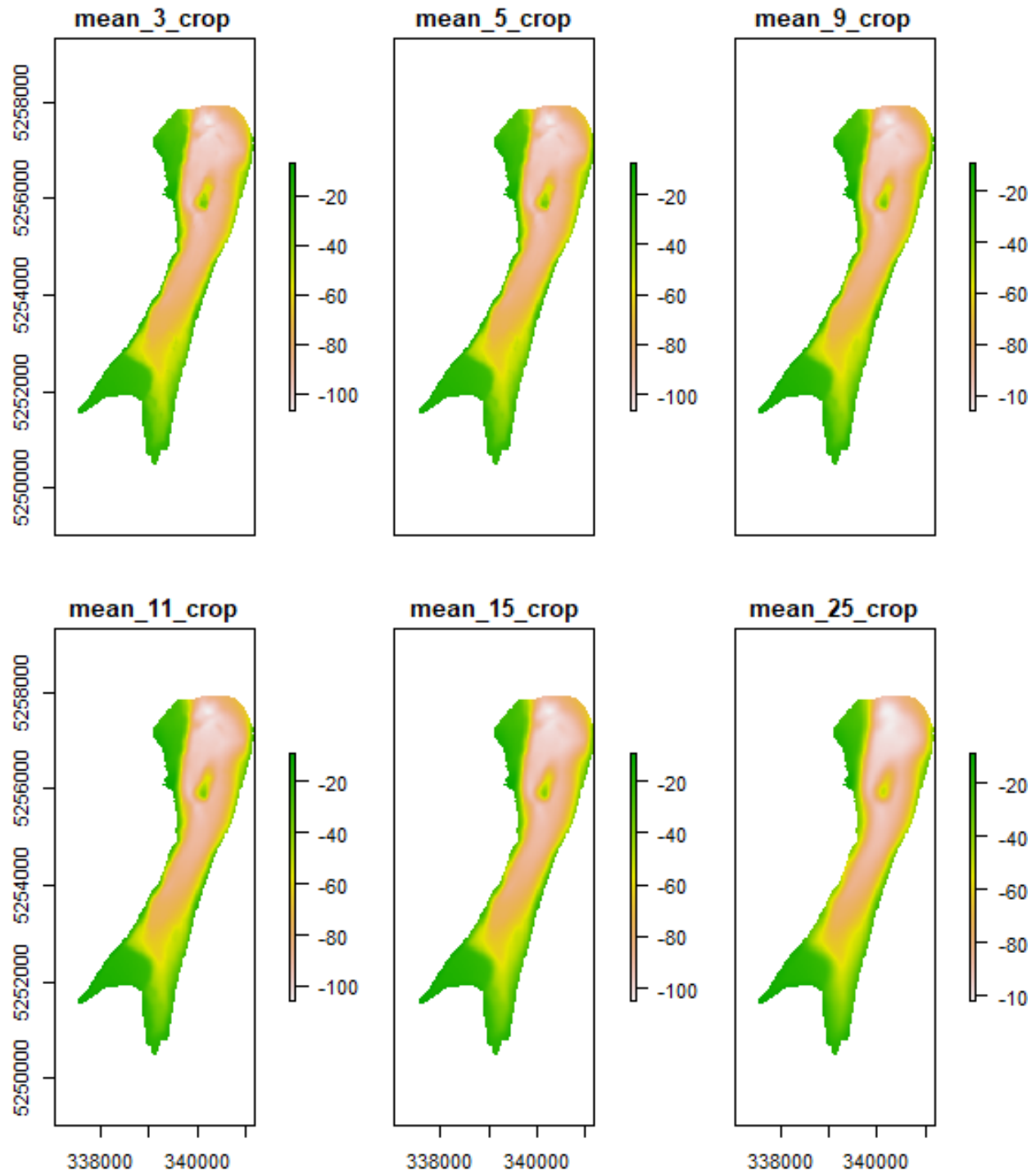


Figure A-5. Raster of the study site, Holyrood Bay, with derived Local Mean overlaid, calculated at multiple scales; (A) 3 x 3 window, (B) 5 x 5 window, (C) 9 x 9 window, (D) 11 x 11 window, (E) 15 x 15 window, and (F) 25 x 25 window. The data is gridded at 10m x 10m using projection 22N.

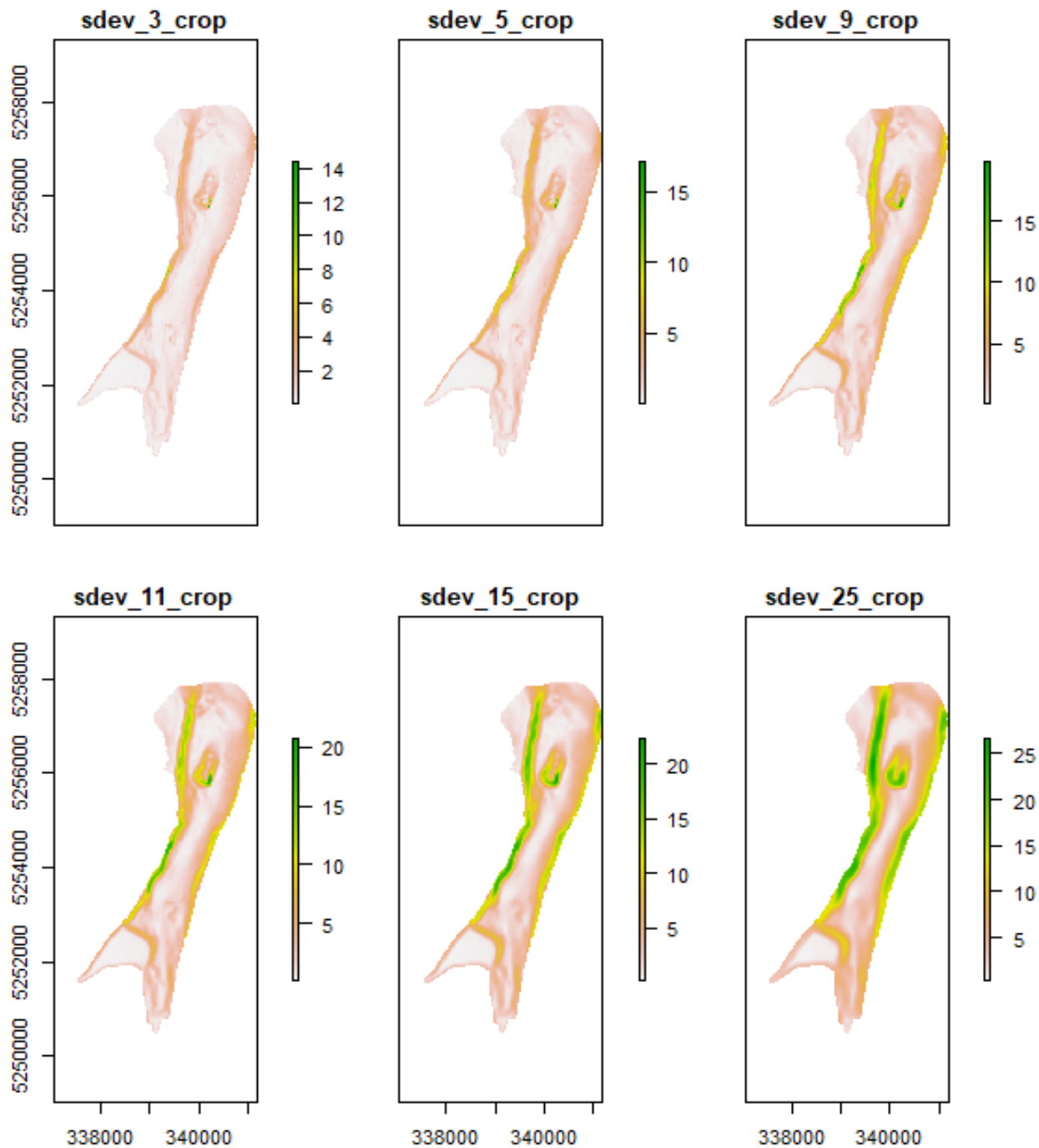


Figure A-6. Raster of the study site, Holyrood Bay, with derived Local Standard Deviation overlaid, calculated at multiple scales; (A) 3 x 3 window, (B) 5 x 5 window, (C) 9 x 9 window, (D) 11 x 11 window, (E) 15 x 15 window, and (F) 25 x 25 window. The data is gridded at 10m x 10m using projection UTM 22N.

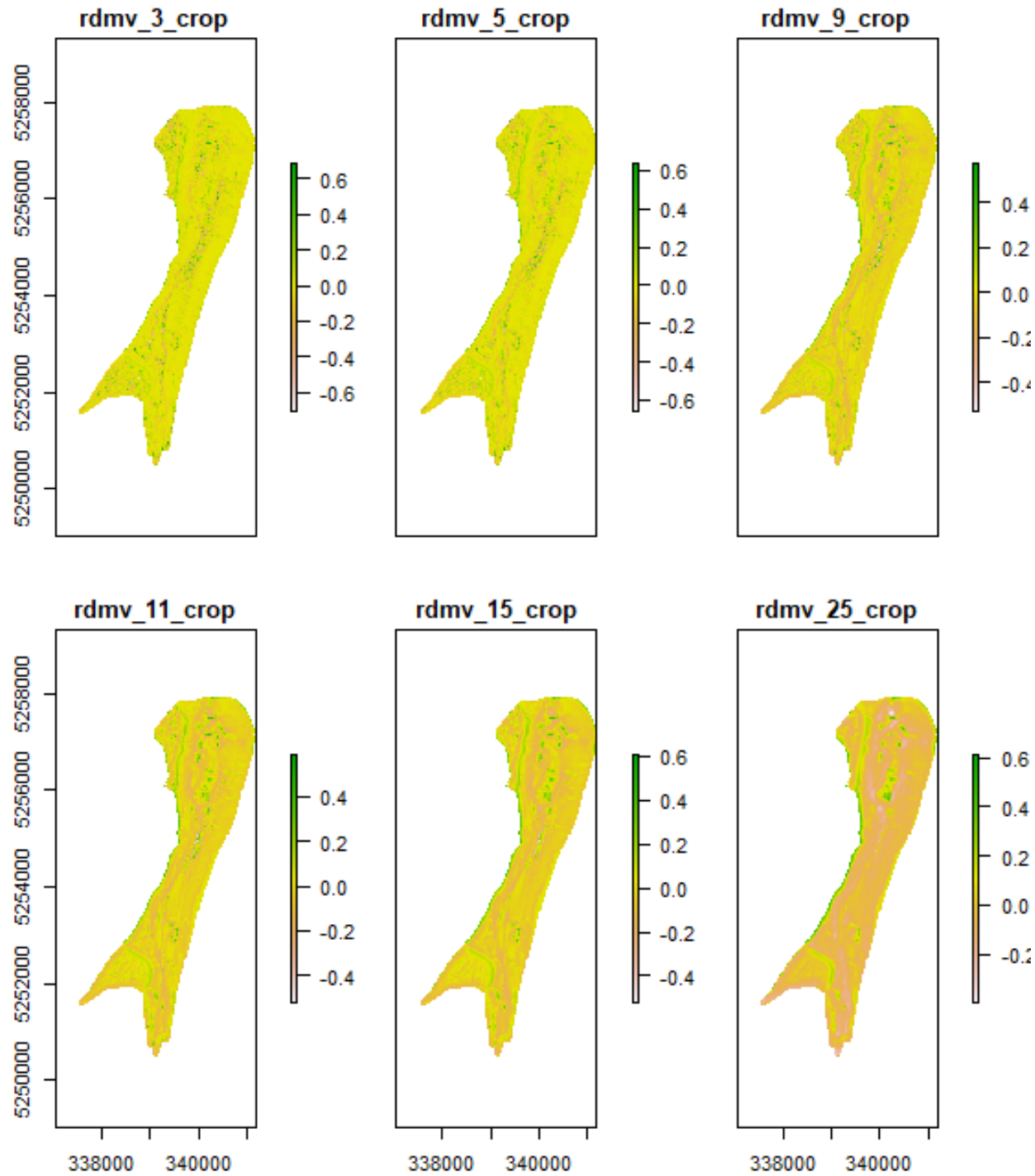


Figure A-7. Raster of the study site, Holyrood Bay, with derived Relative Deviation from the Mean Value (RDMV) overlayed, calculated at multiple scales; (A) 3 x 3 window, (B) 5 x 5 window, (C) 9m x 9m window, (D) 11m x 11m window, (E) 15m x 15m window, and (F) 25m x 25m window. The data is gridded at 10m x 10m using projection UTM 22N.

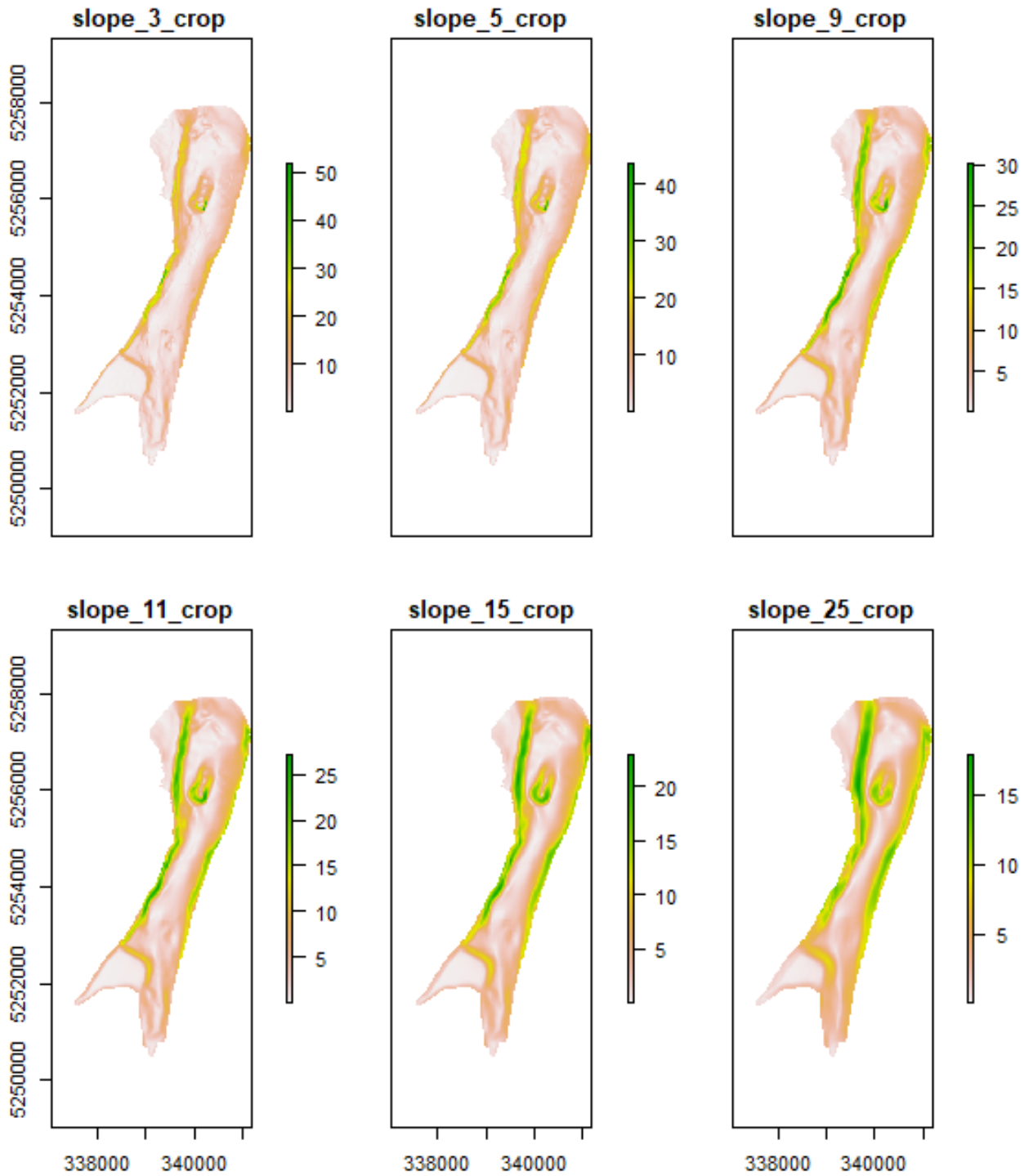


Figure A-8. Raster of the study site, Holyrood Bay, with derived Slope overlaid, calculated at multiple scales; (A) 3 x 3 window, (B) 5 x 5 window, (C) 9 x 9 window, (D) 11 x 11 window, (E) 15 x 15 window, and (F) 25 x 25 window. The data is gridded at 10m x 10m using projection UTM 22N.

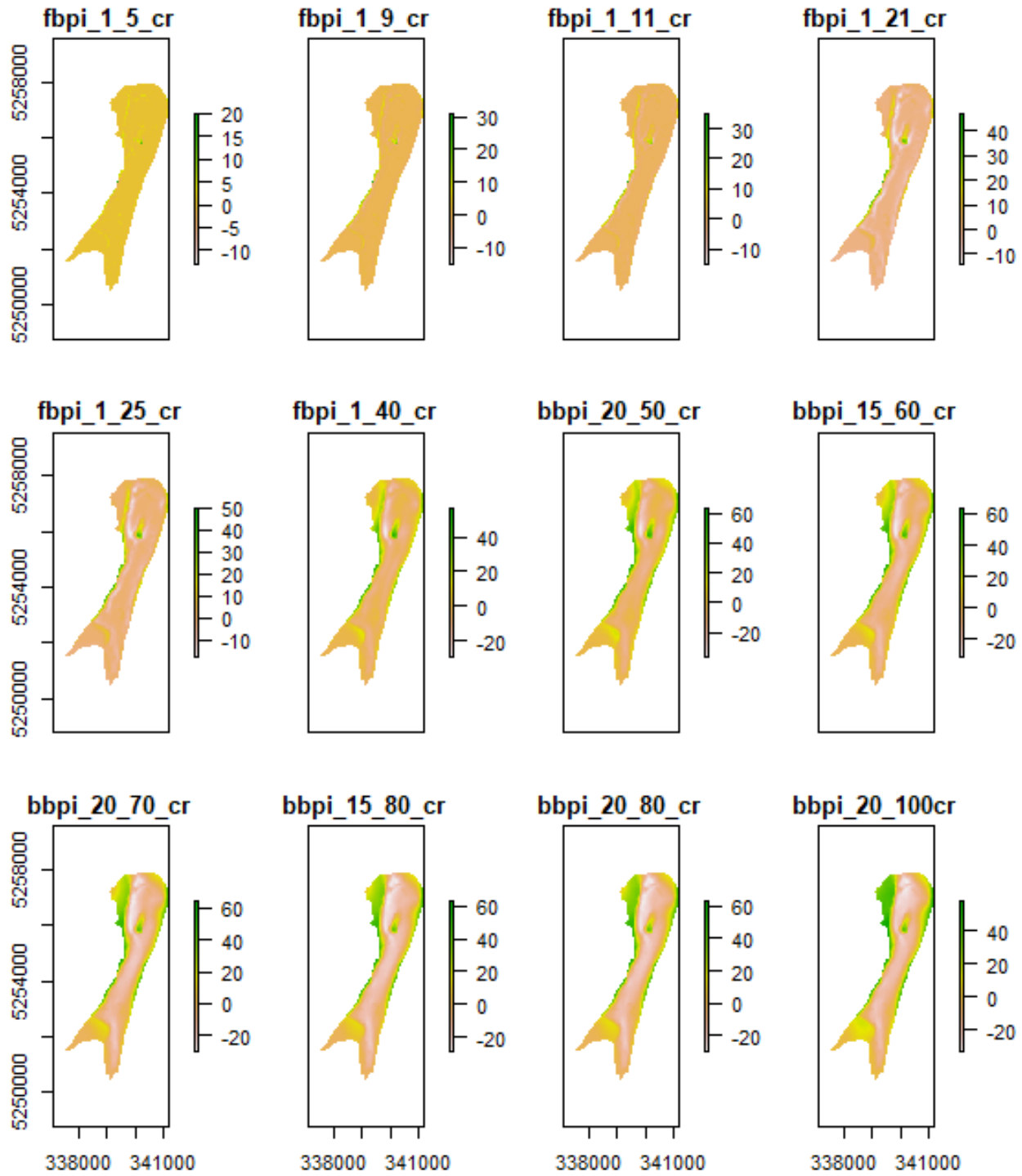


Figure A-9. Raster of the study site, Holyrood Bay, with derived Bathymetric Position Index (BPI) overlayed, calculated at multiple inner diameters and outer diameters (ID-OD); (A) 1-5, (B) 1-9, (C) 1-11, (D) 1-21, (E) 1-25, (F) 1-40, (G) 20-50, (H) 15-60, (I) 20-70, (J) 15-80, (K) 20-80, and (L) 20-100. The data is gridded at 10m x 10m using projection UTM 22N.

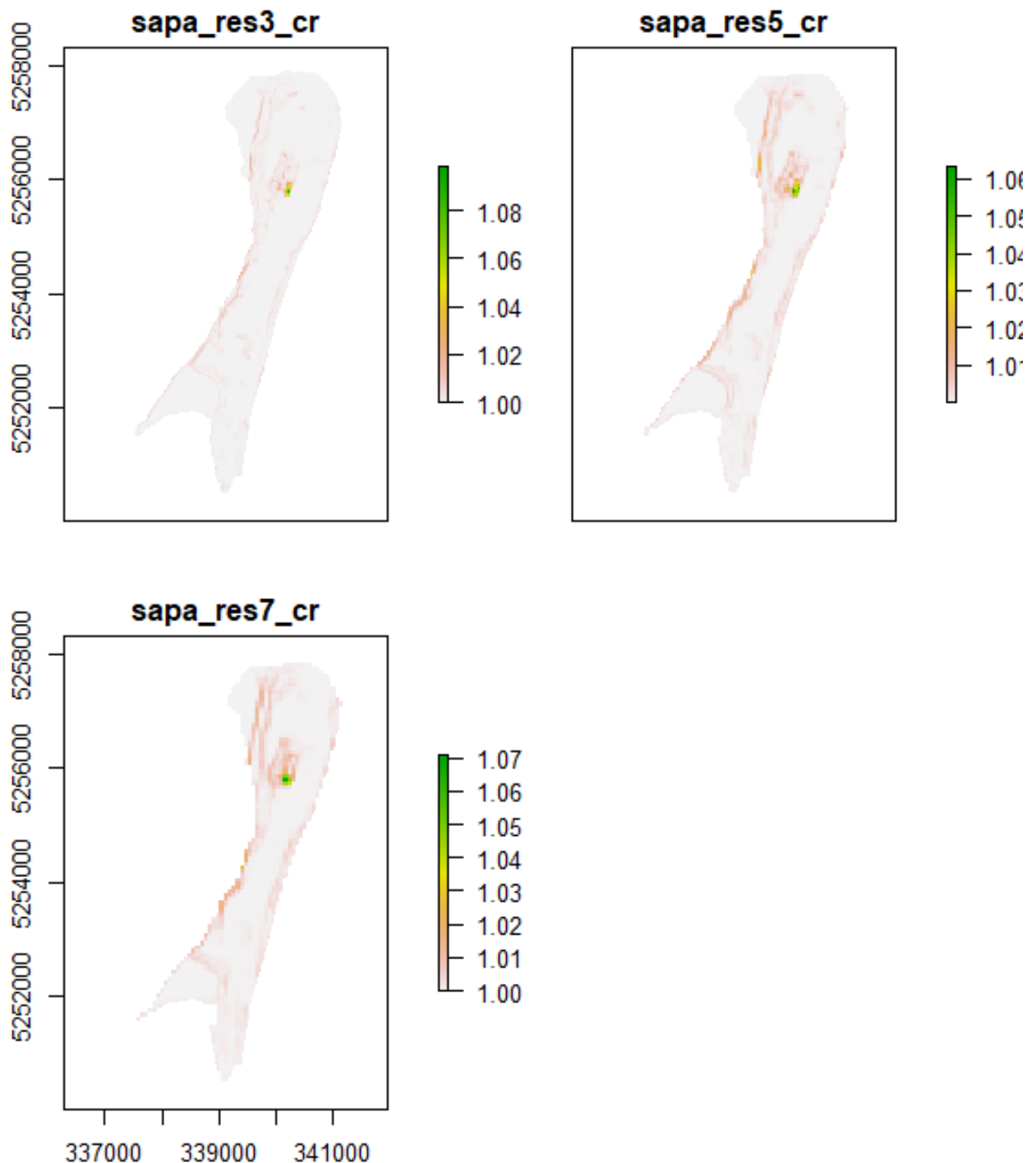


Figure A-10. Raster of the study site, Holyrood Bay, with derived Surface Area to Planar Area Ratio overlaid, calculated at multiple scales; (A) 3 x 3 window, (B) 5 x 5 window, and (C) 7 x 7 window. The data is gridded at 10m x 10m using projection UTM 22N.

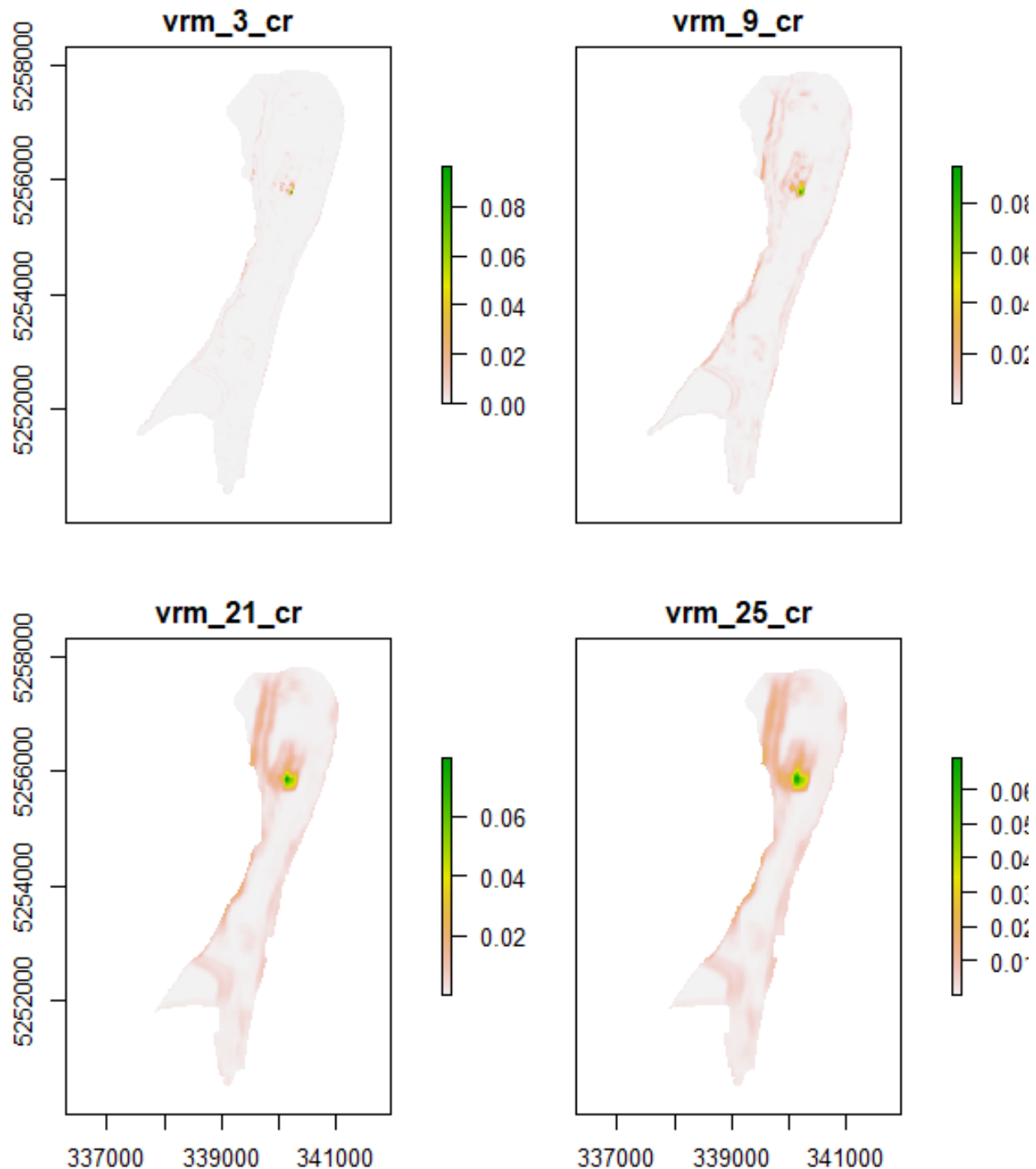


Figure A-11. Raster of the study site, Holyrood Bay, with derived Vector Ruggedness Measure overlaid, calculated at multiple scales; (A) 3 x 3 window, (B) 9 x 9 window, (C) 21 x 21 window, and (D) 25 x 25 window. The data is gridded at 10m x 10m using projection UTM 22N.

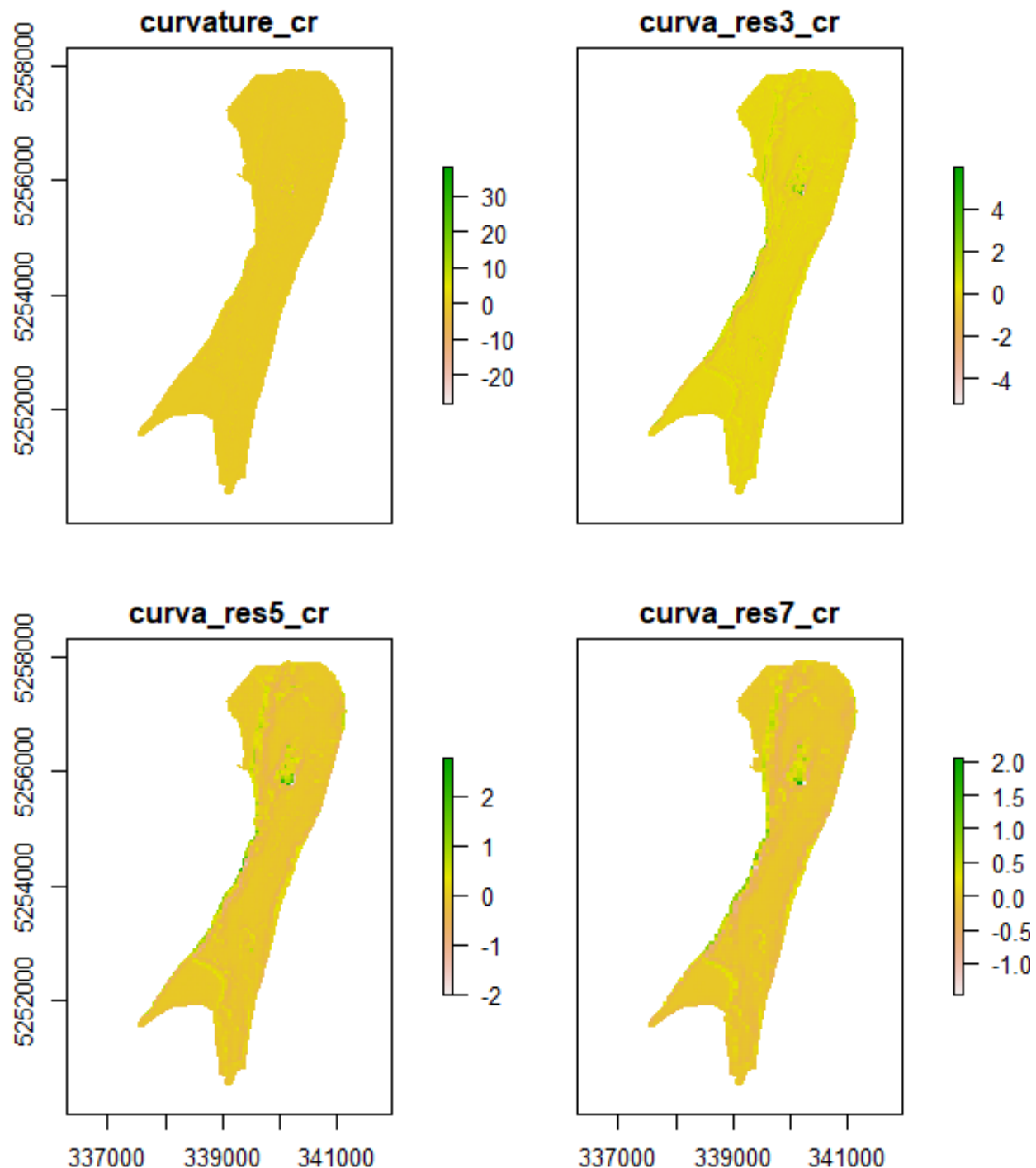


Figure A-12. Raster of the study site, Holyrood Bay, with derived Curvature overlaid, calculated at multiple scales; (A) 3 x 3 window, (B) 9 x 9 window, (C) 15 x 15 window, and (D) 21 x 21 window. The data is gridded at 10m x 10m using projection UTM 22N.

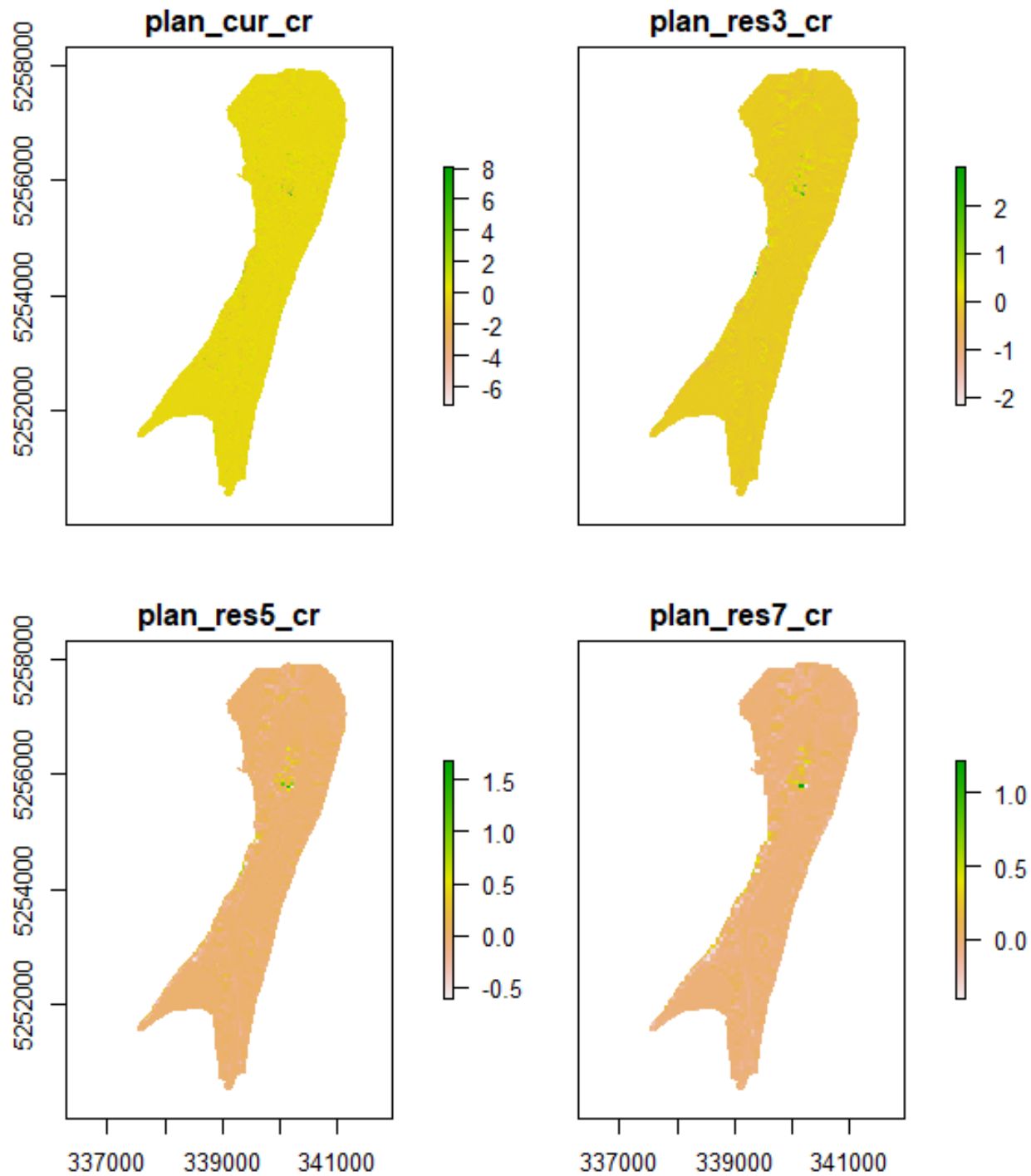


Figure A-13. Raster of the study site, Holyrood Bay, with derived Planar Curvature overlaid, calculated at multiple scales; (A) 3 x 3 window, (B) 9 x 9 window, (C) 15 x 15 window, and (D) 21 x 21 window. The data is gridded at 10m x 10m using projection UTM 22N.

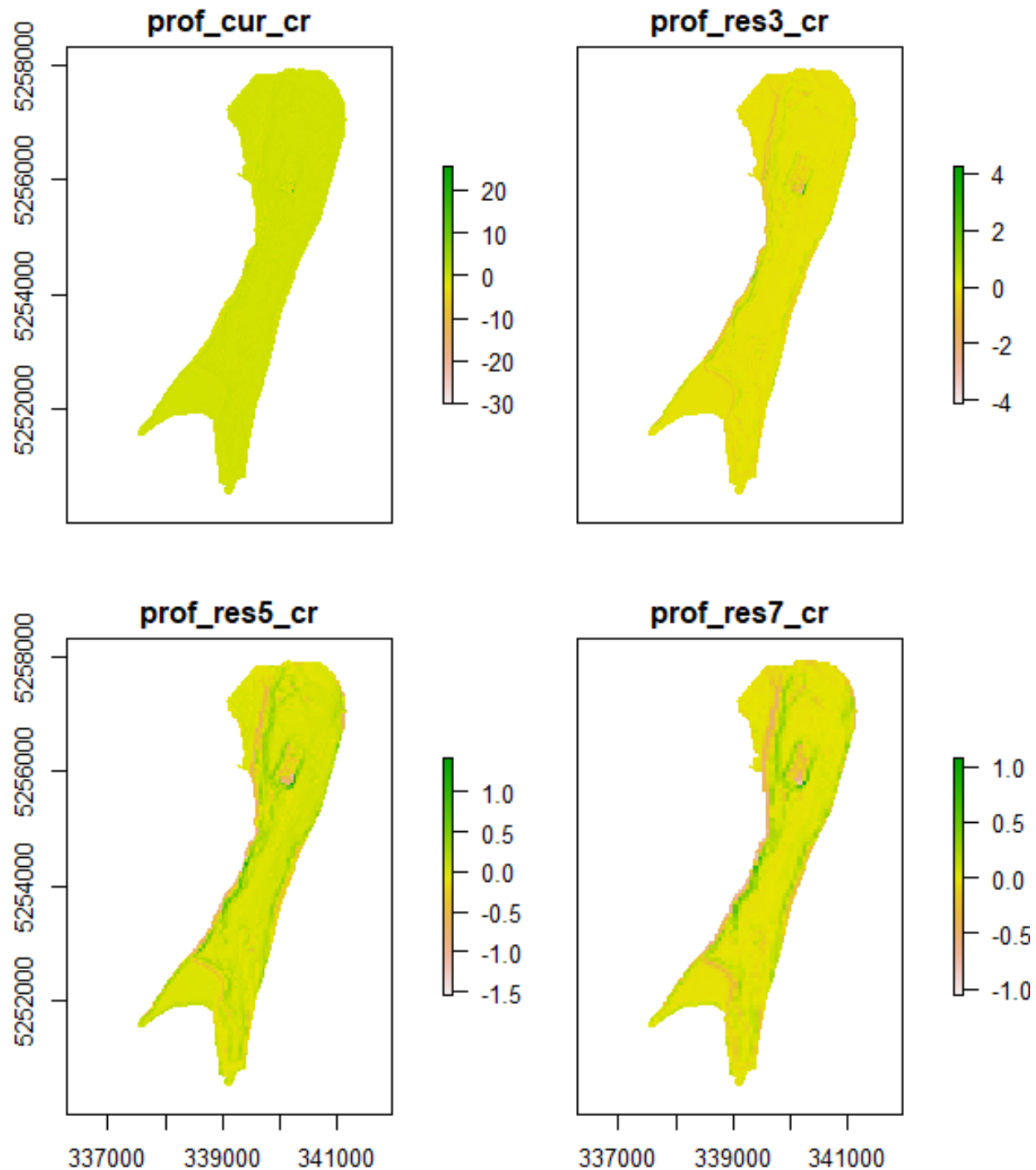


Figure A-14. Raster of the study site, Holyrood Bay, with derived Profile Curvature overlaid, calculated at multiple scales; (A) 3 x 3 window, (B) 9 x 9 window, (C) 15 x 15 window, and (D) 21 x 21 window. The data is gridded at 10m x 10m using projection UTM 22N.

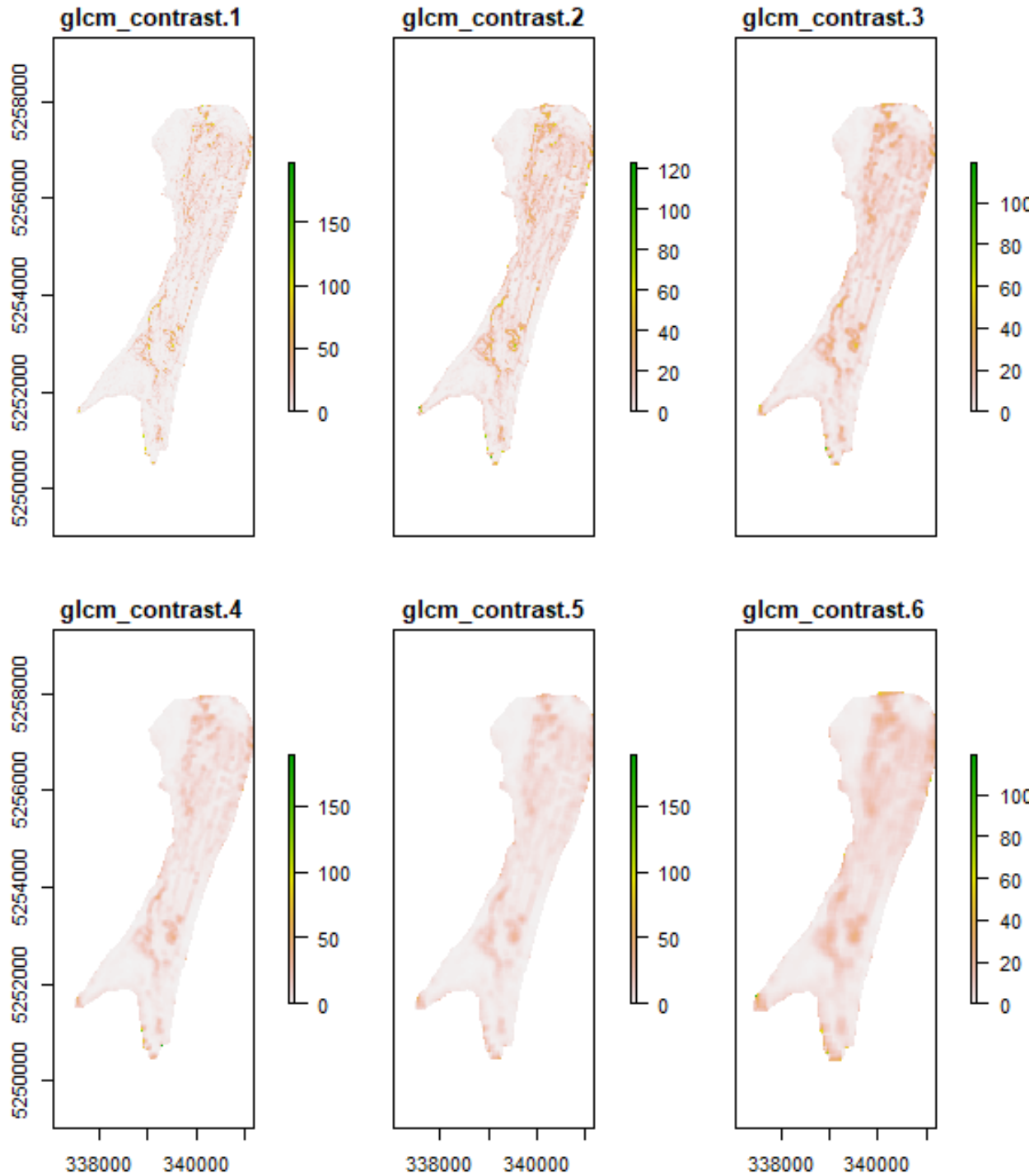


Figure A-15. Raster of the study site, Holyrood Bay, with derived GLCM Contrast overlaid, calculated at multiple scales; (A) 3 x 3 window, (B) 5 x 5 window, (C) 9 x 9 window, (D) 11 x 11 window, (E) 15 x 15 window, (F) 21 x 21 window. The data is gridded at 10m x 10m using projection UTM 22N.

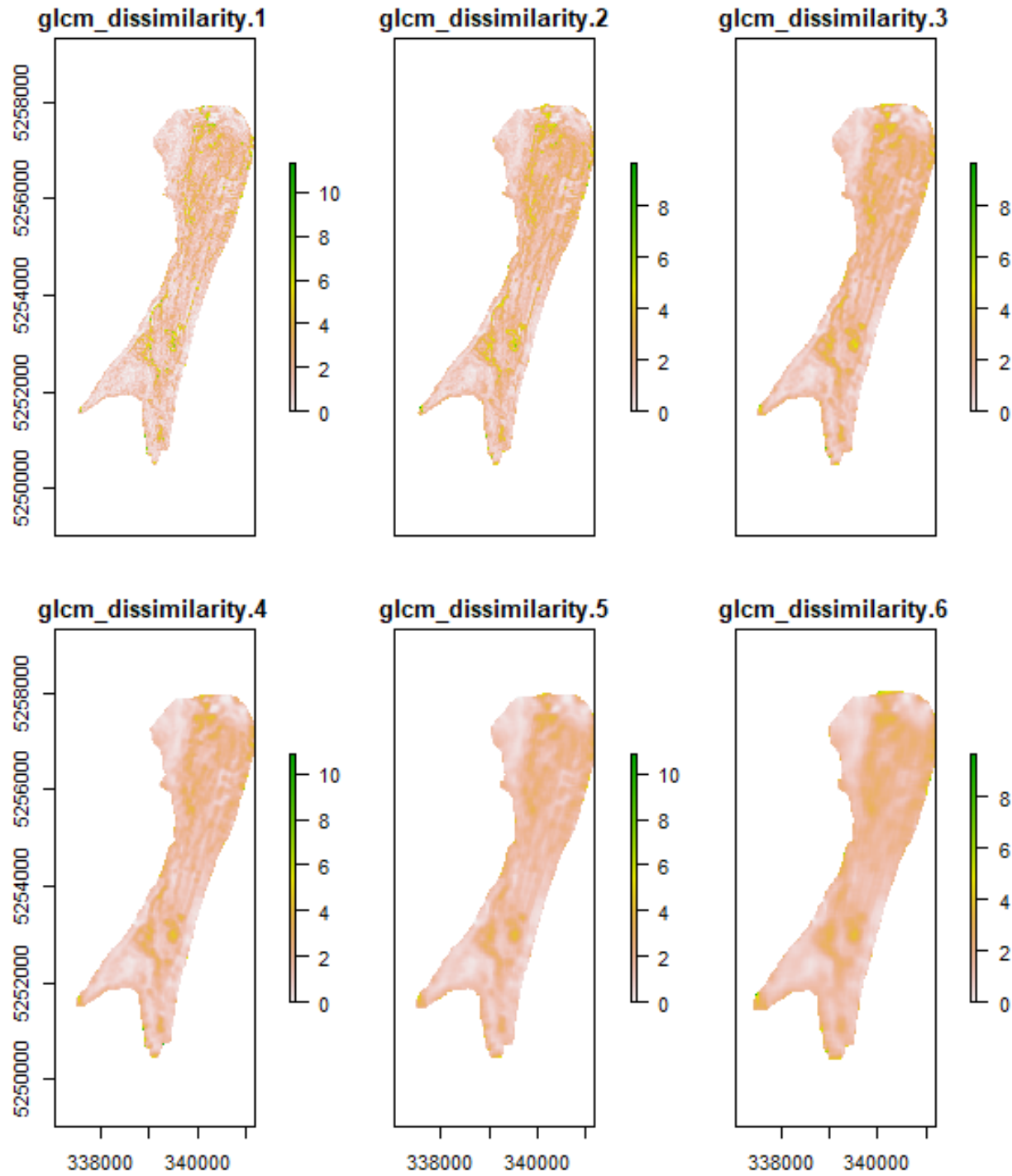


Figure A-16. Raster of the study site, Holyrood Bay, with derived GLCM Dissimilarity overlaid, calculated at multiple scales; (A) 3×3 window, (B) 5×5 window, (C) 9×9 window, (D) 11×11 window, (E) 15×15 window, (F) 21×21 window. The data is gridded at 10m x 10m using projection UTM 22N.

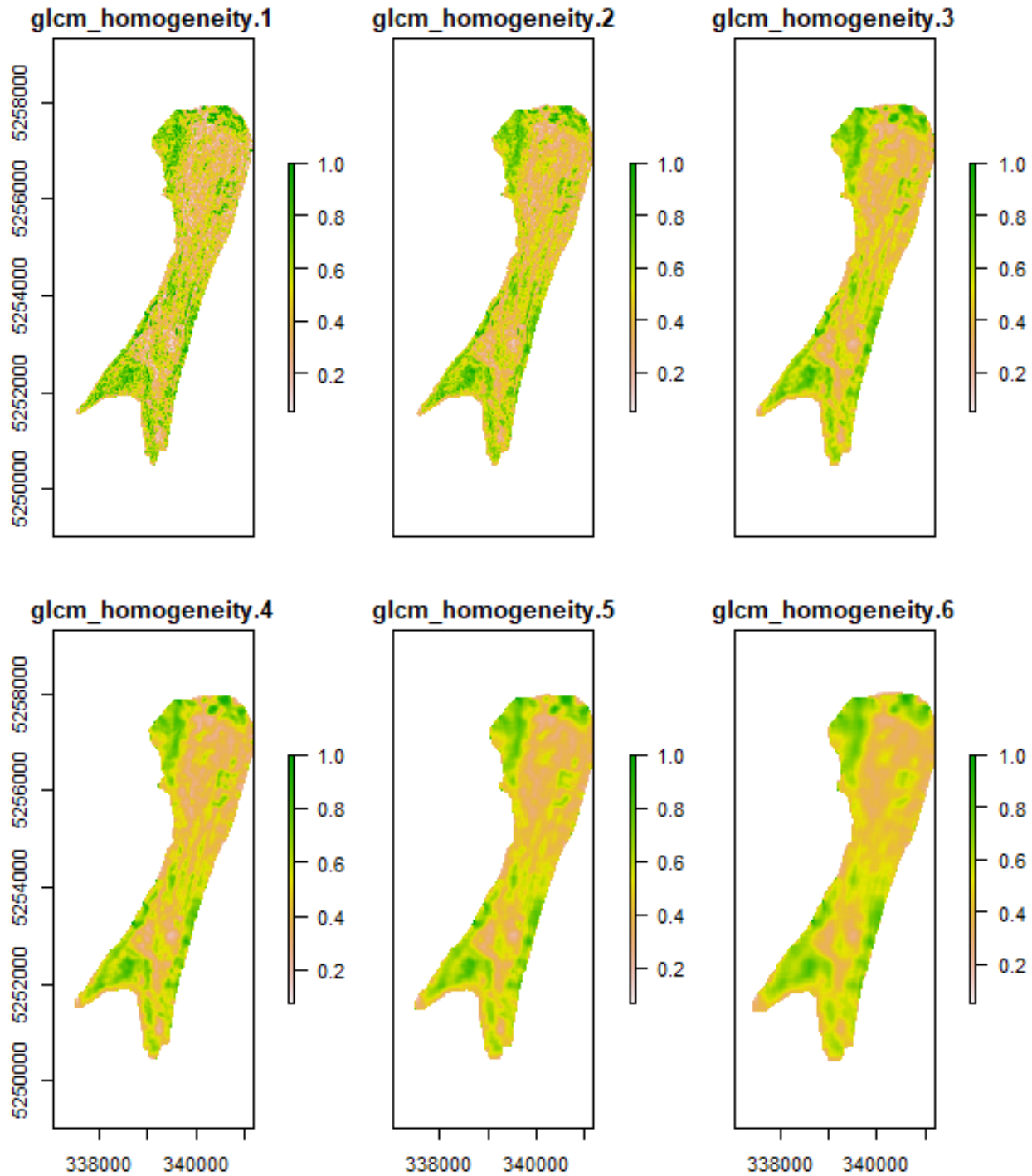


Figure A-17. Raster of the study site, Holyrood Bay, with derived GLCM Homogeneity overlayed, calculated at multiple scales; (A) 3 x 3 window, (B) 5 x 5 window, (C) 9 x 9 window, (D) 11 x 11 window, (E) 15 x 15 window, (F) 21 x 21 window. The data is gridded at 10m x 10m using projection UTM 22N.

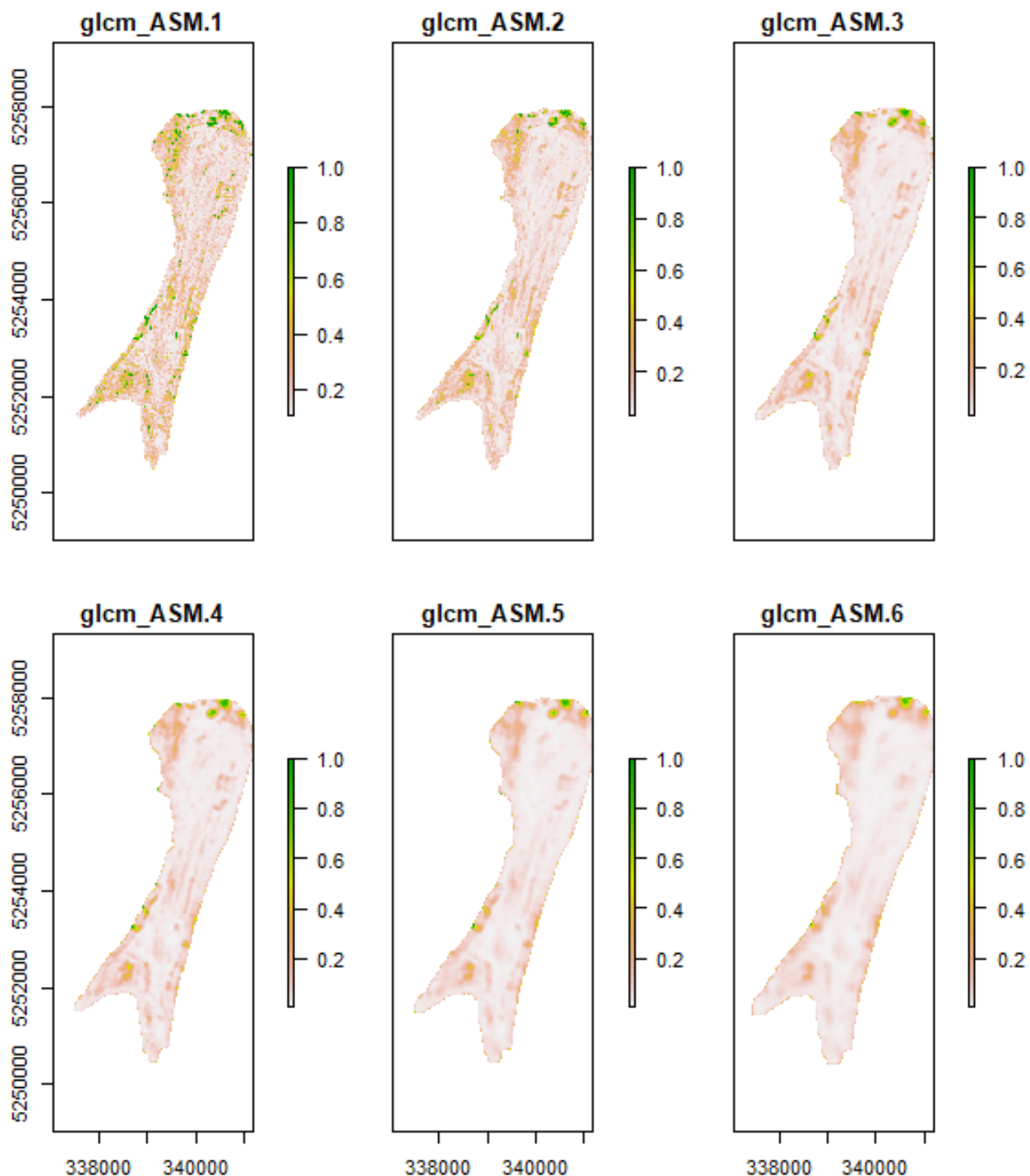


Figure A-18. Raster of the study site, Holyrood Bay, with derived GLCM Angular Second Moment (ASM) overlayed, calculated at multiple scales; (A) 3 x 3 window, (B) 5 x 5 window, (C) 9 x 9 window, (D) 11 x 11 window, (E) 15 x 15 window, (F) 21 x 21 window. The data is gridded at 10m x 10m using projection UTM 22N.

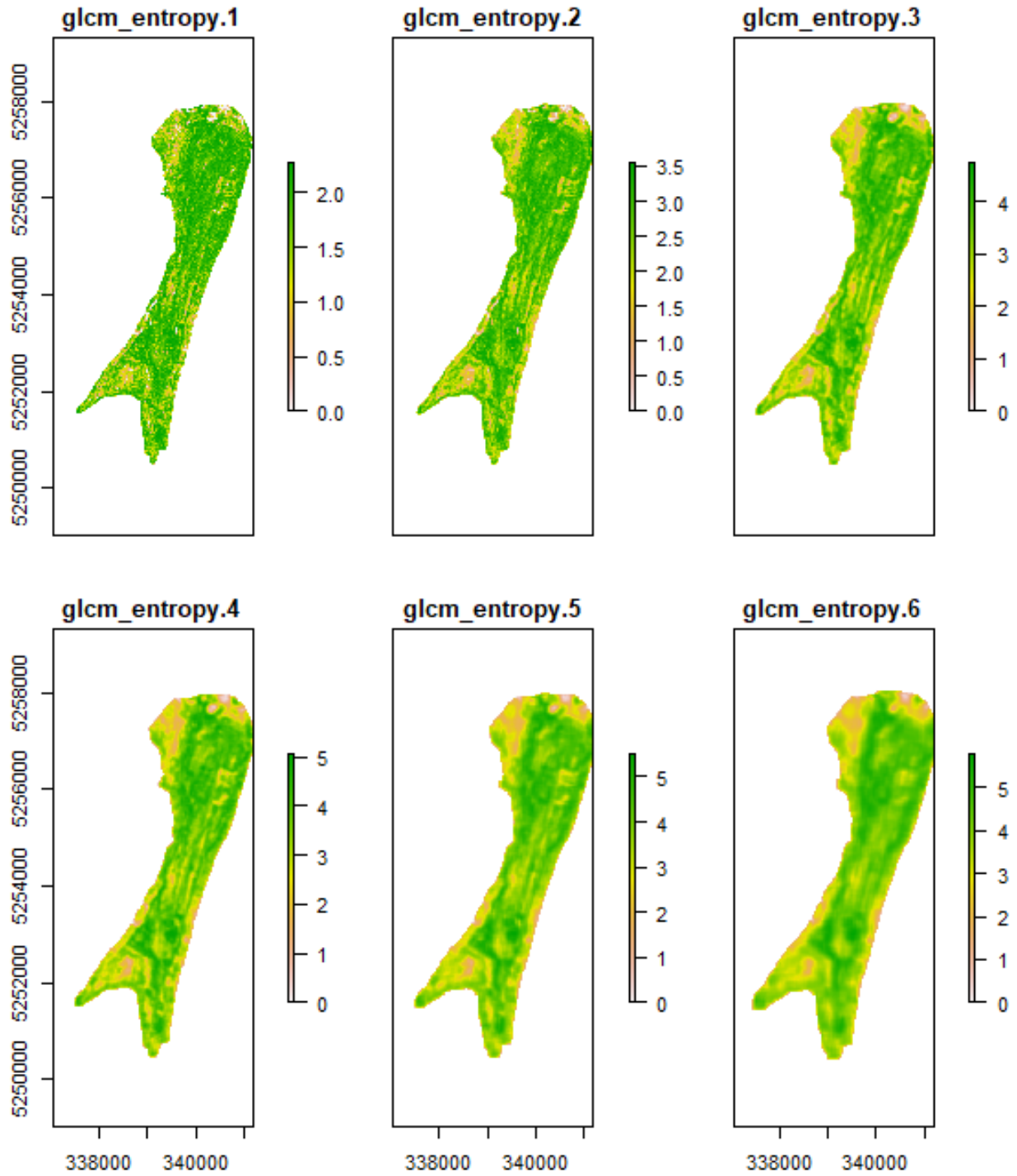


Figure A-19. Raster of the study site, Holyrood Bay, with derived GLCM Entropy overlayed, calculated at multiple scales; (A) 3 x 3 window, (B) 5 x 5 window, (C) 9 x 9 window, (D) 11 x 11 window, (E) 15 x 15 window, (F) 21 x 21 window. The data is gridded at 10m x 10m using projection UTM 22N.

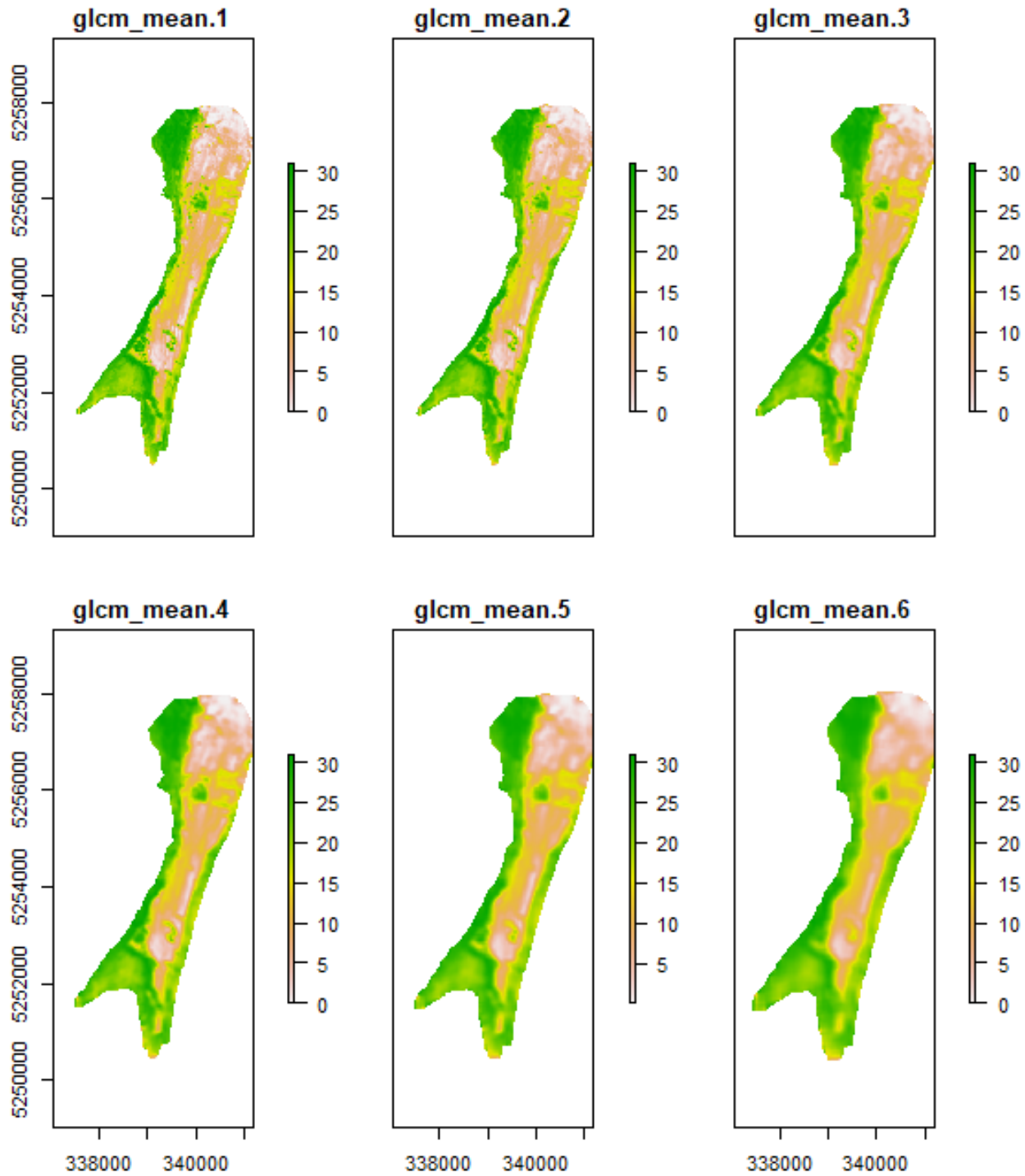


Figure A-20. Raster of the study site, Holyrood Bay, with derived GLCM Mean overlayed, calculated at multiple scales; (A) 3 x 3 window, (B) 5 x 5 window, (C) 9 x 9 window, (D) 11 x 11 window, (E) 15 x 15 window, (F) 21 x 21 window. The data is gridded at 10m x 10m using projection UTM 22N.

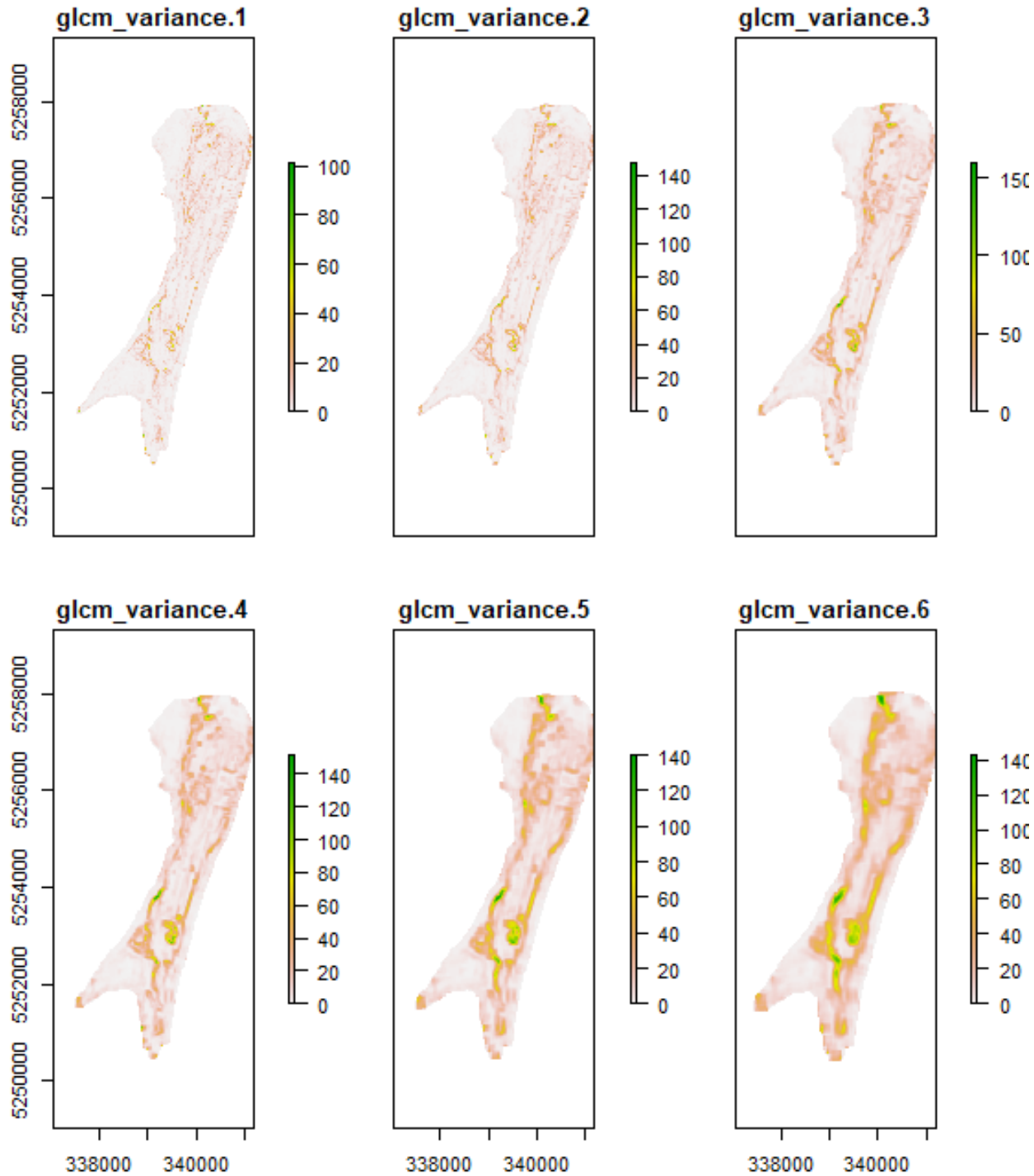


Figure A-21. Raster of the study site, Holyrood Bay, with derived GLCM Variance overlayed, calculated at multiple scales; (A) 3 x 3 window, (B) 5 x 5 window, (C) 9 x 9 window, (D) 11 x 11 window, (E) 15 x 15 window, (F) 21 x 21 window. The data is gridded at 10m x 10m using projection UTM 22N.

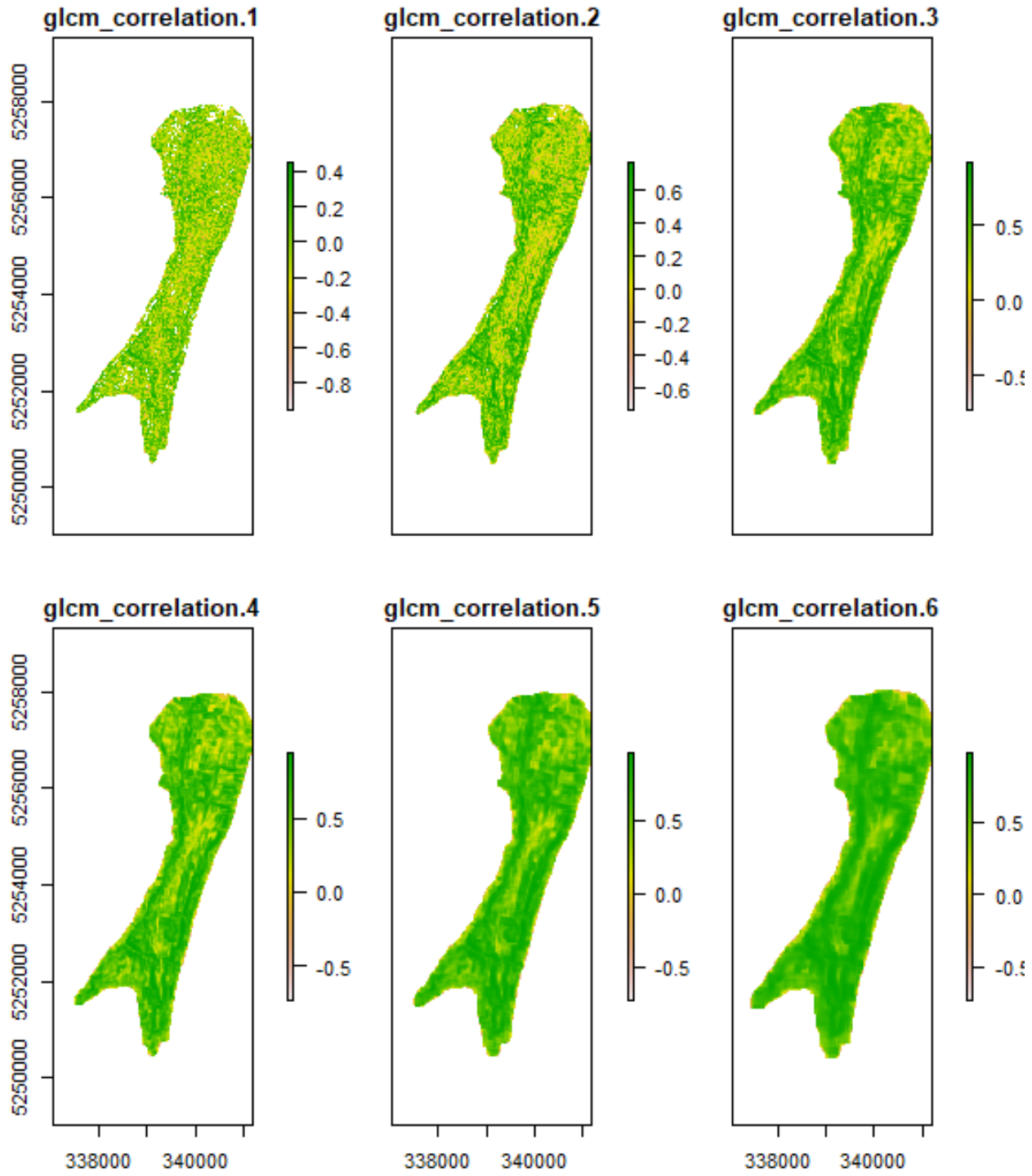


Figure A-22. Raster of the study site, Holyrood Bay, with derived GLCM Correlation overlayed, calculated at multiple scales; (A) 3 x 3 window, (B) 5 x 5 window, (C) 9 x 9 window, (D) 11 x 11 window, (E) 15 x 15 window, (F) 21 x 21 window. The data is gridded at 10m x 10m using projection UTM 22N.

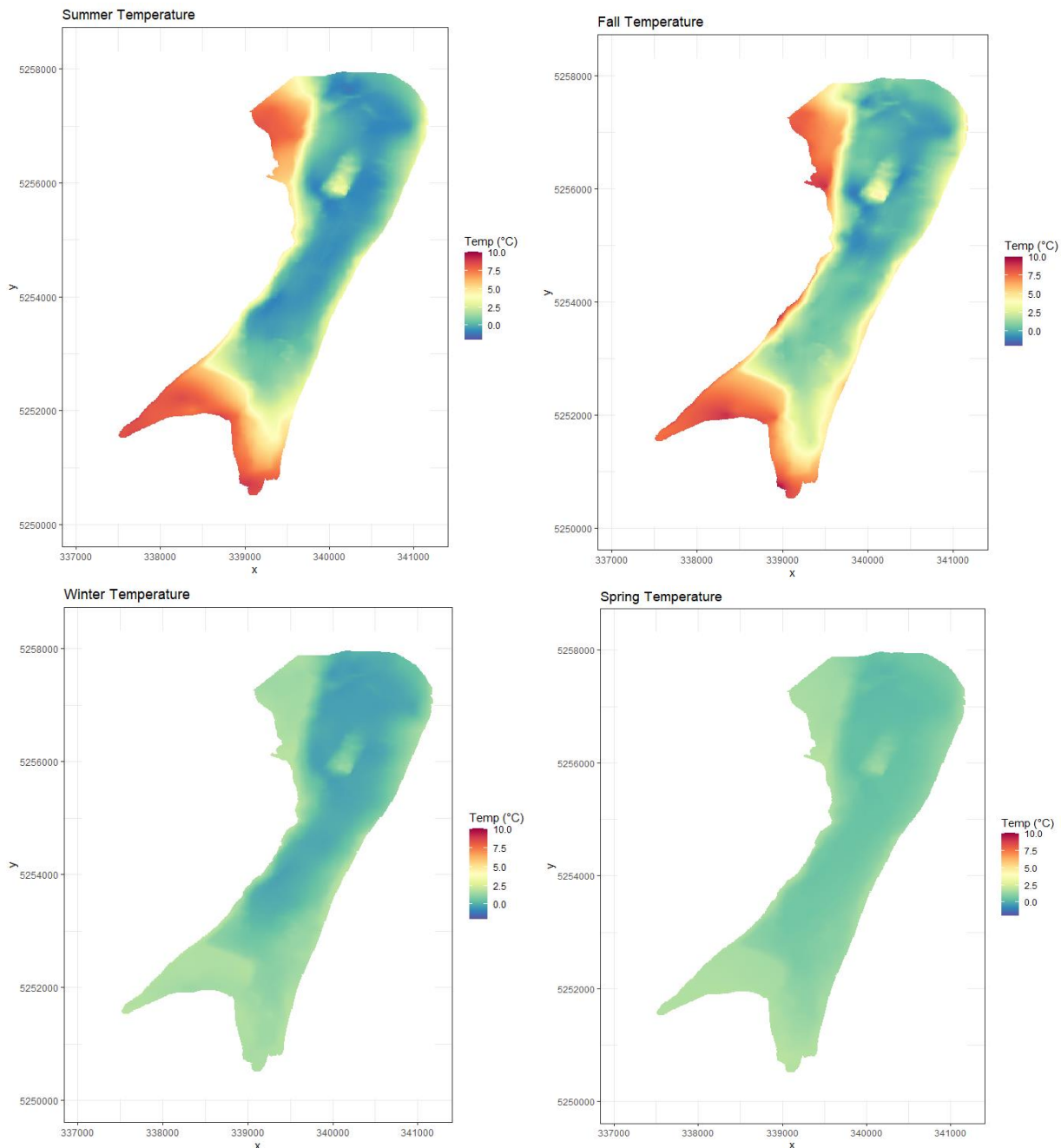


Figure A-23. Raster of the study site, Holyrood Bay, with predicted maps of temperature (°C) across the seasons from July 2020 - April 2021 overlaid; (A) Summer 2020, (B) Fall 2020, (C) Winter 2021, and (D) Spring 2021. The data is gridded

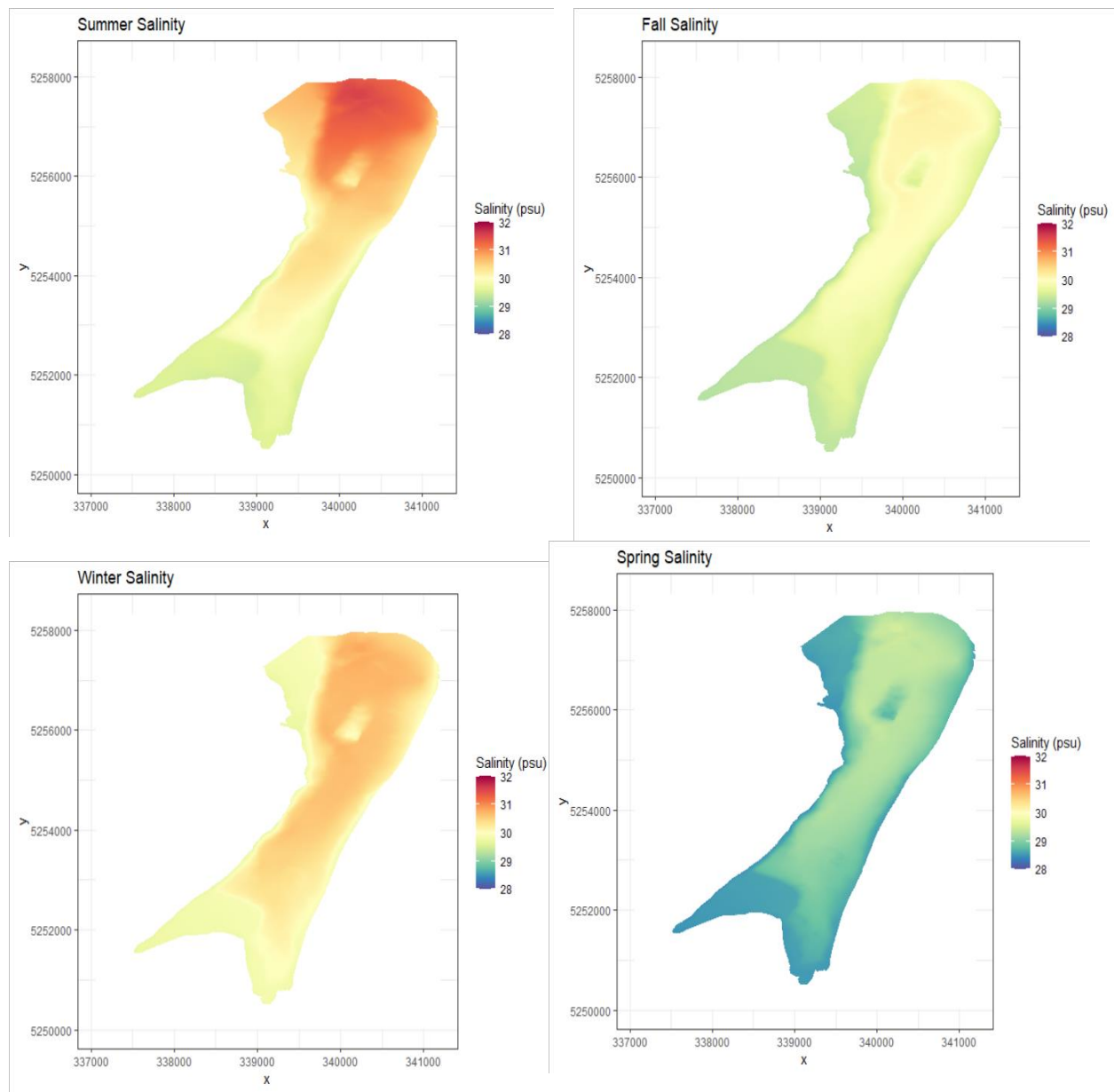


Figure A-24. Raster of the study site, Holyrood Bay, with predicted maps of salinity (psu) across the seasons from July 2020 - April 2021 overlayed; (A) Summer 2020, (B) Fall 2020, (C) Winter 2021, and (D) Spring 2021. The data is gridded at 10m x 10m using projection UTM 22N.

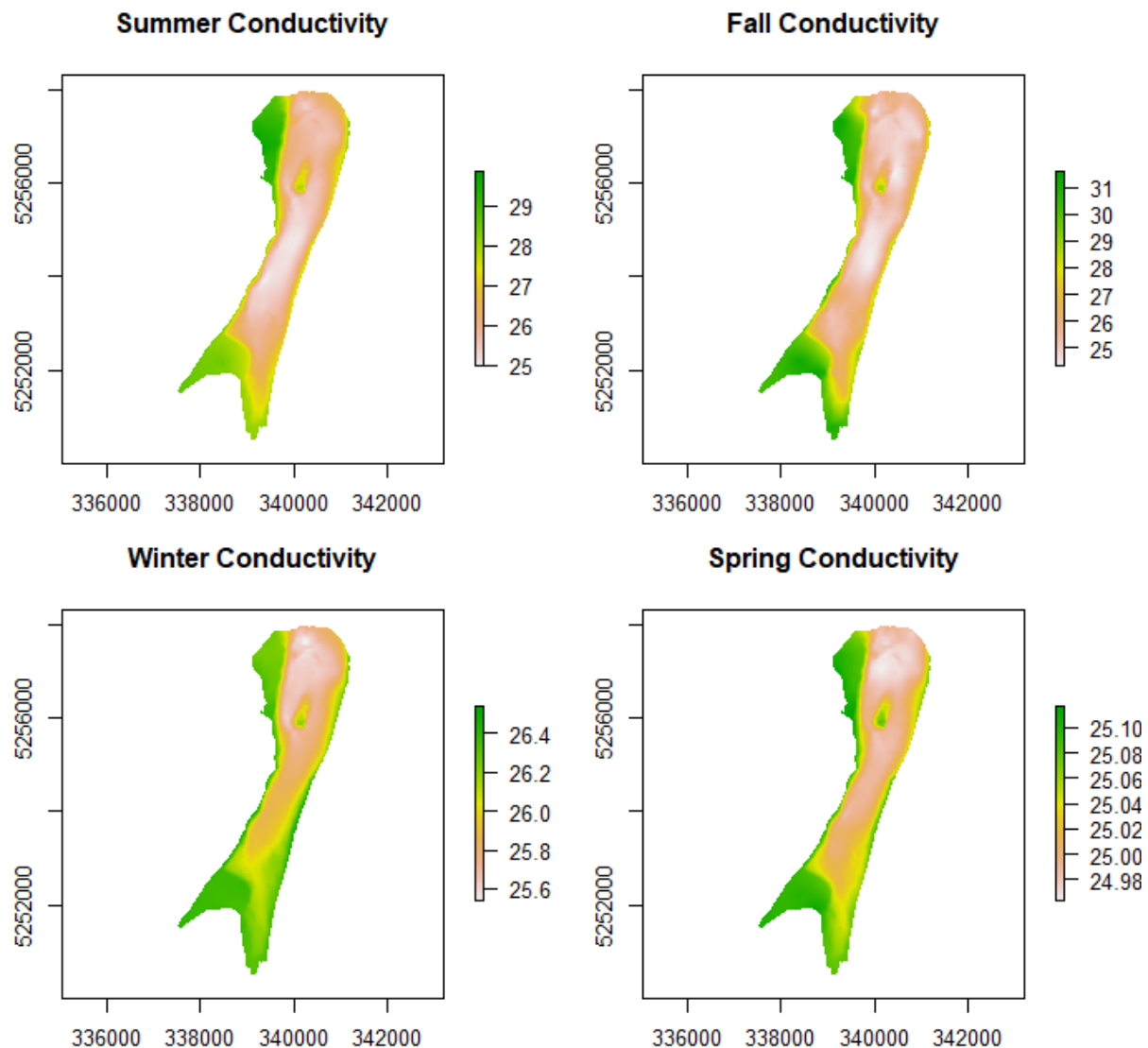


Figure A-25. Raster of the study site, Holyrood Bay, with predicted maps of conductivity (mS/cm) across the seasons from July 2020 - April 2021 overlaid; (A) Summer 2020, (B) Fall 2020, (C) Winter 2021, (D) Spring 2021. The data is gridded at 10m x 10m using projection UTM 22N.

Appendix B – Species Catalogue

This catalogue compiles the observed megabenthic species > 2 cm observed during ground-truthing in Holyrood Bay, Newfoundland and Labrador. Taxonomic information is given to the lowest identifiable level for each species. No biological samples were taken during this project, so identification is based solely on video observations.

Annelida

Class	Order	Family	Genus	Species	Example Image
Polychaeta	Sabellida	Sabellidae	<i>Myxicola</i>	<i>infundibulum</i>	

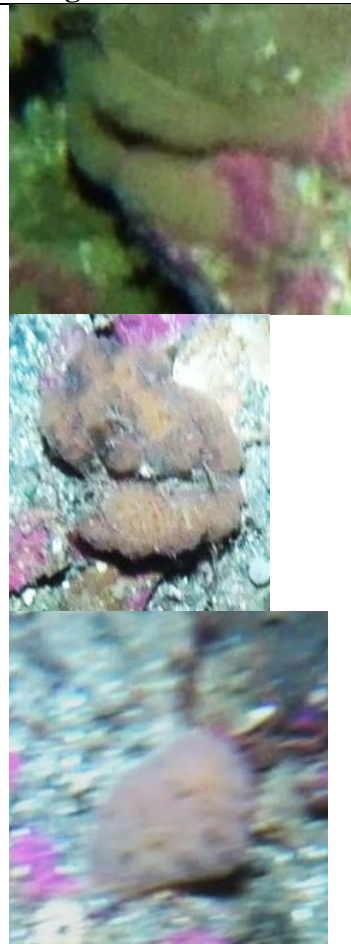
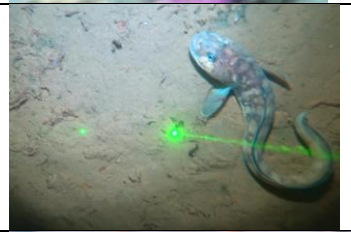
Arthropoda

Class	Order	Family	Genus	Species	Image
-------	-------	--------	-------	---------	-------

Malacostraca	Decapoda	Cancridae	<i>Cancer</i>	<i>irroratus</i>		
Malacostraca	Decapoda	Oregoniidae	<i>Chionoecetes</i>	<i>opilio</i>		
Malacostraca	Decapoda	Oregoniidae	<i>Hyas</i>	<i>coarctatus</i>		

Malacostraca	Decapoda	Oregoniidae	<i>Hyas</i>	<i>araneus</i>		
Malacostraca	Decapoda	Paguridae	<i>Pagurus</i>	sp.		
Malacostraca	Decapoda	Pandalidae	<i>Pandalus</i>	sp.		

Chordata

Phylum	Class	Order	Family	Genus	Species	Image
Chordata	Asciidiacea				sp. 1	
Chordata	Actinopterygii	Perciformes	Zoarcidae	<i>Zoarces</i>	<i>americanus</i>	
Chordata	Actinopterygii	Perciformes	Zoarcidae	<i>Lycodes</i>	<i>reticulatus</i>	

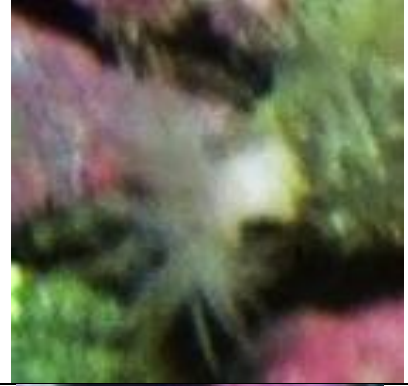
Chordata	Actinopterygii	Perciformes	Zoarcidae	<i>Zoarces</i>	sp. 1	
Chordata	Actinopterygii	Perciformes	Pholidae	<i>Pholis</i>	<i>gunnellus</i>	
Chordata	Actinopterygii	Perciformes	Cottidae	<i>Myoxocephalus</i>	spp.	

Chordata					sp. 6	
Chordata					sp. 7	
Chordata	Actinopterygii	Perciformes	Cottidae		sp. 1	
Chordata	Actinopterygii	Pleuronectiformes	Pleuronectidae	<i>Pseudopleuronectes americanus</i>		

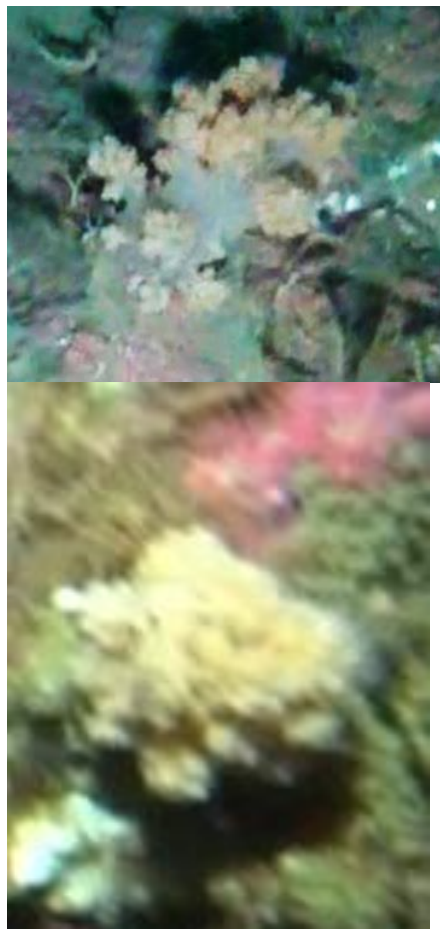
Chordata	Actinopterygii	Pleuronectiformes	Pleuronectidae	<i>Hippoglossoides</i>	<i>platessoides</i>	
----------	----------------	-------------------	----------------	------------------------	---------------------	---

Cnidaria

Class	Order	Family	Genus	Species	Image
Anthozoa	Actiniaria	Metridiidae	<i>Metridium</i>	sp.	

						
Anthozoa	Actiniaria	Actiniidae		sp.	 	

Anthozoa	Actiniaria	Hormathiidae	<i>Hormathia</i>	sp.		
Anthozoa	Actiniaria	Actinostolidae	<i>Stomphia</i>	<i>coccinea</i>	 	

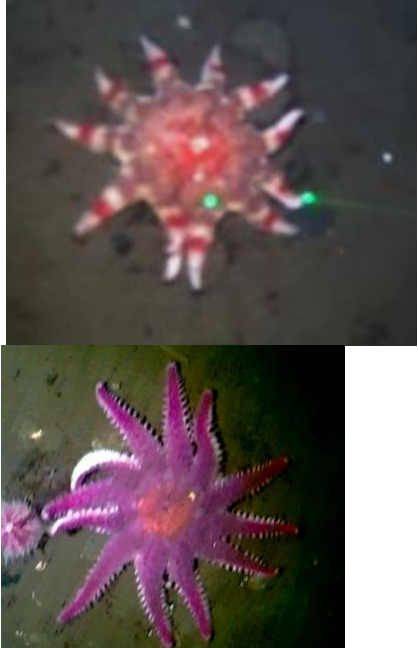
Anthozoa	Malacalcyon acea	Nephtheidae		sp.	
Hydrozoa	Anthoathecata	Corymorphidae	<i>Corymorpha</i>	<i>pendula</i>	

Hydrozoa	Trachymedusae	Ptychogastriidae	<i>Ptychogastria</i>	<i>polaris</i>	
Anthozoa	Spirularia	Cerianthidae	<i>Pachycerianthus</i>	<i>borealis</i>	

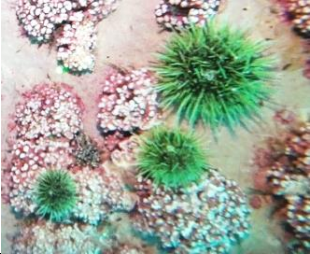
Echinodermata

Class	Order	Family	Genus	Species	Image
Asteroidea	Forcipulatida	Asteriidae	<i>Asterias</i>	sp.	
Asteroidea	Spinulosida	Echinasteridae	<i>Henricia</i>	sp.	

Asteroide a				sp. 10		
Asteroide a	Forcipulat ida	Asteriidae	<i>Leptasterias</i>	<i>polaris</i>		

Asteroidea a	Valvatida	Solasteridae	<i>Crossaster</i>	<i>papposus</i>		
Asteroidea a	Valvatida	Solasteridae	<i>Solaster</i>	<i>endeca</i>		

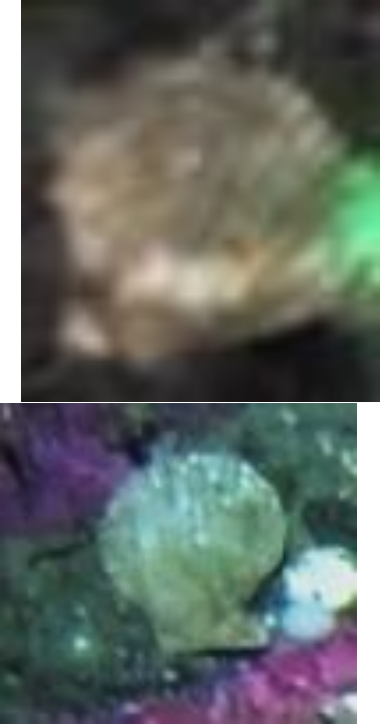
Asteroidea a	Valvatida	Poraniidae	<i>Porania</i>	<i>pulvillus</i>		
Asteroidea a	Velatida	Pterasteridae	<i>Pteraster</i>	spp.		
Ophiuroid ea				sp.	 	

Echnioidea	Camarodonta	Strongylocentrotidae	<i>Strongylocentrotus</i>	<i>droebachiensis</i>	  	
Echnioidea	Echinolampadacea	Echinorachnidae	<i>Echinorachnius</i>	<i>parma</i>	 	
Holothuroidea	Dendrochirotida	Cucumariidae	<i>Cucumaria</i>	<i>frondosa</i>		

Holothuroidea	Dendrochirotida	Psolidae	<i>Psolus</i>	<i>phantapus</i>	
---------------	-----------------	----------	---------------	------------------	--

Mollusca

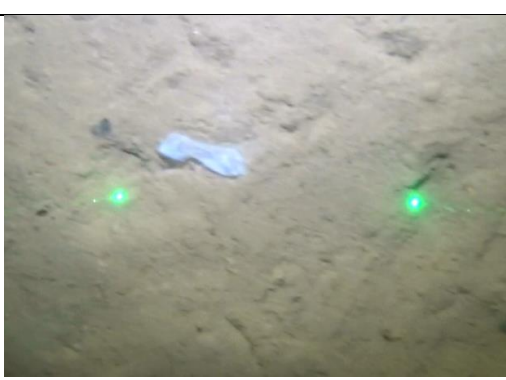
Class	Order	Family	Genus	Species	Image
Bivalvia	Ostreida	Ostreidae	<i>Crassostrea</i>	sp.	

Bivalvia	Pectinida	Pectinidae	<i>Chlamys</i>	sp. 1		
Bivalvia	Venerida	Arcticidae	<i>Arctica</i>	<i>islandica</i>		

Bivalvia	Venerida	Mesodesmatidae	<i>Mesodesma</i> <i>a</i>	<i>arctatum</i>	
Bivalvia	Arcida	Arcidae	<i>Lunarca</i>	<i>ovalis</i>	

Bivalvia	Mytilida	Mytilidae				 The image consists of four separate photographs of bivalve shells, likely from the genus Mytilus, arranged vertically. The top photograph shows a dark brown, irregularly shaped shell resting on a light-colored, pebbled substrate. The second photograph down shows a dark, elongated shell with a distinct blue-grey or purple iridescence along its edge, also resting on a greenish substrate. The third photograph shows a white, ribbed shell with a dark, circular base, resting on a light-colored substrate. The bottom photograph shows a large, dark, textured shell with a prominent purple or blue iridescent band near the base, resting on a greenish substrate.
----------	----------	-----------	--	--	--	---

Bivalvia	Adapedonta	Pharidae	<i>Ensis</i>	spp.	
Gastropoda	Neogastropoda	Buccinidae	<i>Buccinum</i>	<i>undatum</i>	 02:31PM

Gastropoda				sp. 3	
Gastropoda				sp. 4	
Gastropoda				sp. 5	
Gastropoda	Nudibranchia			sp. 1	

Gastropoda	Nudibranchia	Flabellinidae	<i>Flabellina</i>	sp. 1	
Gastropoda	Nudibranchia	Dendronotidae	<i>Dendronotus</i>	<i>frondosus</i>	

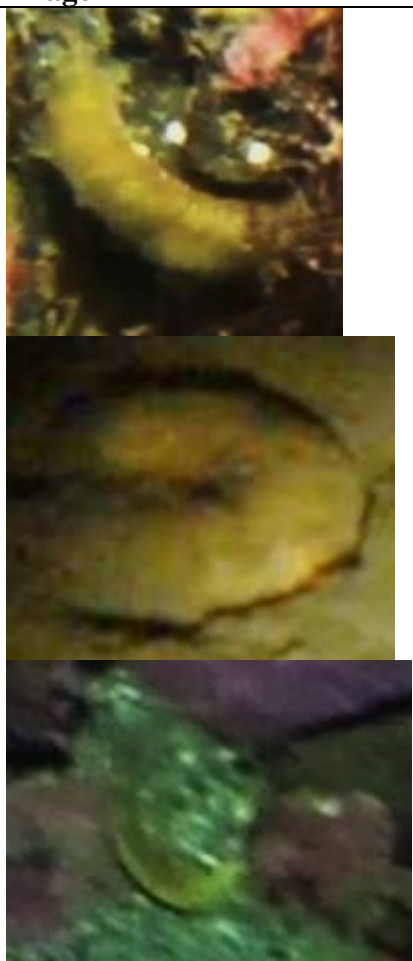
Porifera

Class	Order	Family	Genus	Species	Image
-------	-------	--------	-------	---------	-------

				sp. 15	
				sp. 16	
Demosp ongiae	Tetractine llida	Geodiidae	<i>Geodia</i>	sp.	

				sp. 17	
				sp. 31	
Demospongiae	Poeciliosclerida	Mycalidae	<i>Mycale</i>	sp.	

Unclassified

Class	Order	Family	Genus	Species	Image
Unknown				sp. 9	

Appendix C – SIMPER, IndVal, ANOSIM Results

SUMMER

> summary(simper, ordered=TRUE)

Contrast: Red_Orange

taxa	average	sd	ratio	ava	avb	cumsum	p
<i>Strongylocentrotus droebachiensis</i>	0.29781	0.20065	1.48420	0.21740	1.60780	0.352	0.001 ***
<i>Asterias</i> spp.	0.22938	0.15676	1.46330	0.98770	0.15520	0.624	0.001 ***
<i>Echinorachnius parma</i>	0.11382	0.20053	0.56760	1.08740	0.00000	0.758	0.001 ***
<i>Henricia</i> spp.	0.11168	0.07071	1.57930	0.47630	0.03180	0.890	0.001 ***
Porifera sp. 15	0.01713	0.05212	0.32870	0.00000	0.13090	0.910	0.167
<i>Solaster endeca</i>	0.01085	0.02176	0.49840	0.01620	0.03240	0.923	0.105
<i>Pachycerianthus borealis</i>	0.00758	0.02719	0.27890	0.00000	0.02540	0.932	0.848
<i>Ophiuroidea</i> spp.	0.00740	0.03035	0.24390	0.00000	0.02010	0.941	1.000
<i>Mytilidae</i> spp.	0.00697	0.01148	0.60720	0.02240	0.00610	0.949	0.002 **
<i>Hyas araneus</i>	0.00532	0.01146	0.46460	0.00000	0.02860	0.956	0.549
<i>Pagurus</i> spp.	0.00514	0.02207	0.23280	0.00000	0.01100	0.962	0.401
<i>Pseudopleuronectes americanus</i>	0.00497	0.00929	0.53490	0.00800	0.01340	0.968	0.047 *
<i>Hyas coarctatus</i>	0.00401	0.01333	0.30040	0.00000	0.01160	0.972	0.117
<i>Leptasterias polaris</i>	0.00371	0.01358	0.27320	0.00000	0.01400	0.977	0.179
<i>Lunارca ovalis</i>	0.00367	0.00830	0.44200	0.00000	0.02150	0.981	0.114
<i>Pteraster</i> spp.	0.00330	0.00766	0.43160	0.01140	0.00000	0.985	0.412
<i>Ptychogastria polaris</i>	0.00272	0.00840	0.32320	0.00000	0.00650	0.988	0.982
<i>Metridium</i> spp.	0.00264	0.00837	0.31490	0.01000	0.00000	0.991	0.017 *
<i>Mesodesma arctatum</i>	0.00234	0.00943	0.24790	0.00000	0.00720	0.994	0.630
<i>Flabellina</i> sp. 1	0.00173	0.00807	0.21450	0.00000	0.00290	0.996	0.680
<i>Crossaster papposus</i>	0.00157	0.00454	0.34660	0.00300	0.00150	0.998	0.440
<i>Chionoecetes opilio</i>	0.00108	0.00438	0.24530	0.00000	0.00300	0.999	0.997
<i>Hippoglossoides platessoides</i>	0.00073	0.00235	0.31000	0.00230	0.00000	1.000	0.885
<i>Psolus phantapus</i>	0.00000	0.00000	NA	0.00000	0.00000	1.000	1.000
Gastropoda sp. 3	0.00000	0.00000	NA	0.00000	0.00000	1.000	0.965
<i>Pandalus</i> spp.	0.00000	0.00000	NA	0.00000	0.00000	1.000	0.997

Signif. codes: 0 **** 0.001 ** 0.01 * 0.05 . 0.1 ‘ ’ 1

Contrast: Red_Blue

taxa	average	sd	ratio	ava	avb	cumsum	p
<i>Psolus phantapus</i>	0.5801	0.3215	1.8043	0.0000	44.0600	0.608	0.001 ***
<i>Asterias</i> spp.	0.1227	0.1381	0.8884	0.9877	0.0400	0.736	0.001 ***
<i>Echinarachnius parma</i>	0.0668	0.1534	0.4353	1.0874	0.0100	0.806	0.039 *
<i>Henricia</i> spp.	0.0564	0.0629	0.8968	0.4763	0.0200	0.865	0.001 ***
<i>Strongylocentrotus droebachiensis</i>	0.0388	0.0655	0.5921	0.2174	0.2900	0.906	0.999
<i>Pachycerianthus borealis</i>	0.0256	0.0828	0.3093	0.0000	2.1400	0.932	0.619
<i>Solaster endeca</i>	0.0085	0.0229	0.3702	0.0162	0.2900	0.941	0.220
<i>Ophiuroidea</i> spp.	0.0071	0.0143	0.4922	0.0000	0.6900	0.949	1.000
Porifera sp. 15	0.0064	0.0166	0.3843	0.0000	0.0400	0.955	0.567
Gastropoda sp. 3	0.0050	0.0111	0.4480	0.0000	0.0600	0.960	0.044 *
<i>Mesodesma arctatum</i>	0.0049	0.0126	0.3905	0.0000	0.0300	0.966	0.124
<i>Chionoecetes opilio</i>	0.0045	0.0109	0.4158	0.0000	0.0800	0.970	0.880
<i>Hyas araneus</i>	0.0040	0.0186	0.2129	0.0000	0.0200	0.975	0.701
<i>Mytilidae</i> spp.	0.0038	0.0071	0.5351	0.0224	0.0100	0.979	0.134
<i>Pseudopleuronectes americanus</i>	0.0032	0.0059	0.5351	0.0080	0.0200	0.982	0.305
<i>Ptychogastria polaris</i>	0.0028	0.0060	0.4657	0.0000	0.1900	0.985	0.993
<i>Crossaster papposus</i>	0.0027	0.0105	0.2603	0.0030	0.0300	0.988	0.267
<i>Flabellina</i> sp. 1	0.0023	0.0113	0.2033	0.0000	0.0100	0.990	0.528
<i>Hippoglossoides platessoides</i>	0.0021	0.0062	0.3314	0.0023	0.0100	0.992	0.377
<i>Pandalus</i> spp.	0.0019	0.0065	0.2848	0.0000	0.0000	0.994	0.976
<i>Pteraster</i> spp.	0.0017	0.0053	0.3246	0.0114	0.0000	0.996	0.749
<i>Metridium</i> spp.	0.0017	0.0058	0.2864	0.0100	0.1000	0.998	0.155
<i>Lunارca ovalis</i>	0.0011	0.0051	0.2231	0.0000	0.2500	0.999	0.690
<i>Pagurus</i> spp.	0.0007	0.0032	0.2077	0.0000	0.0000	1.000	0.908
<i>Hyas coarctatus</i>	0.0004	0.0011	0.3153	0.0000	0.0800	1.000	0.815
<i>Leptasterias polaris</i>	0.0000	0.0000	NA	0.0000	0.0000	1.000	0.925

Signif. codes: 0 **** 0.001 ** 0.01 * 0.05 . 0.1 ‘ ’ 1

Contrast: Red_Yellow

taxa	average	sd	ratio	ava	avb	cumsum	p
<i>Ophiuroidea</i> spp.	0.55910	0.25803	2.16670	0.00000	10.95500	0.566	0.001 ***
<i>Asterias</i> spp.	0.09600	0.09245	1.03800	0.98770	0.00000	0.663	0.009 **
<i>Psolus phantapus</i>	0.09190	0.13858	0.66310	0.00000	2.11700	0.756	0.999
<i>Echinarachnius parma</i>	0.05930	0.13531	0.43850	1.08740	0.00000	0.816	0.100 .
<i>Pachycerianthus borealis</i>	0.04730	0.15269	0.30970	0.00000	0.56000	0.864	0.306
<i>Henricia</i> spp.	0.04430	0.04136	1.07020	0.47630	0.00000	0.908	0.009 **
<i>Strongylocentrotus droebachiensis</i>	0.02950	0.04203	0.70230	0.21740	0.21600	0.938	0.997
<i>Ptychogastria polaris</i>	0.01880	0.03212	0.58550	0.00000	0.64200	0.957	0.161
<i>Chionoecetes opilio</i>	0.00870	0.01748	0.49500	0.00000	0.06800	0.966	0.505
<i>Pandalus</i> spp.	0.00780	0.01622	0.48070	0.00000	0.06300	0.974	0.784
<i>Pteraster</i> spp.	0.00690	0.01315	0.52460	0.01140	0.20800	0.981	0.038 *
<i>Flabellina</i> sp. 1	0.00330	0.01130	0.29070	0.00000	0.03800	0.984	0.360
<i>Hippoglossoides platessoides</i>	0.00260	0.00398	0.64590	0.00230	0.03400	0.987	0.217
<i>Mytilidae</i> spp.	0.00220	0.00471	0.47630	0.02240	0.00000	0.989	0.551
<i>Solaster endeca</i>	0.00220	0.00819	0.26870	0.01620	0.00300	0.991	0.884
<i>Pagurus</i> spp.	0.00160	0.00364	0.43730	0.00000	0.06900	0.993	0.698
<i>Metridium</i> spp.	0.00140	0.00417	0.34210	0.01000	0.00500	0.994	0.304
<i>Leptasterias polaris</i>	0.00140	0.00439	0.32060	0.00000	0.01800	0.996	0.463
<i>Crossaster papposus</i>	0.00110	0.00243	0.45020	0.00300	0.00700	0.997	0.542
<i>Hyas araneus</i>	0.00100	0.00305	0.33700	0.00000	0.00700	0.998	0.947
Porifera sp. 15	0.00090	0.00182	0.48540	0.00000	0.01300	0.999	0.954
<i>Pseudopleuronectes americanus</i>	0.00080	0.00226	0.37010	0.00800	0.00000	1.000	0.963
<i>Hyas coarctatus</i>	0.00030	0.00100	0.26260	0.00000	0.00300	1.000	0.876
<i>Lunارca ovalis</i>	0.00000	0.00000	NA	0.00000	0.00000	1.000	0.897
<i>Mesodesma arctatum</i>	0.00000	0.00000	NA	0.00000	0.00000	1.000	0.920
Gastropoda sp. 3	0.00000	0.00000	NA	0.00000	0.00000	1.000	0.956

Signif. codes: 0 *** 0.001 ** 0.01 * 0.05 . 0.1 ‘ ’ 1

Contrast: Red_Purple

taxa	average	sd	ratio	ava	avb	cumsum	p
<i>Pandalus</i> spp.	0.36300	0.09658	3.75900	0.00000	3.80900	0.375	0.001 ***
<i>Asterias</i> spp.	0.14480	0.11123	1.30100	0.98770	0.00000	0.524	0.011 *

<i>Chionoecetes opilio</i>	0.10780	0.12051	0.89500	0.00000	1.93500	0.636	0.002 **
<i>Echinorachnius parma</i>	0.08380	0.15994	0.52400	1.08740	0.10200	0.722	0.065 .
<i>Henricia</i> spp.	0.06640	0.04876	1.36200	0.47630	0.00000	0.791	0.019 *
<i>Psolus phantapus</i>	0.05320	0.07997	0.66500	0.00000	0.30600	0.846	0.995
<i>Ptychogastria polaris</i>	0.04500	0.06541	0.68900	0.00000	0.91700	0.892	0.028 *
<i>Strongylocentrotus droebachiensis</i>	0.04000	0.05397	0.74100	0.21740	0.08900	0.933	0.880
<i>Hyas araneus</i>	0.02990	0.02494	1.19800	0.00000	0.14700	0.964	0.006 **
<i>Pagurus</i> spp.	0.02250	0.03270	0.68900	0.00000	0.45800	0.988	0.024 *
<i>Mytilidae</i> spp.	0.00340	0.00640	0.52900	0.02240	0.00000	0.991	0.285
<i>Solaster endeca</i>	0.00310	0.01126	0.27900	0.01620	0.00000	0.994	0.575
<i>Pteraster</i> spp.	0.00190	0.00487	0.39000	0.01140	0.00000	0.996	0.512
<i>Metridium</i> spp.	0.00160	0.00545	0.28600	0.01000	0.00000	0.998	0.245
<i>Pseudopleuronectes americanus</i>	0.00130	0.00310	0.41000	0.00800	0.00000	0.999	0.669
<i>Crossaster papposus</i>	0.00050	0.00172	0.28500	0.00300	0.00000	1.000	0.577
<i>Hippoglossoides platessoides</i>	0.00040	0.00144	0.28200	0.00230	0.00000	1.000	0.794
<i>Leptasterias polaris</i>	0.00000	0.00000	NA	0.00000	0.00000	1.000	0.585
<i>Lunارca ovalis</i>	0.00000	0.00000	NA	0.00000	0.00000	1.000	0.624
Porifera sp. 15	0.00000	0.00000	NA	0.00000	0.00000	1.000	0.901
<i>Mesodesma arctatum</i>	0.00000	0.00000	NA	0.00000	0.00000	1.000	0.709
<i>Hyas coarctatus</i>	0.00000	0.00000	NA	0.00000	0.00000	1.000	0.705
<i>Ophiuroidea</i> spp.	0.00000	0.00000	NA	0.00000	0.00000	1.000	0.997
Gastropoda sp. 3	0.00000	0.00000	NA	0.00000	0.00000	1.000	0.778
<i>Flabellina</i> sp. 1	0.00000	0.00000	NA	0.00000	0.00000	1.000	0.610
<i>Pachycerianthus borealis</i>	0.00000	0.00000	NA	0.00000	0.00000	1.000	0.811

Signif. codes: 0 *** 0.001 ** 0.01 * 0.05 . 0.1 ‘ ’ 1

Contrast: Orange_Blue

taxa	average	sd	ratio	ava	avb	cumsum	p
<i>Psolus phantapus</i>	0.60550	0.31481	1.92340	0.00000	44.06000	0.641	0.001 ***
<i>Strongylocentrotus droebachiensis</i>	0.18260	0.20363	0.89670	1.60780	0.29000	0.834	0.001 ***
<i>Pachycerianthus borealis</i>	0.03030	0.08481	0.35740	0.02540	2.14000	0.866	0.620
Asterias spp.	0.02210	0.03724	0.59320	0.15520	0.04000	0.890	0.996
Porifera sp. 15	0.01640	0.04130	0.39610	0.13090	0.04000	0.907	0.060 .
<i>Ophiuroidea</i> spp.	0.01120	0.02680	0.41630	0.02010	0.69000	0.919	1.000
<i>Solaster endeca</i>	0.00980	0.02601	0.37560	0.03240	0.29000	0.929	0.064 .

<i>Hyas araneus</i>	0.00710	0.02148	0.33250	0.02860	0.02000	0.937	0.315
<i>Henricia</i> spp.	0.00710	0.01700	0.41620	0.03180	0.02000	0.944	0.999
<i>Mesodesma arctatum</i>	0.00640	0.01537	0.41560	0.00720	0.03000	0.951	0.008 **
Gastropoda sp. 3	0.00570	0.01332	0.42610	0.00000	0.06000	0.957	0.001 ***
<i>Chionoecetes opilio</i>	0.00550	0.01299	0.42220	0.00300	0.08000	0.963	0.861
<i>Ptychogastria polaris</i>	0.00430	0.00844	0.51230	0.00650	0.19000	0.967	0.977
<i>Pseudopleuronectes americanus</i>	0.00430	0.00883	0.48750	0.01340	0.02000	0.972	0.023 *
<i>Pagurus</i> spp.	0.00370	0.01725	0.21390	0.01100	0.00000	0.976	0.642
<i>Flabellina</i> sp. 1	0.00350	0.01387	0.25470	0.00290	0.01000	0.980	0.290
<i>Lunارка ovalis</i>	0.00340	0.00798	0.42180	0.02150	0.25000	0.983	0.081 .
<i>Mytilidae</i> spp.	0.00290	0.00802	0.36690	0.00610	0.01000	0.986	0.302
<i>Crossaster papposus</i>	0.00290	0.01106	0.26120	0.00150	0.03000	0.989	0.291
<i>Hyas coarctatus</i>	0.00270	0.01055	0.25770	0.01160	0.08000	0.992	0.160
<i>Pandalus</i> spp.	0.00230	0.00819	0.27740	0.00000	0.00000	0.995	0.988
<i>Hippoglossoides platessoides</i>	0.00220	0.00789	0.28350	0.00000	0.01000	0.997	0.300
<i>Leptasterias polaris</i>	0.00220	0.01061	0.20750	0.01400	0.00000	0.999	0.446
<i>Echinorachnius parma</i>	0.00040	0.00158	0.22190	0.00000	0.01000	1.000	0.994
<i>Metridium</i> spp.	0.00030	0.00125	0.22320	0.00000	0.10000	1.000	0.810
<i>Pteraster</i> spp.	0.00000	0.00000	NA	0.00000	0.00000	1.000	1.000

Signif. codes: 0 ‘***’ 0.001 ‘**’ 0.01 ‘*’ 0.05 ‘.’ 0.1 ‘ ’ 1

Contrast: Red_Yellow

taxa	average	sd	ratio	ava	avb	cumsum	p
<i>Ophiuroidea</i> spp.	0.57920	0.25980	2.22960	0.02010	10.95500	0.603	0.001 ***
<i>Strongylocentrotus droebachiensis</i>	0.13710	0.13912	0.98510	1.60780	0.21600	0.746	0.099 .
<i>Psolus phantapus</i>	0.09590	0.14441	0.66420	0.00000	2.11700	0.846	1.000
<i>Pachycerianthus borealis</i>	0.05160	0.15737	0.32790	0.02540	0.56000	0.899	0.229
<i>Ptychogastria polaris</i>	0.01970	0.03225	0.61230	0.00650	0.64200	0.920	0.102
<i>Asterias</i> spp.	0.01330	0.02688	0.49510	0.15520	0.00000	0.934	0.997
<i>Chionoecetes opilio</i>	0.00970	0.02025	0.48090	0.00300	0.06800	0.944	0.499
Porifera sp. 15	0.00970	0.03210	0.30160	0.13090	0.01300	0.954	0.443
<i>Pandalus</i> spp.	0.00860	0.01887	0.45790	0.00000	0.06300	0.963	0.860
<i>Pteraster</i> spp.	0.00650	0.01341	0.48150	0.00000	0.20800	0.970	0.004 **
<i>Flabellina</i> sp. 1	0.00400	0.01257	0.31730	0.00290	0.03800	0.974	0.230

<i>Pagurus</i> spp.	0.00320	0.01022	0.31430	0.01100	0.06900	0.977	0.706
<i>Hyas araneus</i>	0.00320	0.00653	0.48840	0.02860	0.00700	0.980	0.808
<i>Solaster endeca</i>	0.00290	0.00814	0.35860	0.03240	0.00300	0.984	0.854
<i>Leptasterias polaris</i>	0.00280	0.00778	0.35880	0.01400	0.01800	0.986	0.299
<i>Hippoglossoides platessoides</i>	0.00250	0.00416	0.60810	0.00000	0.03400	0.989	0.187
<i>Henricia</i> spp.	0.00230	0.00627	0.36870	0.03180	0.00000	0.991	0.999
<i>Lunارca ovalis</i>	0.00170	0.00487	0.35590	0.02150	0.00000	0.993	0.573
<i>Hyas coarctatus</i>	0.00170	0.00647	0.26490	0.01160	0.00300	0.995	0.489
<i>Pseudopleuronectes americanus</i>	0.00150	0.00473	0.30710	0.01340	0.00000	0.996	0.883
<i>Crossaster papposus</i>	0.00110	0.00275	0.40660	0.00150	0.00700	0.998	0.569
<i>Mesodesma arctatum</i>	0.00090	0.00464	0.19490	0.00720	0.00000	0.999	0.907
<i>Mytilidae</i> spp.	0.00080	0.00423	0.19000	0.00610	0.00000	1.000	0.953
<i>Metridium</i> spp.	0.00050	0.00197	0.26300	0.00000	0.00500	1.000	0.596
<i>Echinorachnius parma</i>	0.00000	0.00000	NA	0.00000	0.00000	1.000	0.979
Gastropoda sp. 3	0.00000	0.00000	NA	0.00000	0.00000	1.000	0.981

Signif. codes: 0 *** 0.001 ** 0.01 * 0.05 . 0.1 ‘ ’ 1

Contrast: Orange_Purple

taxa	average	sd	ratio	ava	avb	cumsum	p
<i>Pandalus</i> spp.	0.39200	0.10817	3.62400	0.00000	3.80900	0.415	0.001 ***
<i>Strongylocentrotus droebachiensis</i>	0.19790	0.16053	1.23300	1.60780	0.08900	0.625	0.076 .
<i>Chionoecetes opilio</i>	0.11170	0.12166	0.91800	0.00300	1.93500	0.744	0.001 ***
<i>Psolus phantapus</i>	0.05750	0.08593	0.66900	0.00000	0.30600	0.804	0.999
<i>Ptychogastria polaris</i>	0.04750	0.06550	0.72500	0.00650	0.91700	0.855	0.014 *
<i>Hyas araneus</i>	0.03080	0.02701	1.14100	0.02860	0.14700	0.887	0.002 **
<i>Pagurus</i> spp.	0.02550	0.03355	0.76000	0.01100	0.45800	0.914	0.010 **
<i>Asterias</i> spp.	0.01940	0.03524	0.55000	0.15520	0.00000	0.935	0.869
<i>Echinorachnius parma</i>	0.01920	0.02864	0.66900	0.00000	0.10200	0.955	0.426
Porifera sp. 15	0.01250	0.04209	0.29600	0.13090	0.00000	0.968	0.243
<i>Pachycerianthus borealis</i>	0.00470	0.01875	0.25300	0.02540	0.00000	0.974	0.762
<i>Ophiuroidea</i> spp.	0.00440	0.01951	0.22300	0.02010	0.00000	0.978	0.998
<i>Solaster endeca</i>	0.00400	0.01088	0.36600	0.03240	0.00000	0.982	0.521
<i>Henricia</i> spp.	0.00320	0.00822	0.39100	0.03180	0.00000	0.986	0.959
<i>Lunارca ovalis</i>	0.00250	0.00635	0.39300	0.02150	0.00000	0.988	0.271
<i>Hyas coarctatus</i>	0.00240	0.00873	0.27500	0.01160	0.00000	0.991	0.221

<i>Leptasterias polaris</i>	0.00240	0.00936	0.25200	0.01400	0.00000	0.993	0.230
<i>Pseudopleuronectes americanus</i>	0.00220	0.00645	0.34600	0.01340	0.00000	0.996	0.458
<i>Mesodesma arctatum</i>	0.00140	0.00633	0.22600	0.00720	0.00000	0.997	0.587
<i>Mytilidae</i> spp.	0.00130	0.00572	0.22400	0.00610	0.00000	0.999	0.607
<i>Flabellina</i> sp. 1	0.00080	0.00391	0.21500	0.00290	0.00000	1.000	0.593
<i>Crossaster papposus</i>	0.00040	0.00196	0.21500	0.00150	0.00000	1.000	0.638
<i>Pteraster</i> spp.	0.00000	0.00000	NA	0.00000	0.00000	1.000	0.940
<i>Gastropoda</i> sp. 3	0.00000	0.00000	NA	0.00000	0.00000	1.000	0.882
<i>Hippoglossoides platessoides</i>	0.00000	0.00000	NA	0.00000	0.00000	1.000	0.958
<i>Metridium</i> spp.	0.00000	0.00000	NA	0.00000	0.00000	1.000	0.661

Signif. codes: 0 ***, 0.001 **, 0.01 *, 0.05 ., 0.1 ‘ ’ 1

Contrast: Blue_Yellow

taxa	average	sd	ratio	ava	avb	cumsum	p
<i>Psolus phantapus</i>	0.4174	0.3265	1.2784	44.0600	2.1170	0.458	0.032 *
<i>Ophiuroidea</i> spp.	0.3679	0.2964	1.2413	0.6900	10.9550	0.862	0.001 ***
<i>Pachycerianthus borealis</i>	0.0500	0.1319	0.3793	2.1400	0.5600	0.916	0.185
<i>Strongylocentrotus droebachiensis</i>	0.0147	0.0235	0.6262	0.2900	0.2160	0.933	1.000
<i>Ptychogastria polaris</i>	0.0141	0.0266	0.5315	0.1900	0.6420	0.948	0.390
<i>Chionoecetes opilio</i>	0.0054	0.0120	0.4554	0.0800	0.0680	0.954	0.859
<i>Pandalus</i> spp.	0.0049	0.0120	0.4098	0.0000	0.0630	0.960	0.931
<i>Pteraster</i> spp.	0.0044	0.0110	0.4055	0.0000	0.2080	0.964	0.199
<i>Asterias</i> spp.	0.0039	0.0105	0.3692	0.0400	0.0000	0.969	1.000
Porifera sp. 15	0.0034	0.0094	0.3620	0.0400	0.0130	0.972	0.879
<i>Solaster endeca</i>	0.0033	0.0111	0.2969	0.2900	0.0030	0.976	0.853
<i>Flabellina</i> sp. 1	0.0025	0.0092	0.2747	0.0100	0.0380	0.979	0.547
<i>Gastropoda</i> sp. 3	0.0024	0.0059	0.4106	0.0600	0.0000	0.981	0.501
<i>Hyas araneus</i>	0.0022	0.0096	0.2329	0.0200	0.0070	0.984	0.952
<i>Mesodesma arctatum</i>	0.0022	0.0067	0.3345	0.0300	0.0000	0.986	0.697
<i>Hippoglossoides platessoides</i>	0.0020	0.0040	0.4993	0.0100	0.0340	0.988	0.378
<i>Crossaster papposus</i>	0.0020	0.0071	0.2780	0.0300	0.0070	0.991	0.554
<i>Henricia</i> spp.	0.0018	0.0069	0.2590	0.0200	0.0000	0.993	1.000
<i>Pagurus</i> spp.	0.0014	0.0033	0.4206	0.0000	0.0690	0.994	0.867
<i>Pseudopleuronectes americanus</i>	0.0013	0.0033	0.3994	0.0200	0.0000	0.996	0.947
<i>Lunارка ovalis</i>	0.0011	0.0049	0.2228	0.2500	0.0000	0.997	0.800

<i>Leptasterias polaris</i>	0.0009	0.0034	0.2698	0.0000	0.0180	0.998	0.706
<i>Mytilidae</i> spp.	0.0007	0.0023	0.3120	0.0100	0.0000	0.999	0.977
<i>Metridium</i> spp.	0.0006	0.0018	0.3174	0.1000	0.0050	0.999	0.675
<i>Hyas coarctatus</i>	0.0005	0.0013	0.3981	0.0800	0.0030	1.000	0.836
<i>Echinorachnius parma</i>	0.0002	0.0011	0.2107	0.0100	0.0000	1.000	0.998

Signif. codes: 0 ‘***’ 0.001 ‘**’ 0.01 ‘*’ 0.05 ‘.’ 0.1 ‘ ’ 1

Contrast: Blue_Purple

taxa	average	sd	ratio	ava	avb	cumsum	p
<i>Psolus phantapus</i>	0.4776	0.3396	1.4063	44.0600	0.3060	0.511	0.094 .
<i>Pandalus</i> spp.	0.2271	0.1745	1.3016	0.0000	3.8090	0.753	0.001 ***
<i>Chionoecetes opilio</i>	0.0725	0.1002	0.7238	0.0800	1.9350	0.831	0.048 *
<i>Ptychogastria polaris</i>	0.0321	0.0517	0.6210	0.1900	0.9170	0.865	0.106
<i>Pachycerianthus borealis</i>	0.0232	0.0781	0.2976	2.1400	0.0000	0.890	0.472
<i>Strongylocentrotus droebachiensis</i>	0.0194	0.0278	0.7004	0.2900	0.0890	0.911	0.985
<i>Hyas araneus</i>	0.0177	0.0232	0.7618	0.0200	0.1470	0.930	0.041 *
<i>Pagurus</i> spp.	0.0157	0.0262	0.6012	0.0000	0.4580	0.947	0.102
<i>Echinorachnius parma</i>	0.0107	0.0213	0.5021	0.0100	0.1020	0.958	0.575
<i>Ophiuroidea</i> spp.	0.0062	0.0131	0.4736	0.6900	0.0000	0.965	0.999
<i>Asterias</i> spp.	0.0059	0.0140	0.4232	0.0400	0.0000	0.971	0.990
<i>Porifera</i> sp. 15	0.0043	0.0123	0.3538	0.0400	0.0000	0.976	0.580
<i>Solaster endeca</i>	0.0043	0.0145	0.2967	0.2900	0.0000	0.980	0.482
Gastropoda sp. 3	0.0034	0.0077	0.4424	0.0600	0.0000	0.984	0.230
<i>Mesodesma arctatum</i>	0.0033	0.0089	0.3660	0.0300	0.0000	0.988	0.316
<i>Henricia</i> spp.	0.0028	0.0094	0.2972	0.0200	0.0000	0.990	0.983
<i>Crossaster papposus</i>	0.0019	0.0088	0.2112	0.0300	0.0000	0.992	0.365
<i>Pseudopleuronectes americanus</i>	0.0018	0.0041	0.4376	0.0200	0.0000	0.994	0.567
<i>Flabellina</i> sp. 1	0.0013	0.0071	0.1873	0.0100	0.0000	0.996	0.570
<i>Lunارca ovalis</i>	0.0011	0.0051	0.2217	0.2500	0.0000	0.997	0.543
<i>Hippoglossoides platessoides</i>	0.0011	0.0041	0.2736	0.0100	0.0000	0.998	0.599
<i>Mytilidae</i> spp.	0.0011	0.0031	0.3490	0.0100	0.0000	0.999	0.690
<i>Hyas coarctatus</i>	0.0003	0.0011	0.3141	0.0800	0.0000	1.000	0.671
<i>Metridium</i> spp.	0.0003	0.0012	0.2218	0.1000	0.0000	1.000	0.649
<i>Leptasterias polaris</i>	0.0000	0.0000	NA	0.0000	0.0000	1.000	0.858

<i>Pteraster</i> spp.	0.0000	0.0000	NA	0.0000	0.0000	1.000	0.981
-----------------------	--------	--------	----	--------	--------	-------	-------

Signif. codes: 0 ‘***’ 0.001 ‘**’ 0.01 ‘*’ 0.05 ‘.’ 0.1 ‘ ’ 1

Contrast: Yellow_Purple

taxa	average	sd	ratio	ava	avb	cumsum	p
<i>Ophiuroidea</i> spp.	0.45400	0.25844	1.75650	10.95500	0.00000	0.480	0.012 *
<i>Pandalus</i> spp.	0.19360	0.12071	1.60390	0.06300	3.80900	0.684	0.001 ***
<i>Psolus phantapus</i>	0.07720	0.11427	0.67600	2.11700	0.30600	0.766	0.997
<i>Chionoecetes opilio</i>	0.07360	0.09165	0.80250	0.06800	1.93500	0.844	0.037 *
<i>Ptychogastria polaris</i>	0.04360	0.04727	0.92260	0.64200	0.91700	0.890	0.026 *
<i>Pachycerianthus borealis</i>	0.03670	0.12850	0.28590	0.56000	0.00000	0.929	0.304
<i>Pagurus</i> spp.	0.01680	0.02403	0.70040	0.06900	0.45800	0.946	0.091 .
<i>Strongylocentrotus droebachiensis</i>	0.01590	0.01990	0.79740	0.21600	0.08900	0.963	0.983
<i>Hyas araneus</i>	0.01320	0.01551	0.84820	0.00700	0.14700	0.977	0.104
<i>Echinorachnius parma</i>	0.00870	0.01553	0.55850	0.00000	0.10200	0.986	0.567
<i>Pteraster</i> spp.	0.00540	0.01223	0.44270	0.20800	0.00000	0.992	0.141
<i>Flabellina</i> sp. 1	0.00220	0.00797	0.27940	0.03800	0.00000	0.994	0.392
<i>Hippoglossoides platessoides</i>	0.00200	0.00346	0.56970	0.03400	0.00000	0.996	0.331
<i>Leptasterias polaris</i>	0.00110	0.00371	0.30360	0.01800	0.00000	0.998	0.385
Porifera sp. 15	0.00070	0.00156	0.45920	0.01300	0.00000	0.998	0.867
<i>Crossaster papposus</i>	0.00070	0.00187	0.35210	0.00700	0.00000	0.999	0.541
<i>Metridium</i> spp.	0.00040	0.00155	0.24720	0.00500	0.00000	1.000	0.514
<i>Hyas coarctatus</i>	0.00020	0.00084	0.24990	0.00300	0.00000	1.000	0.740
<i>Solaster endeca</i>	0.00020	0.00084	0.24990	0.00300	0.00000	1.000	0.945
<i>Asterias</i> spp.	0.00000	0.00000	NA	0.00000	0.00000	1.000	0.999
<i>Pseudopleuronectes americanus</i>	0.00000	0.00000	NA	0.00000	0.00000	1.000	0.972
<i>Lunارca ovalis</i>	0.00000	0.00000	NA	0.00000	0.00000	1.000	0.739
<i>Mesodesma arctatum</i>	0.00000	0.00000	NA	0.00000	0.00000	1.000	0.843
Gastropoda sp. 3	0.00000	0.00000	NA	0.00000	0.00000	1.000	0.867
<i>Henricia</i> spp.	0.00000	0.00000	NA	0.00000	0.00000	1.000	0.998
<i>Mytilidae</i> spp.	0.00000	0.00000	NA	0.00000	0.00000	1.000	0.946

Signif. codes: 0 ‘***’ 0.001 ‘**’ 0.01 ‘*’ 0.05 ‘.’ 0.1 ‘ ’ 1

> summary(indval)

taxa	Cluster	indicator_value	probability
<i>Henricia</i> spp.	Red	0.9096	0.0001

<i>Asterias</i> spp.	Red	0.8366	0.0001
<i>Echinorachnius parma</i>	Red	0.3640	0.0103
<i>Strongylocentrotus droebachiensis</i>	Orange	0.6653	0.0007
<i>Psolus phantapus</i>	Blue	0.9479	0.0001
<i>Ophiuroidea</i> spp.	Yellow	0.9393	0.0001
<i>Pteraster</i> spp.	Yellow	0.3793	0.0127
<i>Pandalus</i> spp.	Purple	0.9825	0.0001
<i>Chionoecetes opilio</i>	Purple	0.6197	0.0044
<i>Hyas araneus</i>	Purple	0.4909	0.0059
<i>Pagurus</i> spp.	Purple	0.2829	0.0455

Sum of probabilities = 7.5675

Sum of Indicator Values = 9.36

Sum of Significant Indicator Values = 7.42

Number of Significant Indicators = 11

Significant Indicator Distribution

1 2 3 4 5

3 1 1 2 4

> anosim

Call:

anosim(x = spe.chSummer, grouping = Matrixclust\$spech.UPGMA.g, permutations = 999)

Dissimilarity: euclidean

ANOSIM statistic R: 0.9445

Significance: 0.001

Permutation: free

Number of permutations: 999

FALL

> summary(simper, ordered=TRUE)

Contrast: Brown_Yellow

taxa	average	sd	ratio	ava	avb	cumsum	p
<i>Ophiuroidea</i> spp.	0.58770	0.27965	2.10150	0.00370	5.06800	0.607	0.001 ***
<i>Strongylocentrotus droebachiensis</i>	0.08940	0.12368	0.72270	0.53470	0.11300	0.699	1.000
<i>Psychogastria polaris</i>	0.08800	0.11502	0.76530	0.01800	0.45300	0.790	0.001 ***
<i>Asterias</i> spp.	0.06830	0.11666	0.58570	0.41070	0.00000	0.861	1.000
Porifera sp. 31	0.02150	0.05558	0.38730	0.00370	0.05000	0.883	0.003 **
<i>Henricia</i> spp.	0.01510	0.03457	0.43800	0.09120	0.00000	0.898	1.000
<i>Pachycerianthus borealis</i>	0.00930	0.06470	0.14420	0.07280	0.00000	0.908	0.923
Gastropoda sp. 3	0.00830	0.01928	0.43030	0.00440	0.02200	0.917	0.131
<i>Flabellina</i> sp. 1	0.00830	0.02157	0.38340	0.00190	0.02900	0.925	0.022 *
<i>Hippoglossoides platessoides</i>	0.00760	0.01152	0.65660	0.00520	0.02900	0.933	0.865
<i>Mytilidae</i> spp.	0.00750	0.03765	0.19930	0.04140	0.00000	0.941	0.933
<i>Psolus phantapus</i>	0.00660	0.01309	0.50150	0.00330	0.02400	0.948	0.101
<i>Pandalus</i> spp.	0.00590	0.01223	0.48540	0.00210	0.02100	0.954	1.000
<i>Chionoecetes opilio</i>	0.00490	0.00832	0.58630	0.00910	0.01600	0.959	0.999
<i>Pseudopleuronectes americanus</i>	0.00450	0.00933	0.47690	0.01600	0.00400	0.963	1.000
<i>Arctica islandica</i>	0.00440	0.01203	0.36980	0.01230	0.01000	0.968	0.997
<i>Hyas araneus</i>	0.00400	0.00893	0.44820	0.01070	0.00600	0.972	0.999
<i>Mesodesma arctatum</i>	0.00400	0.01255	0.31510	0.01650	0.00000	0.976	0.998
<i>Pagurus</i> spp.	0.00350	0.00806	0.42980	0.00790	0.00600	0.980	0.988
Porifera sp. 17	0.00340	0.01218	0.27970	0.00950	0.00400	0.983	0.988
<i>Zoarces</i> sp. 1	0.00270	0.00582	0.46960	0.00140	0.01300	0.986	0.800
Gastropoda sp. 4	0.00200	0.00646	0.30690	0.00630	0.00600	0.988	0.996
<i>Solaster endeca</i>	0.00200	0.00795	0.24680	0.00720	0.00600	0.990	0.996
<i>Echinorachnius parma</i>	0.00170	0.00690	0.25060	0.00920	0.00000	0.992	0.989
<i>Leptasterias polaris</i>	0.00170	0.00415	0.40220	0.00720	0.00400	0.994	1.000
<i>Pteraster</i> spp.	0.00160	0.00335	0.48070	0.00120	0.01200	0.995	0.506
<i>Lunaria ovalis</i>	0.00150	0.00443	0.33030	0.00580	0.00200	0.997	0.987
<i>Chlamys</i> sp. 1	0.00130	0.00686	0.18520	0.00540	0.00000	0.998	0.951
Porifera sp. 15	0.00110	0.00352	0.30360	0.00540	0.00000	0.999	0.992
<i>Hyas coarctatus</i>	0.00070	0.00267	0.27090	0.00180	0.00100	1.000	1.000

Signif. codes: 0 *** 0.001 ** 0.01 * 0.05 . 0.1 ' 1

Contrast: Brown_Purple

taxa	average	sd	ratio	ava	avb	cumsum	p
<i>Strongylocentrotus droebachiensis</i>	0.26043	0.23208	1.12220	0.53470	0.02673	0.277	0.054 .
<i>Asterias</i> spp.	0.17516	0.22841	0.76690	0.41070	0.00000	0.464	0.174
<i>Pandalus</i> spp.	0.17376	0.11864	1.46460	0.00210	0.20801	0.649	0.001 ***
<i>Henricia</i> spp.	0.03822	0.06879	0.55560	0.09120	0.00000	0.689	0.198
<i>Arctica islandica</i>	0.03681	0.06285	0.58570	0.01230	0.03942	0.729	0.012 *
<i>Hyas coarctatus</i>	0.03411	0.03649	0.93490	0.00180	0.04086	0.765	0.001 ***
Porifera sp. 17	0.02516	0.04704	0.53500	0.00950	0.02628	0.792	0.070 .
<i>Ptychogastria polaris</i>	0.02480	0.05891	0.42100	0.01800	0.00824	0.818	0.963
<i>Mytilidae</i> spp.	0.02032	0.07942	0.25580	0.04140	0.00000	0.840	0.142
<i>Pachycerianthus borealis</i>	0.01790	0.11504	0.15560	0.07280	0.00000	0.859	0.068 .
<i>Chionoecetes opilio</i>	0.01731	0.02203	0.78590	0.00910	0.01714	0.877	0.028 *
<i>Hyas araneus</i>	0.01599	0.02685	0.59550	0.01070	0.01314	0.894	0.090 .
<i>Mesodesma arctatum</i>	0.01594	0.04442	0.35880	0.01650	0.00000	0.911	0.209
Zoarces sp. 1	0.01074	0.01949	0.55090	0.00140	0.01314	0.923	0.017 *
<i>Pseudopleuronectes americanus</i>	0.01064	0.02019	0.52710	0.01600	0.00000	0.934	0.208
<i>Pagurus</i> spp.	0.00741	0.02242	0.33060	0.00790	0.00000	0.942	0.243
Gastropoda sp. 4	0.00652	0.02141	0.30460	0.00630	0.00000	0.949	0.205
<i>Solaster endeca</i>	0.00552	0.02478	0.22290	0.00720	0.00000	0.955	0.264
<i>Echinorachnius parma</i>	0.00541	0.01857	0.29130	0.00920	0.00000	0.960	0.197
<i>Leptasterias polaris</i>	0.00514	0.01267	0.40560	0.00720	0.00000	0.966	0.253
<i>Hippoglossoides platessoides</i>	0.00499	0.01538	0.32410	0.00520	0.00000	0.971	0.820
<i>Chlamys</i> sp. 1	0.00454	0.02053	0.22110	0.00540	0.00000	0.976	0.121
Gastropoda sp. 3	0.00443	0.01694	0.26140	0.00440	0.00000	0.981	0.536
<i>Lunارка ovalis</i>	0.00351	0.01092	0.32140	0.00580	0.00000	0.984	0.245
Porifera sp. 15	0.00342	0.01062	0.32180	0.00540	0.00000	0.988	0.270
<i>Psolus phantapus</i>	0.00295	0.01517	0.19430	0.00330	0.00000	0.991	0.657
Porifera sp. 31	0.00251	0.01620	0.15520	0.00370	0.00000	0.994	0.939
<i>Ophiuroidea</i> spp.	0.00225	0.01189	0.18900	0.00370	0.00000	0.996	1.000
<i>Flabellina</i> sp. 1	0.00179	0.01160	0.15470	0.00190	0.00000	0.998	0.880
<i>Pteraster</i> spp.	0.00163	0.01061	0.15360	0.00120	0.00000	1.000	0.315

Signif. codes: 0 **** 0.001 *** 0.01 ** 0.05 * 0.1 ' 1

Contrast: Brown_Grey

taxa	average	Sd	ratio	ava	avb	cumsum	p
<i>Strongylocentrotus droebachiensis</i>	0.32770	0.25986	1.26110	0.53470	0.00000	0.334	0.090 .
<i>Asterias spp.</i>	0.19940	0.25326	0.78750	0.41070	0.00000	0.537	0.182
<i>Hippoglossoides platessoides</i>	0.13620	0.09289	1.46660	0.00520	0.12888	0.676	0.001 ***
<i>Solaster endeca</i>	0.04900	0.03524	1.38900	0.00720	0.04296	0.726	0.017 *
<i>Henricia spp.</i>	0.04310	0.07597	0.56790	0.09120	0.00000	0.770	0.155
<i>Ptychogastria polaris</i>	0.02540	0.07976	0.31860	0.01800	0.00000	0.796	0.741
<i>Mytilidae spp.</i>	0.02330	0.08796	0.26450	0.04140	0.00000	0.820	0.082 .
<i>Mesodesma arctatum</i>	0.02100	0.06070	0.34570	0.01650	0.00000	0.841	0.083 .
<i>Pachycerianthus borealis</i>	0.01890	0.12259	0.15430	0.07280	0.00000	0.860	0.041 *
<i>Arctica islandica</i>	0.01820	0.06182	0.29490	0.01230	0.00000	0.879	0.120
<i>Pseudopleuronectes americanus</i>	0.01290	0.02493	0.51730	0.01600	0.00000	0.892	0.174
<i>Hyas araneus</i>	0.01190	0.03214	0.36870	0.01070	0.00000	0.904	0.141
<i>Chionoecetes opilio</i>	0.01160	0.03051	0.37920	0.00910	0.00000	0.916	0.228
Porifera sp. 17	0.01020	0.04328	0.23470	0.00950	0.00000	0.926	0.146
<i>Pagurus spp.</i>	0.00950	0.02947	0.32270	0.00790	0.00000	0.936	0.121
Gastropoda sp. 4	0.00840	0.02765	0.30340	0.00630	0.00000	0.944	0.077 .
<i>Leptasterias polaris</i>	0.00660	0.01738	0.38140	0.00720	0.00000	0.951	0.098 .
<i>Echinorachnius parma</i>	0.00660	0.02283	0.28850	0.00920	0.00000	0.958	0.083 .
Gastropoda sp. 3	0.00560	0.02145	0.26150	0.00440	0.00000	0.964	0.296
<i>Chlamys sp. 1</i>	0.00550	0.02511	0.22070	0.00540	0.00000	0.969	0.042 *
Porifera sp. 15	0.00420	0.01370	0.30540	0.00540	0.00000	0.973	0.070 .
<i>Lunارca ovalis</i>	0.00410	0.01284	0.31990	0.00580	0.00000	0.978	0.076 .
<i>Psolus phantapus</i>	0.00360	0.01864	0.19380	0.00330	0.00000	0.981	0.368
<i>Pandalus spp.</i>	0.00340	0.01573	0.21670	0.00210	0.00000	0.985	0.836
Porifera sp. 31	0.00290	0.01903	0.15430	0.00370	0.00000	0.988	0.754
<i>Ophiuroidea spp.</i>	0.00270	0.01473	0.18410	0.00370	0.00000	0.990	1.000
<i>Zoarces sp. 1</i>	0.00260	0.01229	0.21500	0.00140	0.00000	0.993	0.314
<i>Pteraster spp.</i>	0.00230	0.01469	0.15430	0.00120	0.00000	0.996	0.174
<i>Flabellina sp. 1</i>	0.00220	0.01447	0.15430	0.00190	0.00000	0.998	0.640
<i>Hyas coarctatus</i>	0.00220	0.00979	0.22080	0.00180	0.00000	1.000	0.465

Signif. codes: 0 **** 0.001 ** 0.01 * 0.05 . 0.1 ' 1

<i>Leptasterias polaris</i>	0.00514	0.01267	0.40560	0.00720	0.00000	0.966	0.253
<i>Hippoglossoides platessoides</i>	0.00499	0.01538	0.32410	0.00520	0.00000	0.971	0.820
<i>Chlamys</i> sp. 1	0.00454	0.02053	0.22110	0.00540	0.00000	0.976	0.121
Gastropoda sp. 3	0.00443	0.01694	0.26140	0.00440	0.00000	0.981	0.536
<i>Lunarca ovalis</i>	0.00351	0.01092	0.32140	0.00580	0.00000	0.984	0.245
Porifera sp. 15	0.00342	0.01062	0.32180	0.00540	0.00000	0.988	0.270
<i>Psolus phantapus</i>	0.00295	0.01517	0.19430	0.00330	0.00000	0.991	0.657
Porifera sp. 31	0.00251	0.01620	0.15520	0.00370	0.00000	0.994	0.939
<i>Ophiuroidea</i> spp.	0.00225	0.01189	0.18900	0.00370	0.00000	0.996	1.000
<i>Flabellina</i> sp. 1	0.00179	0.01160	0.15470	0.00190	0.00000	0.998	0.880
<i>Pteraster</i> spp.	0.00163	0.01061	0.15360	0.00120	0.00000	1.000	0.315

Signif. codes: 0 ****, 0.001 **, 0.01 *, 0.05 ., 0.1 ‘ ’ 1

Contrast: Yellow_Green

taxa	average	sd	ratio	ava	avb	cumsum	p
<i>Ophiuroidea</i> spp.	0.67070	0.27317	2.45530	5.06800	0.00000	0.692	0.001 ***
<i>Ptychogastria polaris</i>	0.10890	0.14345	0.75930	0.45300	0.00824	0.805	0.051 .
<i>Pandalus</i> spp.	0.05070	0.04606	1.10130	0.02100	0.20801	0.857	0.090 .
Porifera sp. 31	0.02870	0.07269	0.39420	0.05000	0.00000	0.887	0.079 .
<i>Strongylocentrotus droebachiensis</i>	0.01640	0.02100	0.78210	0.11300	0.02673	0.904	1.000
<i>Arctica islandica</i>	0.01150	0.02221	0.51740	0.01000	0.03942	0.915	0.389
<i>Hyas coarctatus</i>	0.01120	0.01280	0.87390	0.00100	0.04086	0.927	0.086 .
Gastropoda sp. 3	0.01060	0.02568	0.41290	0.02200	0.00000	0.938	0.213
<i>Flabellina</i> sp. 1	0.01010	0.02707	0.37480	0.02900	0.00000	0.948	0.128
<i>Hippoglossoides platessoides</i>	0.00980	0.01507	0.64720	0.02900	0.00000	0.958	0.365
Porifera sp. 17	0.00780	0.01481	0.52710	0.00400	0.02628	0.966	0.349
<i>Psolus phantapus</i>	0.00780	0.01603	0.48630	0.02400	0.00000	0.974	0.194
<i>Chionoecetes opilio</i>	0.00630	0.00833	0.75740	0.01600	0.01714	0.981	0.625
<i>Zoarces</i> sp. 1	0.00520	0.00875	0.59700	0.01300	0.01314	0.986	0.239
<i>Hyas araneus</i>	0.00500	0.00942	0.53470	0.00600	0.01314	0.992	0.664
<i>Pagurus</i> spp.	0.00270	0.00808	0.33510	0.00600	0.00000	0.994	0.736
<i>Pseudopleuronectes americanus</i>	0.00240	0.01013	0.23360	0.00400	0.00000	0.997	0.948
<i>Pteraster</i> spp.	0.00150	0.00258	0.57490	0.01200	0.00000	0.998	0.424
<i>Solaster endeca</i>	0.00040	0.00191	0.23410	0.00600	0.00000	0.999	0.838

Gastropoda sp. 4	0.00040	0.00191	0.23410	0.00600	0.00000	0.999	0.841
<i>Lunarca ovalis</i>	0.00040	0.00186	0.23400	0.00200	0.00000	1.000	0.828
<i>Leptasterias polaris</i>	0.00020	0.00097	0.23410	0.00400	0.00000	1.000	0.965
<i>Asterias</i> spp.	0.00000	0.00000	NA	0.00000	0.00000	1.000	1.000
<i>Henricia</i> spp.	0.00000	0.00000	NA	0.00000	0.00000	1.000	1.000
<i>Mesodesma arctatum</i>	0.00000	0.00000	NA	0.00000	0.00000	1.000	0.981
<i>Echinorachnius parma</i>	0.00000	0.00000	NA	0.00000	0.00000	1.000	0.810
<i>Pachycerianthus borealis</i>	0.00000	0.00000	NA	0.00000	0.00000	1.000	0.326
<i>Mytilidae</i> spp.	0.00000	0.00000	NA	0.00000	0.00000	1.000	0.958
<i>Chlamys</i> sp. 1	0.00000	0.00000	NA	0.00000	0.00000	1.000	0.572
Porifera sp. 15	0.00000	0.00000	NA	0.00000	0.00000	1.000	0.886

Signif. codes: 0 ****, 0.001 **, 0.01 *, 0.05 ., 0.1 ‘ ’ 1

Contrast: Yellow_Grey

taxa	average	sd	ratio	ava	avb	cumsum	p
<i>Ophiuroidea</i> spp.	0.70320	0.27619	2.54590	5.06800	0.00000	0.719	0.081 .
<i>Ptychogastria polaris</i>	0.12090	0.16391	0.73750	0.45300	0.00000	0.843	0.094 .
Porifera sp. 31	0.03300	0.08697	0.37950	0.05000	0.00000	0.876	0.082 .
<i>Hippoglossoides platessoides</i>	0.02860	0.02352	1.21420	0.02900	0.12888	0.906	0.059 .
<i>Strongylocentrotus droebachiensis</i>	0.01450	0.02118	0.68290	0.11300	0.00000	0.920	0.992
<i>Solaster endeca</i>	0.01330	0.01006	1.31680	0.00600	0.04296	0.934	0.076 .
Gastropoda sp. 3	0.01220	0.03061	0.39710	0.02200	0.00000	0.946	0.135
<i>Flabellina</i> sp. 1	0.01120	0.03082	0.36190	0.02900	0.00000	0.958	0.066 .
<i>Psolus phantapus</i>	0.00860	0.01817	0.47120	0.02400	0.00000	0.966	0.102
<i>Pandalus</i> spp.	0.00800	0.01759	0.45370	0.02100	0.00000	0.975	0.534
<i>Chionoecetes opilio</i>	0.00550	0.01172	0.47320	0.01600	0.00000	0.980	0.430
Zoarces sp. 1	0.00330	0.00802	0.41710	0.01300	0.00000	0.984	0.253
<i>Pagurus</i> spp.	0.00300	0.00916	0.32840	0.00600	0.00000	0.987	0.446
<i>Hyas araneus</i>	0.00290	0.00900	0.32660	0.00600	0.00000	0.990	0.600
<i>Pseudopleuronectes americanus</i>	0.00270	0.01170	0.22940	0.00400	0.00000	0.993	0.697
<i>Arctica islandica</i>	0.00240	0.00776	0.30300	0.01000	0.00000	0.995	0.722
Porifera sp. 17	0.00190	0.00592	0.31500	0.00400	0.00000	0.997	0.616
<i>Pteraster</i> spp.	0.00150	0.00271	0.56290	0.01200	0.00000	0.998	0.246
<i>Lunaria ovalis</i>	0.00050	0.00200	0.22940	0.00200	0.00000	0.999	0.731

Gastropoda sp. 4	0.00050	0.00199	0.22940	0.00600	0.00000	0.999	0.726
<i>Hyas coarctatus</i>	0.00040	0.00166	0.22940	0.00100	0.00000	1.000	0.791
<i>Leptasterias polaris</i>	0.00020	0.00101	0.22940	0.00400	0.00000	1.000	0.918
<i>Asterias</i> spp.	0.00000	0.00000	NA	0.00000	0.00000	1.000	1.000
<i>Henricia</i> spp.	0.00000	0.00000	NA	0.00000	0.00000	1.000	1.000
<i>Mesodesma arctatum</i>	0.00000	0.00000	NA	0.00000	0.00000	1.000	0.954
<i>Echinorachnius parma</i>	0.00000	0.00000	NA	0.00000	0.00000	1.000	0.750
<i>Pachycerianthus borealis</i>	0.00000	0.00000	NA	0.00000	0.00000	1.000	0.308
<i>Mytilidae</i> spp.	0.00000	0.00000	NA	0.00000	0.00000	1.000	0.926
<i>Chlamys</i> sp. 1	0.00000	0.00000	NA	0.00000	0.00000	1.000	0.529
Porifera sp. 15	0.00000	0.00000	NA	0.00000	0.00000	1.000	0.839

Signif. codes: 0 ****, 0.001 **, 0.01 *, 0.05 ., 0.1 ‘ ’ 1

Contrast: Purple_Grey

taxa	average	sd	ratio	ava	avb	cumsum	p
<i>Pandalus</i> spp.	0.38420	0.15919	2.41300	0.20801	0.00000	0.384	0.001 ***
<i>Hippoglossoides platessoides</i>	0.23930	0.05997	3.99000	0.00000	0.12888	0.623	0.001 ***
<i>Solaster endeca</i>	0.07980	0.01999	3.99000	0.00000	0.04296	0.703	0.011 *
<i>Hyas coarctatus</i>	0.07660	0.07463	1.02700	0.04086	0.00000	0.780	0.005 **
<i>Arctica islandica</i>	0.05650	0.11305	0.50000	0.03942	0.00000	0.836	0.057 .
<i>Strongylocentrotus droebachiensis</i>	0.03980	0.07969	0.50000	0.02673	0.00000	0.876	0.850
Porifera sp. 17	0.03770	0.07536	0.50000	0.02628	0.00000	0.914	0.072 .
<i>Chionoecetes opilio</i>	0.03090	0.03633	0.85000	0.01714	0.00000	0.945	0.059 .
<i>Hyas araneus</i>	0.01880	0.03768	0.50000	0.01314	0.00000	0.964	0.155
<i>Zoarces</i> sp. 1	0.01880	0.03768	0.50000	0.01314	0.00000	0.982	0.043 *
<i>Ptychogastria polaris</i>	0.01760	0.03517	0.50000	0.00824	0.00000	1.000	0.658
<i>Asterias</i> spp.	0.00000	0.00000	NA	0.00000	0.00000	1.000	0.925
<i>Henricia</i> spp.	0.00000	0.00000	NA	0.00000	0.00000	1.000	0.819
<i>Pseudopleuronectes americanus</i>	0.00000	0.00000	NA	0.00000	0.00000	1.000	0.646
<i>Leptasterias polaris</i>	0.00000	0.00000	NA	0.00000	0.00000	1.000	0.479
<i>Psolus phantapus</i>	0.00000	0.00000	NA	0.00000	0.00000	1.000	0.500
Gastropoda sp. 4	0.00000	0.00000	NA	0.00000	0.00000	1.000	0.326
<i>Pagurus</i> spp.	0.00000	0.00000	NA	0.00000	0.00000	1.000	0.481
<i>Mesodesma arctatum</i>	0.00000	0.00000	NA	0.00000	0.00000	1.000	0.502

<i>Flabellina</i> sp. 1	0.00000	0.00000	NA	0.00000	0.00000	1.000	0.478
<i>Lunaria ovalis</i>	0.00000	0.00000	NA	0.00000	0.00000	1.000	0.334
<i>Ophiuroidea</i> spp.	0.00000	0.00000	NA	0.00000	0.00000	1.000	0.845
<i>Pteraster</i> spp.	0.00000	0.00000	NA	0.00000	0.00000	1.000	0.368
<i>Echinorachnius parma</i>	0.00000	0.00000	NA	0.00000	0.00000	1.000	0.311
<i>Pachycerianthus borealis</i>	0.00000	0.00000	NA	0.00000	0.00000	1.000	0.080 .
<i>Mytilidae</i> spp.	0.00000	0.00000	NA	0.00000	0.00000	1.000	0.443
<i>Chlamys</i> sp. 1	0.00000	0.00000	NA	0.00000	0.00000	1.000	0.137
Gastropoda sp. 3	0.00000	0.00000	NA	0.00000	0.00000	1.000	0.483
Porifera sp. 31	0.00000	0.00000	NA	0.00000	0.00000	1.000	0.332
Porifera sp. 15	0.00000	0.00000	NA	0.00000	0.00000	1.000	0.359

Signif. codes: 0 ****, 0.001 ***, 0.01 **, 0.05 * , 0.1 . 1

Permutation: free

Number of permutations: 999

> summary(indval)

taxa	Cluster	indicator_value	probability
<i>Strongylocentrotus droebachiensis</i>	Brown	0.7547	0.0150
<i>Ophiuroidea</i> spp.	Yellow	0.9993	0.0001
<i>Ptychogastria polaris</i>	Yellow	0.7961	0.0227
<i>Pandalus</i> spp.	Purple	0.8998	0.0051
<i>Hippoglossoides platessoides</i>	Grey	0.7917	0.0141

Sum of probabilities = 10.123

Sum of Indicator Values = 9.96

Sum of Significant Indicator Values = 4.24

Number of Significant Indicators = 5

Significant Indicator Distribution

1 2 3 4

1 2 1 1

> anosim

Call:

```
anosim(x = spe.chFall, grouping = Matrixclust$spech.UPGMA.g, permutations = 999)
```

Dissimilarity: euclidean

ANOSIM statistic R: 0.8875

Significance: 0.001

Permutation: free

Number of permutations: 999

WINTER

```
> summary(simper, ordered=TRUE)
```

Contrast: Brown_Green

taxa	average	sd	ratio	ava	avb	cumsum	p
<i>Ophiuroidea</i> spp.	0.40370	0.31341	1.28800	0.01181	0.91130	0.426	0.001 ***
<i>Pachycerianthus borealis</i>	0.11210	0.19070	0.58760	0.30647	0.00630	0.544	1.000
<i>Strongylocentrotus droebachiensis</i>	0.10720	0.12917	0.83020	0.15515	0.02740	0.657	0.996
<i>Asterias</i> spp.	0.08120	0.12299	0.66010	0.10963	0.00000	0.743	0.993
<i>Psolus phantapus</i>	0.05380	0.09048	0.59470	0.00040	0.05690	0.800	0.001***
<i>Ptychogastria polaris</i>	0.05280	0.10383	0.50900	0.00248	0.05290	0.855	0.001 ***
<i>Pandalus</i> spp.	0.02850	0.06082	0.46890	0.05024	0.01670	0.886	0.503
<i>Henricia</i> spp.	0.02500	0.04829	0.51850	0.03395	0.00000	0.912	0.993
Gastropoda sp. 3	0.01320	0.02241	0.58950	0.00048	0.01180	0.926	0.001 ***
<i>Mytilidae</i> spp.	0.00860	0.02287	0.37470	0.00762	0.00150	0.935	0.996
<i>Arctica islandica</i>	0.00760	0.02107	0.36290	0.01018	0.00130	0.943	0.984
<i>Chionoecetes opilio</i>	0.00740	0.01404	0.52700	0.00181	0.01170	0.951	0.371
<i>Leptasterias polaris</i>	0.00610	0.01404	0.43100	0.01248	0.00140	0.957	0.996
<i>Flabellina</i> sp. 1	0.00600	0.01697	0.35640	0.00021	0.00450	0.964	0.004 **
<i>Echinarachnius parma</i>	0.00570	0.03012	0.19040	0.00543	0.00030	0.970	0.985
<i>Pagurus</i> spp.	0.00540	0.02029	0.26690	0.00665	0.00310	0.975	0.437
<i>Hyas araneus</i>	0.00540	0.01284	0.42000	0.00280	0.00260	0.981	0.911
<i>Solaster endeca</i>	0.00410	0.01089	0.37790	0.00128	0.00310	0.985	0.572

Porifera sp. 16	0.00250	0.01207	0.20520	0.00173	0.00000	0.988	0.977
<i>Hyas coarctatus</i>	0.00200	0.00620	0.32220	0.00130	0.00100	0.990	0.974
Gastropoda sp. 4	0.00170	0.00567	0.29800	0.00060	0.00090	0.992	0.775
Porifera sp. 31	0.00150	0.00392	0.38450	0.00156	0.00060	0.993	0.731
<i>Chlamys</i> sp. 1	0.00150	0.00699	0.21400	0.00159	0.00040	0.995	0.986
<i>Myccale</i> spp.	0.00140	0.00515	0.27220	0.00125	0.00000	0.996	0.995
Chordata sp. 7	0.00110	0.00568	0.20050	0.00050	0.00150	0.998	0.872
Porifera sp. 15	0.00110	0.00481	0.23550	0.00128	0.00000	0.999	0.988
<i>Crossaster papposus</i>	0.00110	0.00399	0.26380	0.00050	0.00030	1.000	0.928

Signif. codes: 0 ‘***’ 0.001 ‘**’ 0.01 ‘*’ 0.05 ‘.’ 0.1 ‘ ’ 1

Permutation: free

Number of permutations: 999

> summary(indval)

taxa	Cluster	indicator_value	probability
<i>Asterias</i> spp.	Brown	0.7179	0.0001
<i>Strongylocentrotus droebachiensis</i>	Brown	0.6974	0.0006
<i>Henricia</i> spp.	Brown	0.5128	0.0002
<i>Pachycerianthus borealis</i>	Brown	0.4773	0.0020
<i>Ophiuroidea</i> spp.	Green	0.9113	0.0001
<i>Ptychogastria polaris</i>	Green	0.6980	0.0001
<i>Psolus phantapus</i>	Green	0.5729	0.0001
Gastropoda sp. 3	Green	0.4434	0.0001
<i>Chionoecetes opilio</i>	Green	0.3998	0.0014
<i>Flabellina</i> sp. 1	Green	0.2203	0.0096

Sum of probabilities = 7.3906

Sum of Indicator Values = 7.6

Sum of Significant Indicator Values = 5.65

Number of Significant Indicators = 10

Significant Indicator Distribution

1 2

4 6

> anosim

Call:

anosim(x = spe.chWinter, grouping = Matrixclust\$spech.UPGMA.g, permutations = 999)

Dissimilarity: euclidean

ANOSIM statistic R: 0.7494

Significance: 0.001

Permutation: free

Number of permutations: 999

SPRING

> summary(simper,ordered=TRUE)

Contrast: Red_Green

taxa	average	sd	ratio	ava	avb	cumsum	p
<i>Psolus phantapus</i>	0.45250	0.28572	1.58380	0.00000	3.33900	0.467	0.270
<i>Echinorachnius parma</i>	0.27200	0.21763	1.24980	1.48710	0.01900	0.748	0.001 ***
<i>Ophiuroidea</i> spp.	0.08200	0.13723	0.59730	0.00000	0.43500	0.832	0.546
<i>Asterias</i> spp.	0.05550	0.05975	0.92870	0.24270	0.02500	0.890	0.017 *
<i>Strongylocentrotus droebachiensis</i>	0.03850	0.07050	0.54610	0.22700	0.02700	0.929	0.891
<i>Henricia</i> spp.	0.02770	0.04595	0.60350	0.09660	0.00500	0.958	0.017 *
<i>Pachycerianthus borealis</i>	0.00900	0.03816	0.23620	0.00000	0.04400	0.967	0.998
<i>Pteraster</i> spp.	0.00850	0.01866	0.45570	0.00000	0.04800	0.976	0.538
<i>Ptychogastria polaris</i>	0.00570	0.00905	0.62510	0.00000	0.03100	0.982	0.934
<i>Mytilidae</i> spp.	0.00280	0.00442	0.62950	0.01360	0.00000	0.985	0.790
<i>Pandalus</i> spp.	0.00250	0.00653	0.38790	0.00000	0.01000	0.987	0.895
Gastropoda sp. 3	0.00250	0.00435	0.57800	0.00000	0.01500	0.990	0.666
<i>Pseudopleuronectes americanus</i>	0.00120	0.00359	0.33070	0.00290	0.00100	0.991	0.293
<i>Chionoecetes opilio</i>	0.00120	0.00336	0.35100	0.00000	0.00500	0.992	0.581
<i>Solaster endeca</i>	0.00110	0.00284	0.40150	0.00000	0.00500	0.993	0.602
Porifera sp. 17	0.00110	0.00281	0.39550	0.00000	0.00700	0.995	0.827
<i>Arctica islandica</i>	0.00110	0.00224	0.47470	0.00310	0.00300	0.996	0.380
<i>Hippoglossoides platessoides</i>	0.00080	0.00264	0.31710	0.00000	0.00400	0.996	0.477
<i>Hyas coarctatus</i>	0.00060	0.00165	0.38040	0.00000	0.00300	0.997	0.888
Porifera sp. 31	0.00050	0.00159	0.32800	0.00000	0.00300	0.998	0.730

Unknown sp. 9	0.00040	0.00189	0.23710	0.00000	0.00200	0.998	0.452
<i>Pagurus</i> spp.	0.00040	0.00196	0.19450	0.00000	0.00200	0.999	0.837
<i>Hyas araneus</i>	0.00040	0.00201	0.18010	0.00000	0.00100	0.999	0.991
<i>Zoarces</i> sp. 1	0.00030	0.00225	0.15040	0.00000	0.00100	0.999	0.817
Gastropoda sp. 4	0.00030	0.00097	0.31200	0.00000	0.00200	1.000	0.418
Porifera sp. 15	0.00030	0.00086	0.29720	0.00070	0.00000	1.000	0.916
<i>Leptasterias polaris</i>	0.00010	0.00052	0.21300	0.00000	0.00000	1.000	0.946

Signif. codes: 0 ‘***’ 0.001 ‘**’ 0.01 ‘*’ 0.05 ‘.’ 0.1 ‘ ’ 1

Contrast: Red_Orange

taxa	average	sd	ratio	ava	avb	cumsum	p
<i>Pachycerianthus borealis</i>	0.35540	0.26360	1.34830	0.00000	1.83700	0.370	0.001 ***
<i>Echinorachnius parma</i>	0.35090	0.25387	1.38230	1.48710	0.00000	0.735	0.001 ***
<i>Asterias</i> spp.	0.08370	0.08068	1.03730	0.24270	0.00780	0.822	0.007 **
<i>Strongylocentrotus droebachiensis</i>	0.08230	0.07842	1.04940	0.22700	0.26040	0.908	0.278
<i>Henricia</i> spp.	0.04060	0.06094	0.66570	0.09660	0.00320	0.950	0.021 *
<i>Psolus phantapus</i>	0.01600	0.02232	0.71660	0.00000	0.05870	0.967	1.000
<i>Pandalus</i> spp.	0.01440	0.03753	0.38440	0.00000	0.02210	0.982	0.120
<i>Mytilidae</i> spp.	0.00360	0.00554	0.65320	0.01360	0.00000	0.985	0.492
Porifera sp. 15	0.00310	0.00665	0.46890	0.00070	0.00640	0.989	0.158
<i>Pseudopleuronectes americanus</i>	0.00170	0.00489	0.34030	0.00290	0.00000	0.990	0.237
<i>Psychogastria polaris</i>	0.00160	0.00418	0.37420	0.00000	0.00230	0.992	0.983
<i>Zoarces</i> sp. 1	0.00160	0.00418	0.37420	0.00000	0.00230	0.994	0.262
Porifera sp. 31	0.00150	0.00349	0.42080	0.00000	0.00320	0.995	0.206
<i>Chionoecetes opilio</i>	0.00110	0.00175	0.61300	0.00000	0.00300	0.996	0.473
<i>Hyas araneus</i>	0.00080	0.00116	0.72620	0.00000	0.00330	0.997	0.684
<i>Arctica islandica</i>	0.00070	0.00129	0.55150	0.00310	0.00000	0.998	0.554
Gastropoda sp. 3	0.00070	0.00144	0.46790	0.00000	0.00270	0.999	0.960
Porifera sp. 17	0.00050	0.00109	0.46600	0.00000	0.00200	0.999	0.853
<i>Solaster endeca</i>	0.00050	0.00109	0.46600	0.00000	0.00200	1.000	0.783
<i>Hyas coarctatus</i>	0.00030	0.00072	0.46790	0.00000	0.00140	1.000	0.817
<i>Hippoglossoides platessoides</i>	0.00000	0.00000	NA	0.00000	0.00000	1.000	0.704

<i>Leptasterias polaris</i>	0.00000	0.00000	NA	0.00000	0.00000	1.000	0.533
<i>Pteraster</i> spp.	0.00000	0.00000	NA	0.00000	0.00000	1.000	0.999
<i>Ophiuroidea</i> spp.	0.00000	0.00000	NA	0.00000	0.00000	1.000	0.991
Gastropoda sp. 4	0.00000	0.00000	NA	0.00000	0.00000	1.000	0.562
<i>Pagurus</i> spp.	0.00000	0.00000	NA	0.00000	0.00000	1.000	0.655
Unknown sp. 9	0.00000	0.00000	NA	0.00000	0.00000	1.000	0.449

Signif. codes: 0 ‘***’ 0.001 ‘**’ 0.01 ‘*’ 0.05 ‘.’ 0.1 ‘ ’ 1

Contrast: Red_Brown

taxa	average	sd	ratio	ava	avb	cumsum	p
<i>Echinorachnius parma</i>	0.49420	0.28399	1.74030	1.48710	0.00649	0.572	0.001 ***
<i>Strongylocentrotus droebachiensis</i>	0.15390	0.13758	1.11900	0.22700	0.28855	0.750	0.004 **
<i>Asterias</i> spp.	0.11740	0.11626	1.01010	0.24270	0.07067	0.886	0.001 ***
<i>Henricia</i> spp.	0.06900	0.09546	0.72250	0.09660	0.01751	0.966	0.001 ***
<i>Mytilidae</i> spp.	0.01260	0.01871	0.67240	0.01360	0.02009	0.980	0.061 .
<i>Pseudopleuronectes americanus</i>	0.00360	0.00755	0.48170	0.00290	0.00267	0.984	0.004 **
<i>Hyas araneus</i>	0.00280	0.00613	0.45040	0.00000	0.00406	0.988	0.231
Porifera sp. 15	0.00210	0.00559	0.36720	0.00070	0.00290	0.990	0.255
<i>Pteraster</i> spp.	0.00120	0.00515	0.23120	0.00000	0.00169	0.991	0.996
<i>Ptychogastria polaris</i>	0.00110	0.00324	0.34700	0.00000	0.00201	0.992	1.000
<i>Leptasterias polaris</i>	0.00100	0.00386	0.26510	0.00000	0.00242	0.994	0.405
<i>Arctica islandica</i>	0.00100	0.00167	0.59000	0.00310	0.00000	0.995	0.395
<i>Psolus phantapus</i>	0.00100	0.00404	0.23630	0.00000	0.00145	0.996	1.000
Porifera sp. 17	0.00090	0.00258	0.33920	0.00000	0.00129	0.997	0.806
<i>Pachycerianthus borealis</i>	0.00090	0.00258	0.33920	0.00000	0.00129	0.998	0.970
Gastropoda sp. 3	0.00050	0.00202	0.23630	0.00000	0.00073	0.998	0.996
<i>Hyas coarctatus</i>	0.00050	0.00211	0.21960	0.00000	0.00056	0.999	0.858
<i>Zoarces</i> sp. 1	0.00040	0.00172	0.23120	0.00000	0.00056	1.000	0.595
<i>Pandalus</i> spp.	0.00040	0.00172	0.23120	0.00000	0.00056	1.000	0.990
Porifera sp. 31	0.00000	0.00000	NA	0.00000	0.00000	1.000	0.892
<i>Hippoglossoides platessoides</i>	0.00000	0.00000	NA	0.00000	0.00000	1.000	0.871
<i>Solaster endeca</i>	0.00000	0.00000	NA	0.00000	0.00000	1.000	0.986
<i>Chionoecetes opilio</i>	0.00000	0.00000	NA	0.00000	0.00000	1.000	0.989

<i>Ophiuroidea</i> spp.	0.00000	0.00000	NA	0.00000	0.00000	1.000	1.000
Gastropoda sp. 4	0.00000	0.00000	NA	0.00000	0.00000	1.000	0.755
<i>Pagurus</i> spp.	0.00000	0.00000	NA	0.00000	0.00000	1.000	0.827
Unknown sp. 9	0.00000	0.00000	NA	0.00000	0.00000	1.000	0.652

Signif. codes: 0 ‘***’ 0.001 ‘**’ 0.01 ‘*’ 0.05 ‘.’ 0.1 ‘ ’ 1

Contrast: Red_Purple

taxa	average	sd	ratio	ava	avb	cumsum	p
<i>Echinorachnius parma</i>	0.52820	0.30058	1.75720	1.48710	0.00565	0.544	0.001 ***
<i>Asterias</i> spp.	0.16180	0.12323	1.31310	0.24270	0.00000	0.711	0.001 ***
<i>Henricia</i> spp.	0.08510	0.10561	0.80570	0.09660	0.00000	0.799	0.005 **
<i>Strongylocentrotus droebachiensis</i>	0.07810	0.11043	0.70730	0.22700	0.05193	0.880	0.330
<i>Ptychogastria polaris</i>	0.07650	0.06469	1.18290	0.00000	0.11411	0.958	0.014 *
<i>Pagurus</i> spp.	0.00850	0.01267	0.66940	0.00000	0.01322	0.967	0.033 *
<i>Mytilidae</i> spp.	0.00560	0.00808	0.69630	0.01360	0.00000	0.973	0.293
<i>Hyas coarctatus</i>	0.00420	0.00634	0.66940	0.00000	0.00661	0.977	0.069 .
<i>Leptasterias polaris</i>	0.00420	0.00634	0.66940	0.00000	0.00661	0.982	0.063 .
<i>Pandalus</i> spp.	0.00420	0.00634	0.66940	0.00000	0.00661	0.986	0.364
<i>Psolus phantapus</i>	0.00390	0.00602	0.64870	0.00000	0.00565	0.990	1.000
<i>Hyas araneus</i>	0.00390	0.00602	0.64870	0.00000	0.00565	0.994	0.153
<i>Pseudopleuronectes americanus</i>	0.00370	0.00891	0.42040	0.00290	0.00000	0.998	0.053 .
<i>Arctica islandica</i>	0.00100	0.00183	0.57420	0.00310	0.00000	0.999	0.315
Porifera sp. 15	0.00080	0.00203	0.39300	0.00070	0.00000	1.000	0.253
Porifera sp. 31	0.00000	0.00000	NA	0.00000	0.00000	1.000	0.668
Porifera.sp..17	0.00000	0.00000	NA	0.00000	0.00000	1.000	0.843
<i>Hippoglossoides platessoides</i>	0.00000	0.00000	NA	0.00000	0.00000	1.000	0.589
<i>Pachycerianthus borealis</i>	0.00000	0.00000	NA	0.00000	0.00000	1.000	0.857
<i>Solaster endeca</i>	0.00000	0.00000	NA	0.00000	0.00000	1.000	0.828
Gastropoda sp. 3	0.00000	0.00000	NA	0.00000	0.00000	1.000	0.969
<i>Chionoecetes opilio</i>	0.00000	0.00000	NA	0.00000	0.00000	1.000	0.901
<i>Pteraster</i> spp.	0.00000	0.00000	NA	0.00000	0.00000	1.000	0.993
<i>Ophiuroidea</i> spp.	0.00000	0.00000	NA	0.00000	0.00000	1.000	0.983

Gastropoda sp. 4	0.00000	0.00000	NA	0.00000	0.00000	1.000	0.433
Zoarces sp. 1	0.00000	0.00000	NA	0.00000	0.00000	1.000	0.445
Unknown sp. 9	0.00000	0.00000	NA	0.00000	0.00000	1.000	0.337

Signif. codes: 0 ‘***’ 0.001 ‘**’ 0.01 ‘*’ 0.05 ‘.’ 0.1 ‘ ’ 1

Contrast: Green_Orange

taxa	average	sd	ratio	ava	avb	cumsum	p
<i>Psolus phantapus</i>	0.45740	0.30096	1.51990	3.33900	0.05870	0.482	0.287
<i>Pachycerianthus borealis</i>	0.29240	0.24641	1.18660	0.04400	1.83700	0.791	0.001 ***
Ophiuroidea spp.	0.08570	0.14885	0.57580	0.43500	0.00000	0.881	0.473
<i>Strongylocentrotus droebachiensis</i>	0.05010	0.05246	0.95430	0.02700	0.26040	0.934	0.673
<i>Pandalus</i> spp.	0.01290	0.04058	0.31780	0.01000	0.02210	0.948	0.092 .
<i>Asterias</i> spp.	0.00960	0.02337	0.40960	0.02500	0.00780	0.958	0.988
<i>Pteraster</i> spp.	0.00900	0.02036	0.43990	0.04800	0.00000	0.967	0.473
<i>Ptychogastria polaris</i>	0.00600	0.00944	0.63930	0.03100	0.00230	0.973	0.853
<i>Echinarachnius parma</i>	0.00460	0.01944	0.23920	0.01900	0.00000	0.978	1.000
Gastropoda sp. 3	0.00280	0.00472	0.60220	0.01500	0.00270	0.981	0.469
<i>Henricia</i> spp.	0.00260	0.00790	0.32440	0.00500	0.00320	0.984	0.987
Porifera sp. 15	0.00230	0.00637	0.36480	0.00000	0.00640	0.986	0.151
<i>Chionoecetes opilio</i>	0.00170	0.00361	0.47390	0.00500	0.00300	0.988	0.216
Zoarces sp. 1	0.00160	0.00514	0.30810	0.00100	0.00230	0.990	0.189
Porifera sp. 17	0.00150	0.00358	0.41970	0.00700	0.00200	0.992	0.565
Porifera sp. 31	0.00150	0.00332	0.44680	0.00300	0.00320	0.993	0.157
<i>Solaster endeca</i>	0.00140	0.00307	0.46440	0.00500	0.00200	0.995	0.361
<i>Hyas araneus</i>	0.00100	0.00305	0.33500	0.00100	0.00330	0.996	0.709
<i>Hippoglossoides platessoides</i>	0.00090	0.00291	0.30920	0.00400	0.00000	0.997	0.365
<i>Hyas coarctatus</i>	0.00090	0.00186	0.46440	0.00300	0.00140	0.998	0.640
<i>Arctica islandica</i>	0.00090	0.00317	0.26930	0.00300	0.00000	0.998	0.520
Unknown sp. 9	0.00050	0.00214	0.22780	0.00200	0.00000	0.999	0.327
<i>Pagurus</i> spp.	0.00040	0.00231	0.18190	0.00200	0.00000	0.999	0.735
Gastropoda sp. 4	0.00030	0.00100	0.30640	0.00200	0.00000	1.000	0.322
<i>Pseudopleuronectes americanus</i>	0.00020	0.00066	0.25660	0.00100	0.00000	1.000	0.985

<i>Leptasterias polaris</i>	0.00010	0.00056	0.20690	0.00000	0.00000	1.000	0.932
<i>Mytilidae</i> spp.	0.00000	0.00000	NA	0.00000	0.00000	1.000	1.000

Signif. codes: 0 ‘***’ 0.001 ‘**’ 0.01 ‘*’ 0.05 ‘.’ 0.1 ‘ ’ 1

Contrast: Green_Brown

taxa	average	sd	ratio	ava	avb	cumsum	p
<i>Psolus phantapus</i>	0.61320	0.31048	1.97510	3.33900	0.00145	0.639	0.001 ***
Ophiuroidea spp.	0.11910	0.19641	0.60660	0.43500	0.00000	0.764	0.056
<i>Strongylocentrotus droebachiensis</i>	0.10500	0.13543	0.77540	0.02700	0.28855	0.873	0.002 **
<i>Asterias</i> spp.	0.03140	0.05087	0.61790	0.02500	0.07067	0.906	0.528
<i>Pachycerianthus borealis</i>	0.01360	0.05192	0.26100	0.04400	0.00129	0.920	0.995
<i>Pteraster</i> spp.	0.01310	0.02742	0.47610	0.04800	0.00169	0.934	0.182
<i>Mytilidae</i> spp.	0.00940	0.02140	0.43770	0.00000	0.02009	0.943	0.028 *
<i>Echinarachnius parma</i>	0.00890	0.02653	0.33670	0.01900	0.00649	0.953	1.000
<i>Ptychogastria polaris</i>	0.00880	0.01296	0.67990	0.03100	0.00201	0.962	0.758
<i>Henricia</i> spp.	0.00780	0.01606	0.48310	0.00500	0.01751	0.970	0.871
<i>Pandalus</i> spp.	0.00490	0.01361	0.36040	0.01000	0.00056	0.975	0.618
Gastropoda sp. 3	0.00390	0.00687	0.56860	0.01500	0.00073	0.979	0.061
<i>Hyas araneus</i>	0.00290	0.01014	0.28500	0.00100	0.00406	0.982	0.118
Porifera sp. 17	0.00240	0.00618	0.39360	0.00700	0.00129	0.985	0.096 .
<i>Solaster endeca</i>	0.00180	0.00432	0.41800	0.00500	0.00000	0.986	0.185
<i>Chionoecetes opilio</i>	0.00180	0.00498	0.35230	0.00500	0.00000	0.988	0.238
<i>Arctica islandica</i>	0.00150	0.00588	0.25700	0.00300	0.00000	0.990	0.156
<i>Hyas coarctatus</i>	0.00140	0.00436	0.32090	0.00300	0.00056	0.991	0.419
<i>Hippoglossoides platessoides</i>	0.00130	0.00401	0.33710	0.00400	0.00000	0.993	0.213
<i>Pseudopleuronectes americanus</i>	0.00120	0.00287	0.40730	0.00100	0.00267	0.994	0.307
Porifera sp. 15	0.00120	0.00530	0.21760	0.00000	0.00290	0.995	0.395
Zoarces sp. 1	0.00100	0.00471	0.21560	0.00100	0.00056	0.996	0.396
<i>Leptasterias polaris</i>	0.00090	0.00346	0.27420	0.00000	0.00242	0.997	0.345
Porifera sp. 31	0.00080	0.00269	0.31120	0.00300	0.00000	0.998	0.482
Unknown sp. 9	0.00080	0.00308	0.24590	0.00200	0.00000	0.999	0.310
<i>Pagurus</i> spp.	0.00070	0.00345	0.19110	0.00200	0.00000	1.000	0.718

Gastropoda sp. 4	0.00040	0.00125	0.31360	0.00200	0.00000	1.000	0.403
------------------	---------	---------	---------	---------	---------	-------	-------

Signif. codes: 0 ‘***’ 0.001 ‘**’ 0.01 ‘*’ 0.05 ‘.’ 0.1 ‘ ’ 1

Contrast: Green_Purple

taxa	average	sd	ratio	ava	avb	cumsum	p
<i>Psolus phantapus</i>	0.64300	0.31454	2.04440	3.33900	0.00565	0.674	0.014 *
Ophiuroidea spp.	0.12720	0.20999	0.60550	0.43500	0.00000	0.808	0.202
<i>Ptychogastria polaris</i>	0.05810	0.08981	0.64640	0.03100	0.11411	0.868	0.025 *
<i>Strongylocentrotus droebachiensis</i>	0.02730	0.04988	0.54750	0.02700	0.05193	0.897	0.771
Asterias spp.	0.01730	0.04186	0.41240	0.02500	0.00000	0.915	0.711
<i>Pachycerianthus borealis</i>	0.01370	0.05515	0.24900	0.04400	0.00000	0.930	0.952
<i>Pteraster</i> spp.	0.01360	0.02932	0.46310	0.04800	0.00000	0.944	0.166
<i>Echinorachnius parma</i>	0.00960	0.02729	0.35030	0.01900	0.00565	0.954	0.987
<i>Pagurus</i> spp.	0.00710	0.01441	0.49350	0.00200	0.01322	0.961	0.034 *
<i>Pandalus</i> spp.	0.00620	0.01172	0.53320	0.01000	0.00661	0.968	0.274
Gastropoda sp. 3	0.00390	0.00739	0.53250	0.01500	0.00000	0.972	0.197
<i>Hyas coarctatus</i>	0.00390	0.00677	0.57190	0.00300	0.00661	0.976	0.059 .
<i>Leptasterias polaris</i>	0.00350	0.00717	0.49370	0.00000	0.00661	0.980	0.071 .
<i>Hyas araneus</i>	0.00340	0.00728	0.47310	0.00100	0.00565	0.984	0.182
<i>Henricia</i> spp.	0.00330	0.01330	0.24960	0.00500	0.00000	0.987	0.875
Porifera sp. 17	0.00230	0.00628	0.35890	0.00700	0.00000	0.989	0.306
<i>Solaster endeca</i>	0.00200	0.00466	0.42020	0.00500	0.00000	0.991	0.185
<i>Chionoecetes opilio</i>	0.00190	0.00535	0.35060	0.00500	0.00000	0.993	0.144
<i>Arctica islandica</i>	0.00170	0.00589	0.28440	0.00300	0.00000	0.995	0.148
<i>Hippoglossoides platessoides</i>	0.00150	0.00432	0.34120	0.00400	0.00000	0.997	0.140
Porifera sp. 31	0.00090	0.00295	0.31060	0.00300	0.00000	0.998	0.231
Unknown sp. 9	0.00080	0.00336	0.24860	0.00200	0.00000	0.998	0.111
Zoarces sp. 1	0.00080	0.00490	0.16470	0.00100	0.00000	0.999	0.262
Gastropoda sp. 4	0.00040	0.00131	0.31190	0.00200	0.00000	1.000	0.129
<i>Pseudopleuronectes americanus</i>	0.00020	0.00091	0.25910	0.00100	0.00000	1.000	0.876
Porifera sp. 15	0.00000	0.00000	NA	0.00000	0.00000	1.000	0.951
Mytilidae spp.	0.00000	0.00000	NA	0.00000	0.00000	1.000	1.000

Signif. codes: 0 ‘***’ 0.001 ‘**’ 0.01 ‘*’ 0.05 ‘.’ 0.1 ‘ ’ 1

Contrast: Orange_Brown

taxa	average	sd	ratio	ava	avb	cumsum	p
<i>Pachycerianthus borealis</i>	0.52710	0.29434	1.79080	1.83700	0.00129	0.617	0.001 ***
<i>Strongylocentrotus droebachiensis</i>	0.15150	0.16938	0.89470	0.26040	0.28855	0.794	0.011 *
<i>Pandalus</i> spp.	0.04430	0.10208	0.43370	0.02210	0.00056	0.846	0.001 ***
<i>Asterias</i> spp.	0.03960	0.05822	0.68030	0.00780	0.07067	0.892	0.273
<i>Psolus phantapus</i>	0.02720	0.03128	0.87100	0.05870	0.00145	0.924	1.000
<i>Mytilidae</i> spp.	0.01440	0.02711	0.53150	0.00000	0.02009	0.941	0.045 *
<i>Henricia</i> spp.	0.00990	0.01652	0.60210	0.00320	0.01751	0.953	0.500
Porifera sp. 15	0.00700	0.01366	0.51560	0.00640	0.00290	0.961	0.004 **
<i>Pychogastria polaris</i>	0.00520	0.01081	0.47840	0.00230	0.00201	0.967	0.789
<i>Zoarces</i> sp. 1	0.00480	0.01089	0.44150	0.00230	0.00056	0.972	0.006 **
<i>Hyas araneus</i>	0.00450	0.01049	0.42460	0.00330	0.00406	0.978	0.095 .
<i>Echinorachnius parma</i>	0.00430	0.01315	0.32780	0.00000	0.00649	0.983	0.936
Porifera sp. 31	0.00310	0.00647	0.47550	0.00320	0.00000	0.986	0.006 **
<i>Chionoecetes opilio</i>	0.00200	0.00315	0.64840	0.00300	0.00000	0.989	0.234
Porifera sp. 17	0.00180	0.00395	0.44540	0.00200	0.00129	0.991	0.449
<i>Pteraster</i> spp.	0.00170	0.00797	0.21020	0.00000	0.00169	0.993	0.983
Gastropoda sp. 3	0.00150	0.00338	0.45620	0.00270	0.00073	0.995	0.867
<i>Pseudopleuronectes americanus</i>	0.00150	0.00373	0.41100	0.00000	0.00267	0.996	0.207
<i>Leptasterias polaris</i>	0.00120	0.00461	0.25350	0.00000	0.00242	0.998	0.271
<i>Hyas coarctatus</i>	0.00120	0.00390	0.29650	0.00140	0.00056	0.999	0.461
<i>Solaster endeca</i>	0.00080	0.00157	0.49170	0.00200	0.00000	1.000	0.686
<i>Hippoglossoides platessoides</i>	0.00000	0.00000	NA	0.00000	0.00000	1.000	0.855
<i>Arctica islandica</i>	0.00000	0.00000	NA	0.00000	0.00000	1.000	0.973
Ophiuroidea spp.	0.00000	0.00000	NA	0.00000	0.00000	1.000	0.999
Gastropoda sp. 4	0.00000	0.00000	NA	0.00000	0.00000	1.000	0.713
<i>Pagurus</i> spp.	0.00000	0.00000	NA	0.00000	0.00000	1.000	0.777
Unknown sp. 9	0.00000	0.00000	NA	0.00000	0.00000	1.000	0.617

Signif. codes: 0 ‘***’ 0.001 ‘**’ 0.01 ‘*’ 0.05 ‘.’ 0.1 ‘ ’ 1

Contrast: Orange_Purple

taxa	average	sd	ratio	ava	avb	cumsum	p
<i>Pachycerianthus borealis</i>	0.56530	0.30555	1.85000	1.83700	0.00000	0.609	0.001 ***
<i>Strongylocentrotus droebachiensis</i>	0.12200	0.09523	1.28110	0.26040	0.05193	0.740	0.161
<i>Ptychogastria polaris</i>	0.09880	0.09834	1.00430	0.00230	0.11411	0.847	0.007 **
<i>Pandalus</i> spp.	0.05040	0.10083	0.50030	0.02210	0.00661	0.901	0.015 *
<i>Psolus phantapus</i>	0.02600	0.03442	0.75620	0.05870	0.00565	0.929	0.999
<i>Pagurus</i> spp.	0.01130	0.01900	0.59290	0.00000	0.01322	0.941	0.019 *
<i>Asterias</i> spp.	0.00760	0.01460	0.51890	0.00780	0.00000	0.950	0.803
Porifera sp. 15	0.00700	0.01484	0.47390	0.00640	0.00000	0.957	0.046 *
<i>Hyas coarctatus</i>	0.00560	0.00942	0.59880	0.00140	0.00661	0.963	0.039 *
<i>Zoarces</i> sp. 1	0.00560	0.01193	0.47220	0.00230	0.00000	0.969	0.052 .
<i>Leptasterias polaris</i>	0.00560	0.00950	0.59290	0.00000	0.00661	0.975	0.040 *
<i>Echinorachnius parma</i>	0.00540	0.00955	0.56700	0.00000	0.00565	0.981	0.686
<i>Hyas araneus</i>	0.00540	0.00946	0.56990	0.00330	0.00565	0.987	0.089 .
<i>Henricia</i> spp.	0.00350	0.00742	0.47390	0.00320	0.00000	0.991	0.658
Porifera sp. 31	0.00350	0.00742	0.47390	0.00320	0.00000	0.995	0.044 *
<i>Chionoecetes opilio</i>	0.00230	0.00360	0.63890	0.00300	0.00000	0.997	0.173
Gastropoda sp. 3	0.00110	0.00228	0.47430	0.00270	0.00000	0.998	0.744
Porifera sp. 17	0.00080	0.00175	0.47430	0.00200	0.00000	0.999	0.628
<i>Solaster endeca</i>	0.00080	0.00175	0.47430	0.00200	0.00000	1.000	0.542
<i>Pseudopleuronectes americanus</i>	0.00000	0.00000	NA	0.00000	0.00000	1.000	0.614
<i>Hippoglossoides platessoides</i>	0.00000	0.00000	NA	0.00000	0.00000	1.000	0.483
<i>Arctica islandica</i>	0.00000	0.00000	NA	0.00000	0.00000	1.000	0.743
<i>Pteraster</i> spp.	0.00000	0.00000	NA	0.00000	0.00000	1.000	0.977
Ophiuroidea spp.	0.00000	0.00000	NA	0.00000	0.00000	1.000	0.954
Gastropoda sp. 4	0.00000	0.00000	NA	0.00000	0.00000	1.000	0.354
Unknown sp. 9	0.00000	0.00000	NA	0.00000	0.00000	1.000	0.279
<i>Mytilidae</i> spp.	0.00000	0.00000	NA	0.00000	0.00000	1.000	0.699

Signif. codes: 0 ‘***’ 0.001 ‘**’ 0.01 ‘*’ 0.05 ‘.’ 0.1 ‘ ’ 1

Contrast: Brown_Purple

taxa	average	sd	ratio	ava	avb	cumsum	p
<i>Strongylocentrotus droebachiensis</i>	0.32480	0.19759	1.64380	0.28855	0.05193	0.396	0.003 **
<i>Ptychogastria polaris</i>	0.23190	0.14877	1.55890	0.00201	0.11411	0.678	0.001 ***
<i>Asterias</i> spp.	0.08280	0.09627	0.85970	0.07067	0.00000	0.779	0.044 *
<i>Mytilidae</i> spp.	0.03450	0.04554	0.75650	0.02009	0.00000	0.821	0.009 **
<i>Pagurus</i> spp.	0.02440	0.03000	0.81400	0.00000	0.01322	0.851	0.001 ***
<i>Henricia</i> spp.	0.01770	0.02770	0.63900	0.01751	0.00000	0.873	0.214
<i>Echinarachnius parma</i>	0.01760	0.02251	0.78410	0.00649	0.00565	0.894	0.748
<i>Hyas araneus</i>	0.01390	0.01419	0.98300	0.00406	0.00565	0.911	0.005 **
<i>Leptasterias polaris</i>	0.01350	0.01511	0.89280	0.00242	0.00661	0.928	0.001 ***
<i>Psolus phantapus</i>	0.01350	0.01641	0.82140	0.00145	0.00565	0.944	1.000
<i>Hyas coarctatus</i>	0.01250	0.01377	0.90900	0.00056	0.00661	0.959	0.001 ***
<i>Pandalus</i> spp.	0.01240	0.01430	0.86370	0.00056	0.00661	0.974	0.116
<i>Pteraster</i> spp.	0.00450	0.01534	0.29380	0.00169	0.00000	0.980	0.714
Porifera sp. 15	0.00380	0.01276	0.29480	0.00290	0.00000	0.984	0.074 .
<i>Pseudopleuronectes americanus</i>	0.00340	0.00656	0.51220	0.00267	0.00000	0.988	0.062 .
Porifera sp. 17	0.00320	0.00725	0.43530	0.00129	0.00000	0.992	0.172
<i>Pachycerianthus borealis</i>	0.00320	0.00725	0.43530	0.00129	0.00000	0.996	0.830
Gastropoda sp. 3	0.00170	0.00561	0.29420	0.00073	0.00000	0.998	0.698
Zoarces sp. 1	0.00150	0.00511	0.29380	0.00056	0.00000	1.000	0.180
Porifera sp. 31	0.00000	0.00000	NA	0.00000	0.00000	1.000	0.816
<i>Hippoglossoides platessoides</i>	0.00000	0.00000	NA	0.00000	0.00000	1.000	0.738
<i>Solaster endeca</i>	0.00000	0.00000	NA	0.00000	0.00000	1.000	0.944
<i>Arctica islandica</i>	0.00000	0.00000	NA	0.00000	0.00000	1.000	0.946
<i>Chionoecetes opilio</i>	0.00000	0.00000	NA	0.00000	0.00000	1.000	0.973
Ophiuroidea spp.	0.00000	0.00000	NA	0.00000	0.00000	1.000	0.999
Gastropoda sp. 4	0.00000	0.00000	NA	0.00000	0.00000	1.000	0.614
Unknown sp. 9	0.00000	0.00000	NA	0.00000	0.00000	1.000	0.481

Signif. codes: 0 ‘***’ 0.001 ‘**’ 0.01 ‘*’ 0.05 ‘.’ 0.1 ‘ ’ 1

Permutation: free

Number of permutations: 999

> summary(indval)

taxa	Cluster	indicator_value	probability
<i>Echinorachnius parma</i>	Red	0.8396	0.0028
<i>Henricia</i> spp.	Red	0.7892	0.0005
<i>Asterias</i> spp.	Red	0.7017	0.0008
<i>Psolus phantapus</i>	Green	0.9568	0.0001
<i>Pteraster</i> spp.	Green	0.5653	0.0318
Ophiuroidea spp.	Green	0.5366	0.0336
<i>Pachycerianthus borealis</i>	Orange	0.9760	0.0001
<i>Ptychogastria polaris</i>	Purple	0.7616	0.0018
<i>Pagurus</i> spp.	Purple	0.4426	0.0135

Sum of probabilities = 6.9617

Sum of Indicator Values = 10.1

Sum of Significant Indicator Values = 6.57

Number of Significant Indicators = 9

Significant Indicator Distribution

1 2 3 5

3 3 1 2

> anosim

Call:

```
anosim(x = spe.chSpring, grouping = Matrixclust$spech.UPGMA.g, permutations = 999)
```

Dissimilarity: euclidean

ANOSIM statistic R: 0.9018

Significance: 0.001

Permutation: free

Number of permutations: 999